

**Assessing the Impact of Grazing on Nutrient Export from Pastureland in an
Ungauged Basin in Manitoba under Climate Change using an Integrated
Modelling Approach**

By
Baiyan Zhou

A thesis submitted to the Faculty of Graduate Studies of
The University of Manitoba
In partial fulfillment of the requirements for the degree of

MASTER OF SCIENCE

Department of Animal Science
University of Manitoba
Winnipeg, Manitoba, Canada

Copyright © 2024 by Baiyan Zhou

ABSTRACT

Assessments of climate change impacts on hydrology and nutrient export from pasturelands are not readily available in Canada. The objective of this study was to implement an integrated modelling approach to predict the impact of climate change on the hydrology and nutrient fluxes on a 46.6 km² pasture-dominated ungauged watershed in Manitoba. The Integrated Farm System Model (IFSM) was used to predict the pasture yield/residues, and manure production. To simulate the hydrological response, the Cold Regions Hydrological Model (CRHM) platform and the Hydrological Predictions for the Environment (HYPE) model were used. Predictions of nutrient exports to stream were also carried out using the HYPE model. Model assessments were conducted for the historical reference period between 2000 and 2019, and for the near (2020 – 2049) and the distant future (2050 - 2079) periods using climate projections under two Representative Concentration Pathways (RCP). Satisfactory model performance was obtained for the three individual models using available observations. Under a changing climate, pasture yields were anticipated to decrease by approximately 2% to 6.8%, with an exception that a 2% increase in pasture yield was predicted in the near future period under RCP 4.5. There was no significant changes observed in manure production. Both CRHM and HYPE models predicted a 20% and 40% reduction in stream discharge in the near future under RCP 4.5, respectively. Meanwhile, CRHM predicted an increase in stream discharge by 26% and 39% in the near future and distant future periods under RCP 8.5. In contrast, HYPE had a marginal increase in stream discharge, averaging 2% under RCP 8.5. An earlier onset of spring snowmelt was predicted by both CRHM and HYPE, ranging from 6 to 21 days in future periods compared to the reference period, implying a potentially longer growing season. Lastly, a 33% and 4.5% reduction was observed in the projected total nitrogen load in future periods under RCP 4.5 and RCP 8.5,

respectively. The total phosphorus loads, on the other hand, had a significant average reduction of 50% and 35% under RCP 4.5 and RCP 8.5, respectively. It was found that the general pattern of nutrient export (N and P) closely mirrored that of the stream discharge. Overall, the predicted reduction in nutrient export implied a lower risk of eutrophication in the study area.

ACKNOWLEDGEMENTS

First and foremost, I would like to express my sincere gratitude to my advisor, Dr. Marcos Cordeiro for the opportunity to extend my studies to the graduate level. His expertise, unwavering support, and invaluable guidance have kept me on the right track throughout the whole journey. I am extremely thankful being one of his students. I also want to thank my committee members, Dr. Kim Ominski, Dr. Masoud Asadzadeh, and Dr. Francis Zvomuya for their time spent on providing constructive comments and advice on my thesis.

I extend my thanks to Dr. Alan Rotz and Logan Fang for their time spent on reviewing the IFSM and the CRHM models, and providing informative feedback for a better model representation.

I am also thankful to our postdoctoral fellows, Dr. Kang Liang and Dr. Befekadu Tadesse Woldegiorgis for their mentorships. Their suggestions are wholeheartedly appreciated. I have learned a lot from them. I would also like to thank Bryan Encabo for sharing the benchmark project template.

Finally, a special thanks goes to my family. They have been a continuous source of encouragement and understanding which has sustained me through all challenges. To my wife, Jiayi Chen, you cannot imagine how grateful I am that you have kept me company for all the time we spent together.

Financial support provided by Manitoba Beef Producers and Mitacs is greatly appreciated.

DEDICATION

To my wife and parents.

FOREWORD

This thesis follows a manuscript-style format based on the Canadian Journal of Animal Science standards and consists of three manuscripts. Each manuscript is comprised of an abstract, introduction, materials and methods, results, discussion and conclusion. Three manuscripts have not been submitted for publication at this time.

Contributions of Authors:

This study was conceived and designed by Dr. Marcos Cordeiro. Model initialization and configuration in the early stage was performed by Dr. Kang Liang (**IFSM**), Dr. Marcos Cordeiro (**CRHM**), and Dr. Befekadu Tadesse Woldegiorgis (**HYPE**). Model refinement, parameterization, calibration and assessment, as well as preparation of future climate datasets, were carried out by Baiyan Zhou (**IFSM, CRHM, and HYPE**). The three manuscripts (**Chapter 3, 4, and 5**) prepared by Baiyan Zhou under the supervision of Dr. Marcos Cordeiro were revised by Dr. Kim Ominski, Dr. Masoud Asadzadeh, and Dr. Francis Zvomuya.

TABLE OF CONTENTS

ABSTRACT.....	ii
ACKNOWLEDGEMENTS.....	iv
DEDICATION	v
FOREWORD	vi
TABLE OF CONTENTS	vii
LIST OF TABLES	x
LIST OF FIGURES	xi
LIST OF ABBREVIATIONS	xiii
CHAPTER 1: GENERAL INTRODUCTION	1
CHAPTER 2: LITERATURE REVIEW	3
2.1. Background.....	3
2.2. Nutrient Pools on Pasturelands	5
2.2.1. Nutrient Pools	6
2.2.1.1. Vegetation	6
2.2.1.2. Manure	8
2.2.1.3. Soil.....	11
2.2.2. Pathways of Nutrient Losses.....	14
2.3. Modelling.....	15
2.3.1. Farm Model.....	16
2.3.2. Hydrological Models	19
2.3.3. Water Quality Model.....	23
2.3.4. Effect of Climate Change.....	25
CHAPTER 3: ASSESSING THE IMPACT OF CLIMATE CHANGE ON PASTURE YIELD AND CATTLE MANURE PRODUCTION IN MANITOBA USING THE INTEGRATED FARM SYSTEM MODEL	29
3.1 Abstract	29
3.2 Introduction.....	30
3.3 Materials and Methods.....	33
3.3.1. Physiography and Study Area Characteristics	33
3.3.2 Datasets	34
3.3.2.1. Historical Climate Data.....	34

3.3.2.2. Future Climate Data.....	36
3.3.3. Integrated Farm System Model.....	37
3.3.4. Assumptions.....	38
3.3.5. Model Assessment	39
3.4 Results.....	41
3.4.1. Future Climate Trends.....	41
3.4.2. Model Assessment	43
3.4.3. Model Hindcast.....	44
3.4.4. Model Forecast.....	45
3.4.4.1. Agronomic Performance	45
3.4.4.2. Manure Production.....	46
3.4.5. Relationship between Yield and Precipitation	49
3.5 Discussion.....	51
3.6 Conclusion	54
BRIDGE TO CHAPTER 4.....	56
CHAPTER 4: IMPACT ASSESSMENT OF CLIMATE CHANGE ON THE HYDROLOGY OF A PASTURE-DOMINATED UNGAUGED WATERSHED IN MANITOBA USING A MULTI- MODEL APPROACH	57
4.1 Abstract.....	57
4.2 Introduction.....	58
4.3 Materials and Methods.....	62
4.3.1. Study Area.....	62
4.3.2. Input Datasets.....	63
4.3.2.1. Historical Weather Data	63
4.3.2.2. Future Climate Data.....	66
4.3.3. Watershed Delineation and Hydrological Response Unit Definition	66
4.3.4. Hydrological Model Configuration.....	68
4.3.4.1. Cold Regions Hydrological Model	68
4.3.4.2. Hydrological Predictions for the Environment (HYPE) Model	72
4.3.5. Model Assessment	75
4.3.6. Relationship between Variables	77
4.4 Results.....	77
4.4.1. Future Climate in the Study Area.....	77

4.4.2. Model Assessment	80
4.4.3. Effect of Climate Modelled Data on Hydrological Simulations.....	81
4.4.4. Model Forecast.....	84
4.4.5. Relationship of Seasonal Precipitation and Annual Discharge.....	88
4.5 Discussion.....	91
4.6 Conclusion	95
BRIDGE TO CHAPTER 5	96
CHAPTER 5: PREDICTING NUTRIENT EXPORT FROM A PASTURE-DOMINATED UNGAUGED WATERSHED IN MANITOBA UNDER CLIMATE CHANGE.....	97
5.1 Abstract	97
5.2 Introduction.....	97
5.3 Materials and Methods.....	102
5.3.1. Study Area.....	102
5.3.2. Input Datasets.....	104
5.3.2.1. Historical Climate Data.....	104
5.3.2.2. Future Climate Data.....	105
5.3.2.3. Datasets for Watershed Delineation and Hydrological Response Unit (HRU) Definition	105
5.3.3. Water Quality Simulations using the Hydrologic Predictions for the Environment (HYPE) Model	106
5.3.4. Model Assessment	108
5.4 Results.....	111
5.4.1. Future Climate	111
5.4.2. Model Assessment	114
5.4.3. Model Hindcast.....	115
5.4.4. Model Forecast.....	117
5.4.5. Relationship between Nutrient Loads and Annual Discharge	119
5.5 Discussion.....	120
5.6 Conclusion	124
CHAPTER 6: GENERAL CONCLUSIONS.....	125
CHAPTER 7: RECOMMENDATIONS FOR FUTURE RESEARCH.....	127
REFERENCES	129

LIST OF TABLES

Table 2.1: Ranges of N intake and excretion by beef cattle.....	10
Table 2.2: Ranges of P intake and excretion by beef cattle.....	11
Table 3.1: Sources of historical weather datasets with respective time steps and derivation method.....	36
Table 3.2: Annual and seasonal precipitation during the reference period for the historical, and the future dataset under RCP 4.5 and RCP 8.5 scenarios	44
Table 4.1: Description of the historical dataset variables, sources, and gap filling method.....	65
Table 4.2: Methods used for disaggregation of daily weather data to an hourly time step for CRHM.....	66
Table 4.3: Input data for watershed delineation.....	67
Table 4.4: Lists of hydrological response units defined in the study area.....	68
Table 4.5: CRHM modules used in the major river valley model.....	70
Table 4.6: HYPE model parameters description, dependency, and values.....	75
Table 4.7: Assessment metrics for simulated water yield and annual ET during the reference period (2000 – 2019) obtained from climate modelled data (RCP 4.5 and 8.5) against the observations.....	84
Table 4.8: Long-term average of ET, streamflow, and time of peak discharge CRHM and HYPE simulations for RCP 4.5 and RCP 8.5 scenarios, respectively.....	88
Table 5.1: Composition of the historical dataset at a daily timestep.....	104
Table 5.2: Information of hydrological response units in the study watershed.....	106
Table 5.3: HYPE model parameters description, dependency, and values.....	108
Table 5.4: Assessment metrics for simulated water yield, total nitrogen, and total phosphorus during the reference period (2000 – 2019) obtained from historical weather data and climate modelled data (RCP 4.5 and 8.5).....	117
Table 5.5: Long-term averages of streamflow, timing of peak discharge, and nutrient loads under RCP 4.5 and 8.5.....	118
Table 5.6: R ² values of annual discharge and nitrogen and phosphorus loads for three climate models under RCP 4.5 and RCP 8.5.....	120

LIST OF FIGURES

Figure 2.1: Typical stages in beef production systems in Canada.....	4
Figure 2.2: Description of an integrated farming system	6
Figure 2.3: Influence of climate change on the ecosystem in cold regions	26
Figure 3.1: Long-term trends of maximum and minimum daily temperature and growing degree days for growing season	42
Figure 3.2: Long-term average seasonal and annual precipitation for the reference, near future, and distant future periods under RCP 4.5 and RCP 8.5.....	43
Figure 3.3: Comparison of growing degree days of the historical dataset and the future climate datasets under RCP 4.5 and RCP 8.5.....	45
Figure 3.4: Long-term average pasture yield for the reference, near future, and distant future periods under RCP 4.5 and RCP 8.5.	46
Figure 3.5: Long-term average manure production, nitrogen and phosphorus content in manure for the reference, near future, and distant future periods under RCP 4.5 and RCP 8.5.....	48
Figure 3.6: Relationship between pasture yield and seasonal precipitation under RCP 4.5 and RCP 8.5.....	50
Figure 4.1: Location and land cover in the study area in the Beaver Creek watershed	63
Figure 4.2: Flowpaths in the soil from one land class assuming no drainage tile.....	74
Figure 4.3: Long-term trends of the projected maximum and minimum daily temperature under RCP 4.5 and RCP 8.5 from 2000 to 2079.....	78
Figure 4.4: Percentage change of ensemble daily mean temperature and total precipitation of each month during the near future and distant future under RCP 4.5.....	78
Figure 4.5: Percentage change of ensemble daily mean temperature and total precipitation of each month during the near future and distant future under RCP 8.5.....	79
Figure 4.6: Long-term trends of precipitation under RCP 4.5 and RCP 8.5.....	80
Figure 4.7: Comparisons of evapotranspiration simulated by CRHM and HYPE models against the long-term average evapotranspiration range in the Prairies ecozone, and the simulated water yield against the published annual water yield reported for the Eastern Prairies and Parkland Prairies ecoprovince.....	81
Figure 4.8: Comparison of CRHM simulated water yield and flow duration curve using historical dataset and climate modelled data for RCP 4.5 and 8.5.....	82
Figure 4.9: Comparison of HYPE simulated water yield and flow duration curve using historical dataset and climate modelled data for RCP 4.5 and 8.5.....	82
Figure 4.10: Comparison of historical measurement of daily maximum and minimum temperature and annual total precipitation against climate modelled data (RCP 4.5 and 8.5) for the reference period from 2000 to 2019 (except 2006).....	83
Figure 4.11: Comparison between evapotranspiration projected by CRHM under RCP 4.5 and RCP 8.5.....	85

Figure 4.12: Comparison between evapotranspiration projected by HYPE under RCP 4.5 and RCP 8.5.....	85
Figure 4.13: Long-term trends of annual stream discharge using CRHM under RCP 4.5 and RCP 8.5.....	86
Figure 4.14: Long-term trends of annual stream discharge using HYPE under RCP 4.5 and RCP 8.5.....	87
Figure 4.15: Relationship between seasonal precipitation and annual cumulative discharge using CRHM for the near and distant future under RCP 4.5 and RCP 8.5.....	89
Figure 4.16: Relationship between seasonal precipitation and annual cumulative discharge using HYPE for the near and distant future under RCP 4.5 and RCP 8.5.....	90
Figure 5.1: Land use in of the study area within the Beaver Creek watershed in Manitoba...	103
Figure 5.2: Long-term trends of the average daily temperature under RCP 4.5 and RCP 8.5 from 2000 to 2079.....	111
Figure 5.3: Long-term averages of monthly mean for the reference period, near future, and distant future under RCP 4.5 and RCP 8.5.....	112
Figure 5.4: Long-term trends of the total precipitation under RCP 4.5 and RCP 8.5 from 2000 to 2079.....	113
Figure 5.5: Long-term averages of monthly cumulative precipitation for the reference period, near future, and distant future under RCP 4.5 and RCP 8.5.....	114
Figure 5.6: Comparisons between estimated observations and simulated total nitrogen and total phosphorus at the study area.....	115
Figure 5.7: Comparison of HYPE simulated water yields and flow duration curves using historical dataset and climate modelled data for RCP 4.5 and 8.5.....	116
Figure 5.8: Comparison of simulated total nitrogen and total phosphorus using historical dataset and climate modelled data for RCP 4.5 and 8.5.....	116
Figure 5.9: Long-term trends of annual cumulative stream discharge under RCP 4.5 and RCP 8.5.....	118
Figure 5.10: Long-term trends of total nitrogen under RCP 4.5 and RCP 8.5.....	119
Figure 5.11: Long-term trends of total phosphorus under RCP 4.5 and RCP 8.5.....	119

LIST OF ABBREVIATIONS

AMCP	Association of Manitoba Community Pastures
CRHM	Cold Regions Hydrological Model
DM	Dry matter
ET	Evapotranspiration
FAO	Food and Agriculture Organization of the United Nations
FTC	Freeze-thaw cycle
HRU	Hydrological response unit
HYPE	Hydrological Predictions for the Environment
IFSM	Integrated Farm System Model
MAE	Mean absolute error
N	Nitrogen
NSE	Nash-Sutcliffe efficiency
P	Phosphorus
PBIAS	Percent bias
RCP	Representative concentration pathways

CHAPTER 1: GENERAL INTRODUCTION

In Canada, 1.16 million tonnes of beef has been produced annually from 2010 to 2021 (Statistics Canada, 2022a). Between 2020 and 2022, the industry generated \$10.4 billion each year (Canadian Cattlemen's Association, 2023). The sector in Canada is comprised of several stages including cow-calf in which calves remain with the cows on pasture until weaning, and finishing during which weaned calves are fed to slaughter weight in confinement, with the potential for a backgrounding stage of varying length on pasture and/or in confinement between the cow-calf and finishing stages (Pogue et al., 2018).

Approximately, 82% of all beef operations in Manitoba are comprised of cow-calf operations (Statistics Canada, 2022b). These operations rely heavily on grazing as the primary feed source during the growing season, as well as in the late fall and winter. Manitoba, one of the three Prairie Provinces in Canada, is home to approximately 17425.5 km² of pasturelands (Census of Agriculture, 2016). These lands offer feed resources for the beef industry in Manitoba.

Due to its reliance on land and water resources, the beef industry has been under increased scrutiny regarding the associated environmental concerns. For example, eutrophication may occur if excess nutrients are exported from pasturelands to streams (Tunney et al., 2007). Assessments of the impacts of cattle grazing on water and nutrient dynamics in the Canadian Prairies are necessary to ensure environmental security; yet, such assessments are not readily available. Moreover, the impacts of climate change should also be included in assessments, given that the responses in pasture yield (Dellar et al., 2018), runoff generation (Escanilla-Minchel et al. 2020; He et al., 2023), and nutrient export (Soana et al., 2023) are expected to be influenced under climate change.

Fertilizer, agricultural by-products (manure), soil, and crop residues have been identified as the sources of nutrient that contribute to eutrophication (Bourke et al., 2008). Quantifying the nutrient content in these pools, as well as the hydrological processes driving the export of nutrient from these pools in pasturelands, can be achieved by modelling. This is convenient, robust, and practical strategy to simulate the interactive and dynamic processes among components at various spatial scales (Nemec, 1993). To assess the impact of climate change on pasturelands, it is also necessary to simulate the hydrological processes because nutrient redistribution and export are driven by water movement (Gordon et al., 1992; Schlesinger, 1997).

The objective of this study was to implement a modelling framework that consisted of integrating a farm model, a hydrological model, and a water quality model to evaluate the impact of climate change on nutrient export from pasturelands utilized for cattle grazing. This thesis is divided into seven chapters. The first chapter introduces an overall concern (i.e., eutrophication) associated with cattle grazing that needs to be assessed, and proposes the modelling framework approach to assess the problem. The second chapter provides a literature review of the nutrient dynamics in the vegetation, soil, and manure pools, as well as the pathways of nutrient export, followed by a brief overview of modelling options with their capabilities. The next three chapters follow a manuscript-style format, with chapter three focusing on predicting the pasture yield, manure production, manure nutrients, and nutrients contained in crop residues within a pasture-dominated ungauged watershed under a changing climate scenario. Chapter four aims to simulate the impacts of climate change on hydrological processes, with emphasis on stream discharge, while chapter five investigates the changes in nutrient exports under climate change. The last two chapters summarize the simulation results of all three models, and provide some recommendations for future research.

CHAPTER 2: LITERATURE REVIEW

2.1. Background

According to the Food and Agriculture Organization of the United Nations (FAO), global beef consumption per capita dropped 4.16% from 9.37 kg/year in 2000 to 8.98 kg/year in 2020 (FAO, 2023). Nonetheless, beef consumption has a positive correlation with the gross domestic product per capita (GDP) of a country. High-income countries, including Australia, European countries and North America, consumed 21kg of beef per capita in 2020, followed by upper-middle-income countries, lower-middle-income countries, and low-income countries (i.e., 11, 3.87, and 3.76 kg, respectively; FAO, 2023). Beef consumption has several nutritional benefits including high density of protein, trace minerals, and vitamins (Li, 2017). To meet both domestic and international demand for beef, Canada produced 1.16 million tonnes of beef between 2010 and 2021, 38.5% of which was exported (Statistics Canada, 2022a). Between 2020 and 2022, \$10.4 billion was generated annually by the cattle sector (Canadian Cattlemen’s Association, 2023), highlighting the importance of beef production from the perspective of economic growth. Pasture plays an important role during the cow-calf and the backgrounding phase due to the reliance on grazing (Fig. 2.1; Government of Manitoba, n.d.).

Despite its importance from a nutritional and economic perspectives, the beef industry in Canada has been under increased scrutiny due to the environmental impacts associated with cattle grazing, such as greenhouse gas (GHG) and ammonia emission (Canadian Cattlemen’s Association, n.d.), land degradation and water consumption (Pulido et al., 2018), and nonpoint source pollution (Hubbard et al., 2004). Among these concerns, excessive nutrient export from pasturelands that can lead to eutrophication in downstream aquatic environments has been identified as a concern. These nutrient issues are critical for Manitoba, as the province

reportedly had 17425.5 km² of pasturelands in 2016, accounting for 9% of all pasturelands in Canada (Census of Agriculture, 2016). In addition, Manitoba has a high proportion of cow-calf operations (i.e., 81.6% of all beef operations in the province; Statistics Canada, 2022b), which rely heavily on grasslands as a feed source during the growing season, as well as in fall/early winter. In order to ensure the sustainability of beef production in the province, it is necessary to assess nutrient cycling on pasturelands, and the associated impact on downstream water bodies caused by nutrient export.

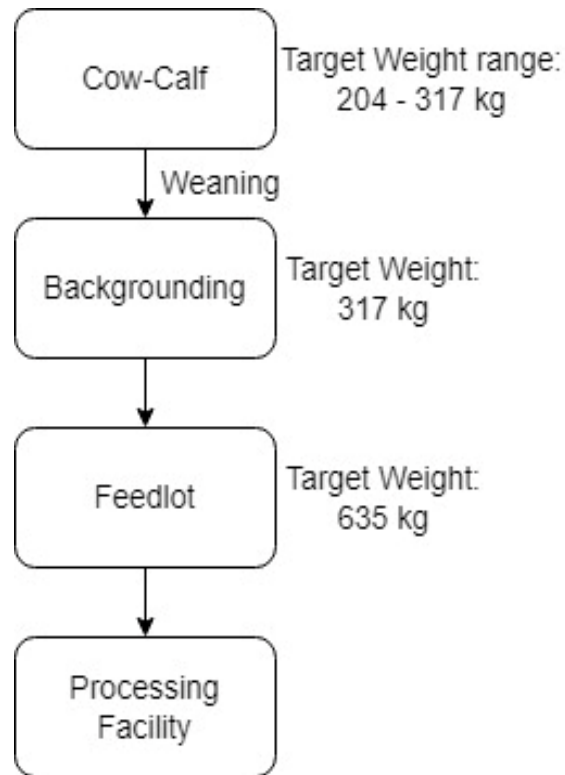


Figure 2.1: Typical stages in beef production systems in Canada (Hoar and Angelos, n.d.).

Nutrient cycle in pasturelands includes the movement of carbon (C), nitrogen (N), phosphorus (P), and other secondary nutrients including calcium, magnesium and sulfur (Bellows, 2001) generated by physical processes in soils, vegetation, and livestock (Beetz, 2002). As a result of the interaction among those nutrient pools, it is essential to examine nutrient losses that could

lead to a reduction in soil quality (Tan et al., 2005), pasture quality and yield (Moore et al., 2019), and nutritional quality of beef (Revilla et al., 2021), as well as causing negative impacts to downstream environments. Because the components of the nutrient cycle are interconnected, developing a holistic approach that encompasses all undergoing processes characterizing nutrient dynamics is important but also challenging.

Hydrology influences nutrient cycling by facilitating nutrient redistribution on pasturelands because nutrients move with water (Ide et al., 2019). Typically, the hydrological cycle on pasturelands is governed by major processes including precipitation, surface runoff, subsurface drainage, infiltration, evapotranspiration, and water storage (Lastoria, 2008). However, snow-related processes such as infiltration through unsaturated frozen soil layers, blowing snow, snowmelt, snow sublimation, snow interception, and the formation of ice layers must be considered when assessing the hydrology of cold regions like the Prairies (Pomeroy et al., 2007). In particular, Glozier et al. (2006) reported that 70% of annual runoff and nutrient losses from a watershed located in Manitoba were attributed to snowmelt runoff in spring, highlighting the importance of accounting for hydrology when conducting nutrient loss analyses.

2.2. Nutrient Pools on Pasturelands

Integrated crop-livestock production systems use crop or pastures to serve as fodder for ruminants, as well as excreta (i.e., urine and manure) as fertilizers to improve soil fertility, thereby benefiting the crop or pasture growth in the next growing season (Fig. 2.2; FAO, 2001). This forms a cycle in which nutrients are recycled through three major pools: vegetation, soil, and livestock. Approximately 10%-30% of the nutrients from ingested foods are absorbed by the ruminants, whereas the rest are excreted and returned to the land (Silveira et al., 2019; Herrero et al., 2009). The absorbed nutrients are exported as meat and milk and therefore do not contribute

to eutrophication. To quantify the nutrient losses that contribute to eutrophication, it is vital to know the concentrations of N and P in the vegetation, soil, and livestock pools respectively, as well as the pathways and processes that govern nutrient movement.

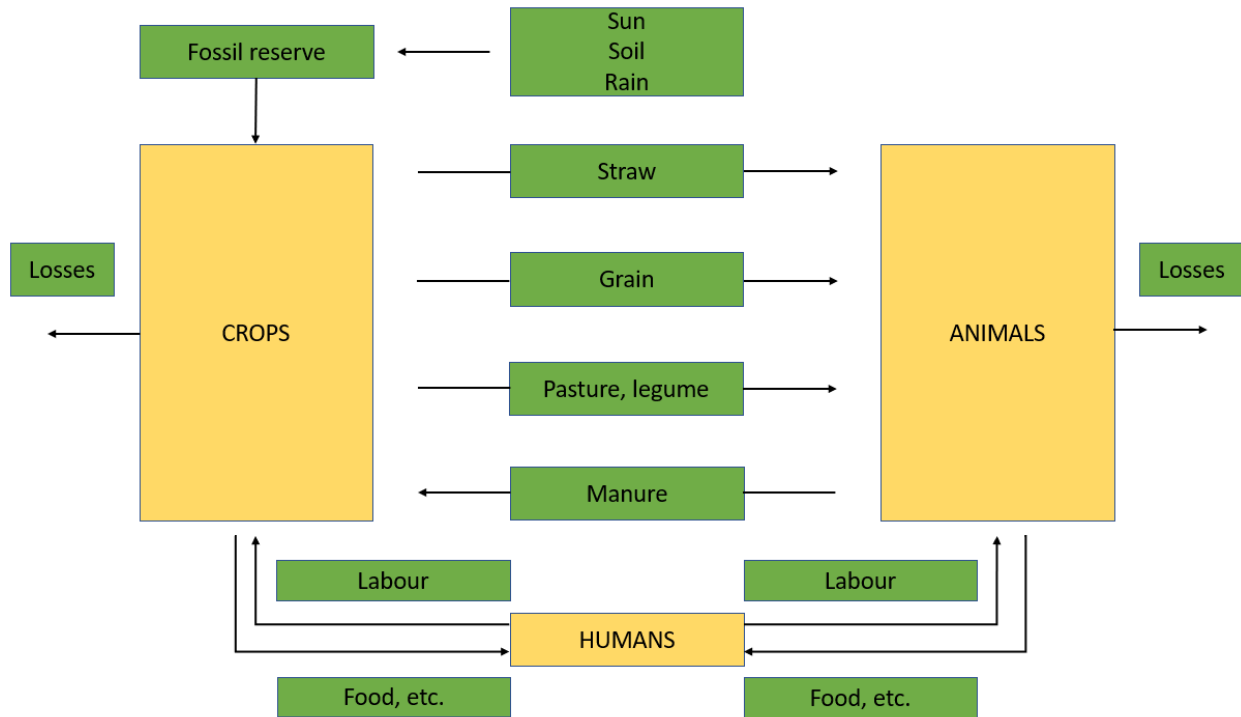


Figure 2.2: Description of an integrated farming system (adapted from FAO, 2001)

2.2.1. Nutrient Pools

2.2.1.1. Vegetation

In cold regions like the Prairies, forage residues that are not harvested and remain following grazing are the primary source of nutrients in the vegetation pool (Costa et al., 2019). These plant residues, both above-ground (i.e., stubbles) and underground biomass (i.e., shoots and roots), are left behind throughout the winter and will undergo multiple freeze-thaw cycles (FTC) depending on the local weather. By definition, an FTC describes the phenomena of water transformation between different states, which occurs when the ambient temperature drops below the freezing point, and then warms up enough to allow defrosting (Zeinali et al., 2020). During

FTC, moisture inside the plant residues undergoes several phase changes (i.e., liquid to solid during freezing, and solid to liquid during thawing). The formation of ice ruptures the plant tissues, and the nutrients contained therein are released in dissolved form when thawing occurs (Roberson et al., 2007). Nutrient release (i.e., forage quality x remaining crop residue) is dictated by various factors, such as plant species (Roberson et al., 2007; Øgaard, 2015), stage of plant development (Roberson et al., 2007), residue composition (i.e., different plant parts; Liu et al., 2013a), local weather condition (Øgaard, 2015), and the number of FTC (Costa et al., 2019; Øgaard, 2015).

A study conducted De Baets et al. (2011), reported the roots of certain annual crops are less cold resilient than those of perennial ryegrass, leading to a greater probability of rupturing during FTCs. Roberson et al. (2007) compared the P concentrations in alfalfa (*Medicago sativa*) and quackgrass (*Agropyron repens*) samples, which are both perennials, observed that the total soluble P in alfalfa ranged from 10 to 264 mg kg⁻¹ of fresh tissue, equivalent to 3% of total P, while the average P in quackgrass was 100 mg kg⁻¹ of fresh tissue (2.67% of total P). Moreover, extraction was performed after air drying the fresh samples at 60°C for 48 hours, and the total soluble P contents roughly increased 13.5 and 21 fold in alfalfa and quackgrass respectively, implying the quackgrass contains a higher P potential than alfalfa.

Numerous studies had shown that the number of FTC also has a substantial effect on nutrient release from plants (Kreyling et al., 2010; Liu et al., 2013a; Cober et al., 2018). Costa et al. (2019) investigated the concentration and cumulative load of nutrients released under various scenarios, including snow alone, a mixture of snow and alfalfa crop residues, and mixtures of deionized water and alfalfa crop residues. They discovered that after five FTC, crop residues released 0.29 (nitrate, NO₃) to 9 (phosphate, PO₄) times more nutrients than those in the snow-

only scenario, indicating that crop residues were responsible for a higher proportion of nutrient compared to snow, primarily during snowmelt events. In a separate study, four continuous or discontinuous FTC resulted in the greatest release of P from multiple catch crops (i.e., crops that grow between two main crops to improve soil conditions; Freyer et al. 2023) compared to a single FTC or no freezing (Liu et al., 2013a). Also, the experimental results produced by Bechmann et al. (2005) also revealed that after repeated FTC, the biomass of annual ryegrass released much higher level of water-extractable P (9.7 mg/L) than those from bare soils (0.14 mg/L) and dairy manure (0.18 mg/L) during simulated snowmelt runoff, implying the vegetation pool has a dominant contribution on nutrient export over the other two pools. In summary, these results indicate that: (1) plant tissues are ruptured and inter- and intracellular solutes are released during FTC; and (2) the more FTC events, the greater the nutrient release, with no further release once the available solutes are depleted.

2.2.1.2. Manure

Nutrients released by ruminant livestock in the form of excreta account for 70 – 90% of the total intake returning to the soil (Williams and Haynes, 1990). Cattle in Canada generated 134,896 thousand of tonnes of manure (i.e., urine and feces) in 2006, accounting for 74.5% of total domestic manure production in Canada (Hofmann, 2008). Compared to swine (1-4 kg/day) and poultry (<1 kg/day), cattle produce between 12 kg (calves) and 62 kg (lactating cows) of fresh weight manure per day (Statistics Canada, 2006).

In general, N excreted in manure can be categorized as organic and inorganic. Although organic-N is not utilized by plants, it can nonetheless contribute to nutrient losses via soil erosion (Chastain and Camberato, 2004). Additionally, soil microorganisms can decompose organic-N

into ammonium, a slow process commonly known as mineralization (Ketterings et al., 2005). In contrast, inorganic N can be utilized by plants instantly upon deposition in the forms of ammonium-N and nitrate-N. Manure N is typically reported levels of organic-N, total-N and ammonium-N since: (1) the amount of nitrate-N in manure is negligible (Government of Manitoba, 2009), and (2) values of ammonium-N often include ammonia-N given the conversion between ammonium and ammonia occurs at pH greater than 8.5 (Clean Water Team, 2004) which is the pH of fresh cow manure (Irshad et al., 2013).

Similar to N, P exists in both organic and inorganic forms, in which inorganic-P (i.e., phosphate) can be generated by the mineralization of organic-P (Rawal et al., 2022). As per research findings by Ajiboye et al. (2004), inorganic-P accounted for 50% in fresh beef manure.

Overall, the broad range of concentrations associated with the nutrients presented in Table 2.1 and 2.2 demonstrated the difficulties when estimating the composition of beef cattle manure. Nutrient concentration of the manure is dependent on diet composition, moisture content of the manure, digestibility of the feeds, environment, and stage of growth (Van Horn, 1997; Lorimor and Powers, 2004). Generally, excreted-N is split almost evenly between urine and feces, whereas excreted-P is primarily from feces (Lorimor and Powers, 2004).

Nutrients loss also varies depending on the timing of manure application. In a laboratory setting, Williams et al. (2011) found that manure that is covered by snowpack, which suggests the manure was applied prior to snowfall, had greater losses and higher concentrations of total N and P in runoff compared to other timings (e.g., during snowfall, after snowfall). This is relevant for grazing operation where manure is deposited and remains on the ground.

Table 2.1: Ranges of N intake and excretion by beef cattle (adapted from Pagliari et al., 2020)

Reference	Farm type, region	Average N input (g/head/d)	Study subject and time frame	Average N excreted (g/head/d)	Feces-N (g/head/d)	Urine-N (g/head/d)
Bernier et al. (2014)	Beef, Canada	122 (low quality forage with supplements)	24 animals, 5mo	104	54	50
Cole and Todd (2009)	Beef, TX, USA	165 (various diets)	>1000 animals, 1 yr	141	50.9	90.5
Gandra et al. (2011)	Beef, Brazil	217 (corn silage and concentrates)	30 animals, 21 d	100	58	42
Hünerberg et al. (2013)	Growing beef, Canada	280 (diets with dried distiller grains)	16 animals, 21 d	235	85	149
Koenig and Beauchemin (2013)	Beef, Canada	166 (barley-based diets)	16 animals, 28 d	112	46	72
Koenig and Beauchemin (2018)	Beef, Canada	290 (finishing diets with tannins)	32 animals, 35 d	205	34	136
Luebbe et al. (2012)	Beef, TX, USA	232 (diets with wet distillers grain)	37 animals, 21 d	153	55	98
Nair et al. (2016)	Beef, Canada	248 (Canola-meal-based)	25 animals, 160 d	191	51	140
Spihs and Varel (2009)	Beef, NE, USA	201 (diets with corn wet distillers grains)	24 animals, 96 h	139	58	81
Zenobi et al. (2015)	Beef, Canada	281 (blended feed pellets)	25 animals, 160 d	209	78	131

Table 2.2: Ranges of P intake and excretion by beef cattle (adapted from Pagliari et al., 2020)

Reference	Farm type, region	Average P input (g/head/d)	Study subject and time frame	Average P excreted (g/head/d)	Feces-P (g/head/d)	Urine-P (g/head/d)
Bernier et al. (2014)	Beef, Canada	17.9 (low quality forage with supplements)	24 animals, 5mo	22.2	18.3	3.9
Cole and Todd (2009)	Beef, TX, USA	28.9 (various diets)	>1000 animals, 1 yr	23.1	14.5	8.6
Geisert et al. (2010)	Beef, NE, USA	28.6 (diets with different P contents)	5 animals, 21 d	17.2	15.5	3.0
Souza et al. (2016)	Beef, Brazil	31.4 (high grain diets)	50 animals, 116 d	18.3	17.2	1.2
Spiehs and Varel (2009)	Beef, NE, USA	31.1 (diets with corn wet distillers grains)	24 animals, 96 h	19.8	10.9	8.9
Zanetti et al. (2017)	Beef, Brazil	13.0 (diets with different P contents)	28 animals, 63 d	8.4	8.2	0.2

2.2.1.3. Soil

It is difficult to quantify the relative contribution of soil to the overall nutrient export because the soil pool receives inputs from manure, decomposition of vegetations (above and below ground), biological fixation, and atmospheric deposition (Drury et al., 2007). As the vegetation and manure pools are addressed in sections 2.2.1.1 and 2.2.1.2 respectively, atmospheric deposition, and the impact of land management on the soil pool will be discussed here.

According to the World Meteorological Organization (2019), there are two types of atmospheric deposition: dry and wet. Dry deposition refers to the settling process of particulate matter from the atmosphere, which is a dynamic process readily transported by wind and precipitation. It is challenging to measure these dry fluxes which could vary spatially, temporally, and under different weather conditions (Freedman, 1995). More importantly, the spreading and accumulation of particulate matter depend on the distance travelled from the sources of emissions, as they are mostly by-products of industrialization (e.g., pollutants) and human activities (Osada et al., 2014). This makes the estimation of dry fluxes more of a regional assessment, and as such, databases of dry deposition records are not readily available in Canada due to the frequent movement of small particle, resulting in substantial variability (Chambers et al., 2001). Nitrogen- and phosphorous-containing substances also enter the nutrient cycle as inputs through wet deposition, such as rainfall, snowfall, and fog. Monitoring wet fluxes can be achieved by nutrient extraction from collected precipitation. For example, the Canadian Air and Precipitation Monitoring Network (CAPMoN) operated by Environment and Climate Change Canada (2020) produced wet deposition maps from 1981-2016 that recorded nitrate, sulfate, and ammonium levels in precipitation. Chambers et al. (2001) found the long-term average of P loading from both dry and wet depositions ranged from 0.01 – 0.74 kg/ha/yr across Canada, and Manitoba reportedly received between 0.8 and 3.4 kg N/ha/yr from precipitation during the 1990s. On the other hand, Köchy and Wilson (2001) reported that 22 kg N/ha/yr deposited at Elk Island in Manitoba from 1994 to 1996, reinforcing the significant spatial and temporal variability in measurements.

Management practices, such as importing nutrients as fertilizers to support plant growth (Silveira et al., 2019), reducing the total P loss in the surface soils by soil inversion (Josan et al.,

2019), and managing the grazing operation (e.g., herd size, duration, and grazing method), all can impact the nutrient dynamics of the soil pool. Decisions in grazing management, on the other hand, can also impact the nutrient cycle by altering the soil structure. As summarized by Roesch et al. (2019) and Man et al. (2022), soil compaction and aggregate disintegration caused by livestock trampling can change soil properties, including particle diameter and pore size distribution, leading to a reduction of water infiltrability into soil and a higher risk of surface runoff and soil erosion. Similar effects were observed by Leuther and Schlüter (2021) when soils were subjected to FTC. Those authors found that the soil porosity and connectivity diminished following the expansion and shrinkage of soil moisture volume. Unarguably, it is inevitable to encounter soil compaction during grazing operations (Houlbrooke and Laurenson, 2013), but its impact can be mitigated by executing the proper management decisions (Hamza and Anderson, 2005). For example, soil moisture can serve as an indicator in spring to determine when to begin grazing, since the trafficability of soil is inversely correlated with the soil moisture. In other words, the soil structure would be impaired if grazing took place while soil moisture levels exceeded the lower plastic limit that could cause a disruption in soil cohesiveness (Müller et al., 2011). Other strategies, like implementing rotational grazing, not only make optimal use of available resources, but also promote sustainability by minimizing soil disturbance and compaction, lowering greenhouse gas emissions, and enhancing water infiltration (Baronti et al., 2022). From the standpoint of nutrient management and optimal usage of feed resources, rotational grazing is advantageous as it facilitates nutrient recycling by avoiding ungrazed or poorly grazed fields, which could lead to a significant amount of underutilized crop residue in a specific area (Eldridge, 2004).

2.2.2. Pathways of Nutrient Losses

While approximately 70-90% of the intake would be excreted and returned to the land as manure (Williams and Haynes, 1990), not all of the nutrients are recycled as fertilizers. As outputs of the nutrient cycle, nutrient losses can take place in various pathways. The pathways of N loss include volatilization, nitrification, denitrification, leaching, erosion and runoff (Ward 2008; Government of Alberta, 2009), whereas P loss can only occur through leaching, erosion and runoff in particulate or soluble form because P does not exist in gaseous form (Prasad and Chakraborty, 2019).

Both volatilization and denitrification cause N loss in gaseous form. Volatilization refers to the loss of ammonium-N due to the conversion of ammonium to ammonia gas when the pH exceeds 5.5 (Jones et al., 2013). With manure is directly deposited on the land, the quantity of conversion are positively correlated with soil moisture, soil pH, temperature and wind condition (Johnson et al., 2005). Additionally, loss through volatilization is affected by land management, since 65% of the ammonium-N can be retained by the soil if incorporation (i.e., by tillage) is performed within a day following manure application. Denitrification, on the other hand, it is the process by which nitrate is reduced by soil microorganisms in anaerobic soils, typically when soils are saturated, or have significant microbial activity under favorable soil pH (Prairie Province's Committee, 2004; Wang et al., 2019). As a result, nitrate-N is eventually lost to the atmosphere in the forms of nitric oxide, nitrous oxide and dinitrogen gas (Johnson et al., 2005).

Nutrient loss in particulate or dissolved form are facilitated by water flow which is governed by soil texture and local weather conditions. For instance, in the presence of water, lands with coarser soil are more susceptible to solutes leaching (e.g., nitrate and dissolved P) because they are highly soluble in water, allowing them to be easily transported through soils via downward

water movement (i.e., infiltration and percolation; Prairie Province's Committee, 2004). The last major pathway, erosion and runoff, is often triggered due to high intensity rainfall events or during snowmelt periods, resulting in overland flow either when soils are saturated, or the water infiltration rate exceeds the soil absorption rate (Oschner, 2019). If there is no manure collection during grazing, manure nutrients in dissolved form seep downward through soil layers, whereas the rest remain on the surface layer, leaving them vulnerable to erosion and runoff loss during the subsequent spring snowmelt. During annual snowmelt runoff of the South Tobacco watershed in Manitoba from 1993 to 2010, 91% of TN and 73% of TP were in dissolved form, confirming that nutrients in dissolved form are the leading causes of eutrophication (Liu et al., 2013b). Moreover, the total water volume of runoff always exceeds that of leachate in simulated snowmelt events due to restricted permeability of frozen soil layers (Williams et al., 2011), except when the temperature of the topsoil layer is around 15°C (Williams et al., 2012), which rarely occurs in the spring snowmelt period. This implies the dominant role of runoff among other pathways that export nutrients.

2.3. Modelling

Although nutrient load and concentration can be measured by sample collections, concentrations can be highly variable depending on the time and location of sampling. The nature of discontinuous measurements renders it less likely that fluctuations that occur between sampling times will be captured, due to changes in vegetation status, hydrological response due to climate, and land management. Hence, using sampling and sequent laboratory analysis is challenging to quantify the relative contribution of each pool to the overall nutrient loss on pasturelands, given the dynamic interactions among vegetation, soil and animal waste, making

the measurement a composite value. It is also impractical to assess the nutrient loss of a large scale area (e.g., farm, watershed) with field-monitoring method due to cost.

Computer modelling, on the other hand, has been implemented in many fields due to its robustness, cost-effectiveness, convenience, and efficiency (Atwell et al., 2016). Computer modelling has also benefited from continuous hardware and software development in recent decades (Noll and Henkel, 2020). Modelling is used to perform simulations under defined conditions as a simplified representation of real-life scenarios, with the objective of having the simulation outputs eventually approach reality (i.e., measured data; Devia et al., 2015; Spence et al., 2022). Models that are well-defined, calibrated, and validated are beneficial to stakeholders to provide an estimate of outputs so that preventive measures can be taken. In this study, a farm model was selected for the estimation of potential nutrient loss from each pool, a hydrological model was chosen to forecast hydrological responses (e.g., surface runoff, subsurface runoff, and stream discharge) over time, and a water quality model was used to estimate nutrient export from each of the nutrient pools.

2.3.1. Farm Model

The Integrated Farm System Model (IFSM) is a process-based whole-farm model developed by Rotz (2004). Comprehensive evaluation and comparison of farm management can be achieved by allowing users to customize the operations of a virtual farm via model parameterization. The following modules are available in IFSM: crop and soil, grazing, machinery, tillage and planting, harvest information, storage management for harvested crops, herd and feeding, manure storage, and economics (Rotz et al., 2022). IFSM can assess nutrient flow by simulating forage yields and quality, manure production, and nutrient loss in different pathways while incorporating different management practices. For example, the forage growth

can be simulated using IFSM to estimate the dry matter (DM) and neutral detergent fiber (NDF), which are functions of daily mean temperature, crop stage, and species (i.e., warm-season grass and cool-season grass) with different coefficients (Rotz et al., 2022).

Howe et al. (2011) used IFSM to determine the phosphorus imbalances in three dairy farms in Vermont: one grass-based organic farm, one full confinement farm, and one mixed system with confined dairy cows and grazed heifers. Phosphorus surplus from these three farms ranged from 5.5– 18.7 kg/ha. Despite the wide range of P surplus under different management scenarios, simulation results indicated that P surplus in each farm was commonly contributed: (1) excessive use of supplements in the diet, (2) low forage yield, and (3) poor feed utilization efficiency (Howe et al., 2011). This study is an example of how IFSM can be used to help farmers identify the sources of pollution, so corresponding remediation strategies can be applied. This technique is beneficial for both farmers and the environment by mitigating the nutrient buildup while ensuring yield.

The use of IFSM is not restricted to monoculture, simulation of mixture of species is also feasible. Jégo et al. (2015) predicted the yield and the NDF content of alfalfa and timothy alone and in mixtures for various locations in Canada. The mean errors of DM yields for alfalfa and timothy were 0.27 and 0.15 tonnes DM/ha, with a Nash-Sutcliffe efficiency (NSE) of 0.51 and 0.85, respectively, suggesting a good performance of IFSM in simulating yields. On the other hand, the NDF contents in both species were underestimated (NSE for alfalfa: -0.35; NSE for timothy: -1.35). For the timothy-alfalfa mixture, the simulated annual DM yield and NDF content were $\pm 18\%$ and $\pm 15\%$ of the measured values. Although model performance was acceptable overall, the negative NSE values of NDF highlighted the need of model improvement, or a better model representation. It was pointed out that IFSM did not model weed growth, which

could partially contribute to the harvested biomass in the second and the third cut (Jégo et al., 2015).

To provide a baseline assessment for the environmental impacts of beef cattle production in the United States, Rotz et al. (2019) used IFSM to simulate different combinations of beef production phases, including cow-calf, cow-calf and backgrounding, and cow-calf to finishing. The results showed that: (1) ammonia loss were higher with warmer temperatures, which aligned with the findings by Huang and Shang (2006); (2) the total reactive N loss at a national scale was 1476 Gg per year for the simulation period from 2013 to 2017, primarily contributed by ammonia release (939 Gg per year); (3) ammonia loss from grazing cattle comprised half of 939 Gg, and the other half was by cattle in confinement (backgrounding and feedlot); (4) more nitrate loss was observed in wetter climate regions due to greater amount of leaching and runoff. Caution should be used when implementing IFSM for the Canadian Prairies, given that the climate in the Prairies is colder than the United States, and IFSM included all precipitation as rainfall, which would lead to misrepresentation for cold climate regions.

Besides assessment of existing farms, IFSM can also be implemented to assess risk of operations before construction. In the early stage of a construction plan for expanding the daily manure storage capacity of a Pennsylvania dairy farm, Duncan et al. (2017) evaluated two manure application methods (i.e., broadcast and injection), and found injection is a better approach as the ammonia loss via volatilization was reduced by 87.5%. Being able to compare outcomes in different scenarios, greatly assists farmers in their decision-making regarding best practices.

2.3.2. Hydrological Models

Hydrological models can simulate the underlying hydrological processes within a watershed, so that the influence of hydrology on nutrient loss can be assessed, particularly focusing on N and P loss through runoff. Rainfall-runoff models are always used in hydrological studies related to runoff simulation (Watson et al., 2022). These models can be grouped into three categories: empirical, conceptual, and physical-based (Dwarakish and Ganasri, 2015). As summarized by Sitterson et al. (2017), empirical models establish a non-linear relationship between input (e.g., precipitation, temperature, evaporation) and output data, in which the predictions could be impacted by overlooking other relevant factors, such as physiographic characteristics of watersheds (e.g., area, slope, elevation, drainage condition, aspect, altitude, land use, soil properties), antecedent moisture content, and climate change. Conceptual models generalize the complicated hydrological processes with simplified mathematical equations. Due to generalization, models may not be representative of the study area, which could lead to inadequate predictions (Bouffard, 2014). Unlike conceptual models, physically-based models utilize physical laws to mimic the complex but more realistic hydrological processes. This makes physically-based models more popular for catchments with sufficient data available, since it accounts for spatial and temporal variability due to land characteristics (Sitterson et al., 2017). However, physically-based models that are well-configured, are still expected to have performance fluctuations when dealing with extreme conditions, different climates and geographic locations. That is due to the fact that physically-based models are built by integrating proven equations to form a structure, so unknowns can be solved sequentially through the structure (Martina and Todini, 2009). Hence, model performance could deviate if the governing equations are no longer applicable or sufficient to represent the designed scenarios.

The winter conditions of the Canadian Prairies can be characterized as cold, snowy, windy, and of long duration (Vickers et al., 2001). Under such conditions, models should be carefully chosen before conducting hydrological simulations. There are many hydrological models available, such as the Soil and Water Assessment Tool (SWAT; Arnold et al., 1998), the Variable Infiltration Capacity model (VIC; Cherkauer et al., 2003), the Arctic Hydrological and Thermal Process Model (ARHYTHM; Zhang et al., 2000), the Hydrological Predictions for the Environment (HYPE; Lindström et al., 2010) model, the Cold Regions Hydrological Model (CRHM; Pomeroy et al., 2007), and HYDRUS (Šimůnek et al., 2012). Because each model has characteristics and strengths that other models might not possess, researchers should base the model selection process on the model that best represents the interactions of hydrological activities within the region of interest.

Among these models, CRHM stands out with its capacity to simulate most physically-based processes relevant to the Prairies, or in general for cold regions (Pomeroy et al., 2007). CRHM was designed to operate using hydrological response units (HRUs), which are the smallest spatial units within a watershed that are defined by the homogeneous properties of slope, soil and land use (Fang et al., 2010). CRHM users can either modify the built-in example projects to fit their watershed, or build their own models by selecting the appropriate modules to simulate specific hydrological processes, such as snowmelt (Mahmood et al., 2017).

CRHM has proven reliable when simulating hydrological processes in watersheds located in various geographic regions with distinct physiographic characteristics (Cordeiro et al., 2017). For example, the spatial variability was evaluated for a 0.33 km² alpine basin (i.e., Izas catchment) located in the Spanish Pyrenees (López-Moreno et al., 2013). The average values of simulated snowpack depth and snowpack duration were 1.71 meter and 188 days from 1996 to 2008, which

were 1.7% lower and 6.8% higher than the observations (i.e., 1.74 meter and 176 days), respectively. Different commencement timings of thawing in HRUs with different sun-exposed slopes were captured, with thawing occurred the latest in a HRU that has a Northwest facing slope (López-Moreno et al., 2013). Despite the variable topography, flat terrain is predominately the landscape type in the Canadian Prairies due to the vast areas of grasslands. Spence et al. (2022) used CRHM to create seven regional models, where each model represented one of the seven classified basin types in the Prairies based on their physio-geographic characteristics, such as climate, geology, streamflow, topography, and land cover. Sensitivity analysis was conducted to determine the variation caused by climate effect, and the results suggested that the annual runoff volume would reduce by 40% with a 6°C warming and a 30% increase in precipitation in the western Prairies, whereas that of the eastern Prairies increased by 55%. This demonstrates the importance of spatiotemporal variability in hydrological analysis, which is a common reason associated with model uncertainties in large-domain hydrological models (Melsen et al., 2016; Ochoa-Rodriguez et al., 2015). Hence, modifying the parameters from these generalized models for a smaller basin at local scale can be considered.

Besides the effect of climate, CRHM is also able to capture hydrological response due to vegetation and soil change, or the combinations of these variations. With future climate projections, vegetation and soil properties are expected to change (e.g., shrub expansion, afforestation or deforestation, and soil porosity). As a result, hydrological responses are expected due to the combined effect of climate, vegetation, and soil properties. Rasouli et al. (2019) performed simulations for three catchments in Canada, and the simulation results suggested the individual effect of climate variation (e.g., temperature, precipitation) could be trivial to the hydrological sensitivity, but the combined effect could significantly amplify the output (i.e.,

hydrological response). However, significant individual variation does not necessarily imply a significant response overall because these parameters can offset each other (Rasouli et al., 2019). In another study, Cordeiro et al. (2022) tested the hydrological response within the La Salle River basin in Manitoba, by converting the land use of some areas from annual cropland to perennial forage. This conversion significantly lowered the surface runoff by 53%, increased the infiltration and annual ET by 66.7% and 34.5%, respectively; resulting in significant reduction in the cumulative annual stream discharge (36.5%) and the peak discharge rate (30%). These studies highlight the flexibility of CRHM in model construction and falsification (i.e., a procedure that selects the appropriate model representation; Palminteri et al., 2017), as well as its promising capability for use in western Canada by accounting for snow processes thereby ensuring a better model representation for watersheds in cold region.

The HYPE model, a dynamic and semi-distributed hydrological model developed by the Swedish Meteorological and Hydrological Institute (SMHI) is also very robust (Lindström et al., 2010) in hydrological simulation. HYPE is an integrated model that has been widely used to investigate water and nutrient fluxes at continental scale, such as in Sweden (S-HYPE; Arheimer et al., 2011), Europe (E-HYPE; Donnelly et al., 2013), India (India-HYPE; Pechlivanidis and Arheimer, 2015), the Baltic sea region (Balt-HYPE; Donnelly et al., 2011), and pan-arctic region (A-HYPE; Andersson et al., 2015) with simulation domains covering up to 23.3 million km² (Bajracharya, 2023). HYPE is a rainfall-runoff model that simulates water dynamics (i.e., runoff generation) with the “fill-and-spill” mechanism, in which water input (e.g., precipitation) would recharge the soil layers as storage, and convert to runoff after exceeding the storage capacity (Coles and McDonnell, 2018). HYPE can be applied to assess hydrology in cold regions, given that the model can handle formation of frozen soil and snowmelt (Lindström et al., 2010).

2.3.3. Water Quality Model

Several different models are available for simulating water quality dynamics those developed by: 1) Williams et al. (2011), which can estimate nutrient release from manure; 2) Costa et al. (2019) for predicting the rate of nutrient released from alfalfa residue; and 3) Roste (2015) for estimating N and P concentration at the edge of the field during snowmelt runoff events.

Alternatively, the Annual Phosphorous Loss Estimator (APLE) 3.0 developed by Vadas and Bolster (2022) is a user-friendly spreadsheet model that quantifies the annual edge-of-field P losses with the options of having different kinds of animal manure applied.

Although employing empirical models could achieve prediction by interpolation or extrapolation with acceptable performance, a process-based model is preferred as it encompasses the dynamic and sophisticated interactions among processes, and captures the spatial and temporal variation, which collectively guarantees a better model representation. For example, modification of existing CRHM modules (e.g., Prairie Blowing Snow, soil, and routing modules), and development of new modules enable CRHM models to simulate biogeochemical processes in cold regions (Costa et al., 2021). These adjustments focused on the water quality aspect that was not addressed in the previous version of CRHM, particularly on the concentration and transport of N and P. The predecessor of these recently added CRHM water quality modules, the winter nutrient field transport (WINTRA) model, was originally developed to estimate the edge-of-the-field nitrate concentration during snowmelt events (Costa et al., 2017). Building upon this, the new modules incorporate the WINTRA model with HYPE, allowing CRHM to simulate processes of nutrient transformation including nitrification, denitrification, dissolution, mineralization, degradation, and sorption-desorption equilibrium (Pomeroy et al., 2022), better capturing the response of nutrient dynamics due to seasonal variation in cold regions.

Furthermore, CRHM now takes management practices (e.g., manure/fertilizer application, tillage, plant residue) information into consideration, which provides greater flexibility to users when assessing the impact of different management strategies on nutrient export. Although integrating the underlying hydrological processes with biogeochemical processes leads to a more complicated model representation, it is more comprehensive and realistic. However, the newly added modules have not been fully-integrated, rendering the simulations at subbasin level unavailable at the present time.

Alternatively, HYPE can also perform simulations of nutrient dynamics. To perform water quality simulations in HYPE, users are required to supply input data such as climatological data, geographical data, land information (e.g., land use, soil texture, soil layers, and stream depth), and nutrient data (Lindström et al., 2010). Concentrations of inorganic (IN) and organic (ON) nitrogen and dissolved (SP) and particulate (PP) phosphorus in runoff are simulated by the model (Lindström et al., 2010). The change of nutrient concentration is driven by nutrient transport and transformation, which are governed by processes including erosion, denitrification, primary production, mineralization, sedimentation, and resuspension. HYPE uses attenuation factors as filters to estimate the nutrient concentration after soil retention. The inclusion of these processes makes simulations more realistic. Lindström et al. (2010) compared the simulation outputs with the observation values at a local scale for the Vindån basin in Sweden and found that the lake water level was well simulated with a R^2 of 0.95, followed by discharge rate, snow depth, and groundwater level (R^2 of 0.94, 0.92, and 0.9, respectively). The performance of total nitrogen (TN) content simulation was satisfactory (R^2 as 0.68), whereas further improvement was needed for total phosphorous (TP) prediction with a R^2 value of 0.41, which was persistently underestimated. This calibrated model was then applied at a regional scale for two different

rivers within the same basin in order to test the parameter transferability. Streamflow in two rivers, and the TP in one of the rivers were well-predicted. However, simulation performance of TN in the other river channel was poor. This showcases that despite the parameter transferability being feasible for regions with similar landscape characteristics, implementing such an approach for an ungauged basin still needs more work.

2.3.4. Effect of Climate Change

Climate change is real and human activities have been hastening this process (Stern and Kaufmann, 2014). When assessing nutrient loss from pasturelands to streams, the variation due to climate change must be considered. Changes in future climate will trigger chain reactions to other ecosystem components, ultimately affecting surface runoff, streamflow and the nutrients contained within (Fig. 2.3).

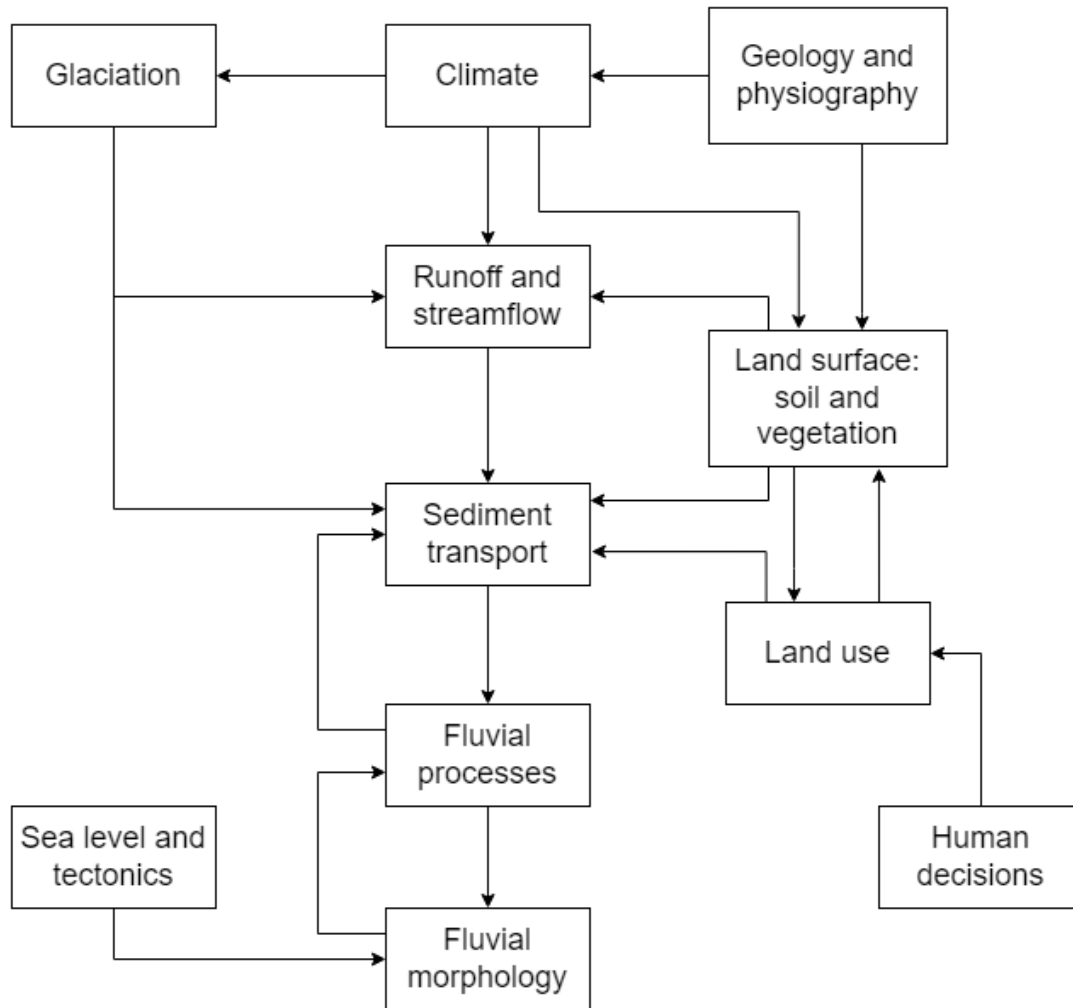


Figure 2.3: Influence of climate change on the ecosystem in cold regions (adapted from Ashmore and Church, 2001)

According to Ashmore and Church (2001), the temperature is expected to rise, resulting in more precipitation as warmer air has more capacity to hold water vapor (Yang et al., 2023). Such increases in precipitation, however, are expected in the form of rain rather than snow (Vogt et al., 2018). Both snow water equivalent (SWE) and duration of snow cover have declined by 5-10% across Canada from 1981 to 2015, and a 5-10% decadal reduction in SWE is anticipated by 2050 (Government of Canada, 2019). Fang and Pomeroy (2007) used CRHM to conduct a drought sensitivity analysis for the Bad Lake watershed in Saskatchewan, and they suggested that snowmelt runoff (or streamflow discharge) would be reduced, with less snowfall, a warmer

winter, and lower level of soil moisture content at the end of the previous growing season. This is critical for hydrological simulations and nutrient tracking in the Canadian Prairies because snowmelt is the major contributor to runoff during spring. Moreover, precipitation change could be partially offset or exacerbate the increase in evapotranspiration in warmer climates, leading to more variable runoff. Nonetheless, the amplification effect, a phenomenon in which runoff response could disproportionately increase with a minor change in precipitation, suggests less impact on wet areas because of the lower elasticity of runoff values in wet regions (Gong et al., 2022). In addition to the intensity and duration of individual precipitation events, Ashmore and Church (2021) also mentioned that the severity of flooding by rainfall is expected in small catchment and by snowmelt in larger catchments. These findings further reinforce the necessity of acknowledging the spatiotemporal variation in discussions of climate change impact on hydrological processes.

Given the fact that pasture yield is impacted by various factors, such as antecedent soil moisture, soil texture, water deficit, solar energy, species, and land management, it is very difficult to predict yield with a high confidence. Yet, studies unanimously suggested that the occurrence of drought will be more frequent (Vogt et al., 2018; van der Kamp et al., 2013), stating that increased precipitation would not compensate for increased annual mean temperature and evapotranspiration (Bonsal et al., 2011). With five general circulation model (GCM) scenarios inferring a warmer climate, Thorpe et al. (2008) predicted that grassland yield in the Canadian Prairies would not change substantially from 2040-2069. However, the impact of climate change on forage growth is uncertain due to weed, insect and crop disease perspectives. Weed growth has been found to increase as a response to the elevation of atmospheric CO₂ level (Ziska, 2003), implying a reduction of forage yield under a warmer climate due to weed

competition (Uddin and Kebraab, 2020). On the other hand, plant pests are favored by a warmer growing environment, which could lead to a lower forage production. In terms of forage quality, Dumont et al. (2015) discovered if atmospheric CO₂ level are elevated, the non-structural carbohydrates in forages would increase by 25% with an 8% drop in the nitrogen content.

CHAPTER 3: ASSESSING THE IMPACT OF CLIMATE CHANGE ON PASTURE YIELD AND CATTLE MANURE PRODUCTION IN MANITOBA USING THE INTEGRATED FARM SYSTEM MODEL

3.1 Abstract

Beef production relies heavily on the grasslands in the Canadian Prairies, which will inevitably face challenges induced by climate change. The objective of this study was to assess the impact of climate change on the availability of grassland in the region, aiming to help beef producers to formulate effective management strategies for adaptation. To this end, the Integrated Farm System Model (IFSM) was parameterized based on the physiographic characteristics of a 33.92 km² pastureland located in Manitoba. A baseline scenario was established by running the model with an observation dataset for the reference period (2000 – 2020). The evaluation of pasture yield predictions for the reference period indicated satisfactory model performance, with the percent bias ranging from -0.4% to 0.8%. The parameterized model was used to simulate grazing for near future (2020 – 2049) and distant future (2050 – 2079) periods using three climate models under two representative concentration pathways (RCP 4.5 and 8.5) of greenhouse gas emissions. The historical simulation yielded a pasture yield of 219.9 t dry matter (DM) km⁻². The predicted pasture yields under RCP 4.5 were 227.5 t DM km⁻² in the near future, and 217.9 t DM km⁻² in the distant future, where yields under RCP 8.5 were 215.1 and 205.4 t DM km⁻² for the near future and distant future periods, respectively. A lower pasture yield with increasing greenhouse gas emission intensity was predicted, predominantly attributable to the elevated ambient temperature and reduced precipitation in the growing seasons. The impact of climate change on manure production was negligible. Simulation of the distant future generated

the greatest discrepancy, which was only 0.39% lower than that of the reference period (13.15 kg DM day⁻¹ of cattle manure) under RCP 8.5.

3.2 Introduction

Beef is a valuable food source that provides enriched protein content, as well as other essential nutrients that humans require. According to the Organization for Economic Co-operation and Development (2022), beef consumption varies by country with Argentina having the highest annual beef consumption (39.3 kg/capita) from 2010 to 2022, followed by the United States, Brazil, Australia, Israel, Kazakhstan, and Canada (25.8, 25.5, 20.5, 21.1, 19.0, and 18.6 kg/capita, respectively). To meet the domestic and global demand for beef, Canada produced 1.16 million tonnes annually between 2010 and 2021, of which 38.5% were exported (Statistics Canada, 2022a). Between 2000 and 2022, the average revenue per year was \$10.4 billion, which contributed \$24 billion to Canadian GDP (Canadian Cattlemen's Association, 2023).

Beef production systems can be categorized into three stages: cow-calf, backgrounding, and finishing (Pogue et al., 2018). Herd sizes from 2010 to 2022 averaged roughly 9.9 million heads per year, with 68.6% of that (i.e., 6.8 million heads) belonging to cow-calf operations (Statistics Canada, 2022b). Because grazing is a common practice that utilizes pasture as the main feed source during the cow-calf stage, large tracts of pasture are needed. Grasslands comprise much of the pastureland with Canada possessing 185,600 km² of grasslands (i.e., tame and native pasture) in 2021, mostly concentrated in the Prairie provinces of Saskatchewan, Alberta, and Manitoba (44%, 36%, and 9%, respectively; Statistics Canada, 2022c).

Given the grassland sensitivity to climate variability (Wu et al., 2021), yield can be impacted by climate change. Harvrilla et al. (2022) predicted a 74% reduction in cool-season grasses in western United States in 2070 due to climate change, whilst warm-season grasses increase by

66%. This aligns with the simulation results by Thorpe et al. (2008), who suggested an increase in warm-season grasses for the Canadian Prairies by 2050, particularly for areas with coarse-textured soil.

Variation in grassland yield may affect current provincial policies. For example, the Manitoba Protein Advantage, a strategy that was proposed by the Government of Manitoba in 2019, aims to promote an increase in animal protein production by 35% through a 15% increase in pasture yield by 2025 (Manitoba Agriculture, 2019). However, to assess the viability of such policy, it is necessary to investigate the change in pasture yield under climate change scenarios.

Nutrient dynamics is another crucial factor potentially impacting the future of the Canadian beef industry due to increased scrutiny regarding environmental sustainability. One of the prominent concerns, eutrophication of downstream waterbodies, is attributed to the export of nitrogen (N) and phosphorus (P) to streams (Huang et al., 2017). Cattle manure has been identified as one of the major sources of nutrient release. Cattle reportedly produced nearly 135,000 thousand of tonnes of manure in 2006, accounting for two-thirds of the total domestic manure production (Hofmann, 2008). Depending on the diet composition, the manure N and P excretion can vary considerably, ranging from 100 to 235 g N head⁻¹ d⁻¹, and 8.4 to 23.1 g P head⁻¹ d⁻¹, respectively (Pagliari et al., 2020). Under the influence of climate change, it is necessary to predict the production of cattle manure, as well as the corresponding nutrient content.

Whole-farm modelling is a tool that has proven essential for predicting the environmental impacts. By examining the whole system, such as crop and livestock growth, fertilizer application, harvesting, nutrient cycling, and economics, process-based models are able to simulate farm operations in both the short- and long-term, and the results are often utilized to aid

the decision-making process (Schils et al., 2007; Del Prado et al., 2013; Ahmed et al., 2020). Whole-farm models are useful to assess the impact of climate change on agronomic performance and nutrient dynamics. There are several whole-farm models available, such as Decision Support System for Agrotechnology Transfer (DSSAT; Jones et al., 2003), Holos (Little et al., 2008), FarmDESIGN (Groot et al., 2012), Agricultural Production Systems sIMulator (APSIM; Holzworth et al., 2014), and the Integrated Farm System Model (IFSM; Rotz et al., 2022). Among them, IFSM has been used to investigate climate change effects in multiple locations across Canada. For example, the projected yield of alfalfa, timothy, and the mixture of both species were assessed and deemed to be lower in the Southwest region of the province of Quebec compared to the Eastern region (Thivierge et al., 2017). The same conclusion was drawn in a separate study by Payant et al. (2021), who also found the yields of four alfalfa-grass mixtures were lower in southwest region compared to the eastern region of Quebec. The yield discrepancy was attributed to the fact that east region will be generally colder than the southwest, so that cool-season grasses have a better chance not exceeding the optimal growth temperature than warm-season species under a warmer climate. Moreover, both studies predicted that the overall forage dry matter yield will increase, mainly due to the greater growing degree days (GDD) and longer growing seasons.

The objective of this study was to evaluate the impact of climate change on pasture yield and manure production in Manitoba using IFSM. Such an assessment is not readily available for western Canada. This assessment was conducted at the watershed scale and provides practical insights about the trend of the pasture growth and adaptability under temperature and water stress, especially for regions with similar landscape characteristics, management practices, and climate.

3.3 Materials and Methods

3.3.1. Physiography and Study Area Characteristics

Site selection was carried out with the following criteria in order to find a study area that is representative in Manitoba, including having the grassland cover proportion over 70%, a relatively large cattle grazing density, data availability for model calibration and validation, and a relatively large watershed area. As a result, the study area was located close to the town of St-Lazare in the southeast of Manitoba (50°23'36" N, 101°21'27" W), which is within the Beaver Creek watershed that drains into the Assiniboine river. The long-term (2000-2020) annual mean, maximum and minimum daily air temperature in the area was 2, 7, and -3°C, respectively, while the annual precipitation for the same period ranged from 320 to 750 mm with 200 mm of precipitation falling during the growing season (Birtle station; Manitoba Agriculture, 2022; Manitoba Agriculture, n.d.a.). The average heat accumulation was 1500 to 1550 GDD above 5°C (Manitoba Agriculture, n.d.a.). From the 30-m resolution digital elevation model (DEM) derived from the NASA Shuttle Radar Topography Mission (SRTM) data, the study area has a relatively flat topography with elevation and slopes ranging from 387 m to 487 m, and 2% to 5%, respectively (U.S. Geological Survey, 2014). According to the Association of Manitoba Community Pasture (AMCP), the plant diversity of this native mixed-grass region consists of 51% cool-season grasses, 27% warm-season grasses, 20% forbs, and 2% legumes. Porcupine-grass (*Hesperostipa spartea*) is the dominant grass species, followed by Western porcupine-grass (*Hesperostipa curtiseta*), and Blue grama (*Bouteloua gracilis*; Association of Manitoba Community Pasture, 2021). Loamy sand is the dominant soil type (95% area coverage) which consists of 8% silt, 6% clay, and 86% sand, followed by clay loam (Cordeiro et al., 2018). Pastureland was the dominant and cover in this area (72%), followed by forest (19%), farmlands

(8%), and other covers (i.e., barren, urban, and wetland; 1%; Agriculture and Agri-Food Canada, 2023).

The study site was simulated on a 33.92 km² pastureland area managed by the AMCP. The 10-year (2010 – 2019) average carrying capacity of the study area was approximately 2612 animal unit months (AUMs), or 77 AUMs km⁻² as the stocking rate (Association of Manitoba Community Pasture, 2021). With the animal unit equivalent (AUE) for cows ranging from 1.0 to 1.5 depending on animal weight, the herd size was calculated as 373 [Equation (3.1)]. Continuous grazing is practiced in the area between May and September with Black Angus as the major breed type of beef cattle in the area (Association of Manitoba Community Pasture, 2021).

$$\text{Herd size} = \frac{\text{AUM}}{\text{AUE} \times \text{Number of months}} \quad (3.1)$$

3.3.2 Datasets

3.3.2.1. Historical Climate Data

Model simulations were performed for three periods: reference (2000-2019), near future (2020-2049), and distant future (2050-2079; Thivierge et al., 2017). Daily meteorological data for the reference period were mainly obtained from the Birtle station from the Manitoba Agriculture Weather Program (50°24'39"N, 100°53'36"W; Manitoba Agriculture, 2022) between 2008 and 2019. Data obtained from other stations were used to fill any data gaps in the Birtle station. Hourly data from the ShoalLake CS station and the Rosburn 4 North station from 2000 to 2007 (50°27' N 100°36' W, and 50°45' N 100°49'12" W; Environment and Climate Change Canada, 2023a) were aggregated to a daily time step to fill this gap. Precipitation data from the Birtle station during the winter months prior to 2017 were replaced due to limitation of the

equipment to record solid precipitation (i.e., Tipping Bucket Rain Gauge). Solar radiation was only available from 2017 onwards; therefore, the Hargreaves and Samani model [Equation (3.2); Aladenola and Madramootoo, 2014] was used to model solar radiation data on a daily time step. Linear interpolation was used to fill small data gaps in the station records. Neither of the supplemental weather stations measured solar radiation.

$$R_s = K_{RS}(\sqrt{T_{max} - T_{min}})R_a \quad (3.2)$$

where K_{RS} , R_a , and R_s refer to an empirical coefficient, the extraterrestrial radiation ($\text{MJ m}^{-2} \text{ day}^{-1}$), and the solar radiation ($\text{MJ m}^{-2} \text{ day}^{-1}$), respectively. The daily value of R_s is dependent on the latitude of the location and the day of the year, and was calculated following the guidelines by Allen et al. (1998).

Another aspect related to solar energy, the GDD, is an index that quantifies the accumulative thermal energy that can be harnessed to facilitate plant growth (McMaster and Wilhelm, 1997). GDD on a daily basis was calculated by subtracting a predetermined base temperature from the daily mean air temperature. This study estimated the seasonal GDD for the growing seasons from April to September with a base temperature of $5\text{ }^\circ\text{C}$ (Manitoba Agriculture, n.d.).

Due to the absence of wind speed records for six consecutive months in the historical dataset in 2006, synthetic data was used to create a complete time series of data. Thus, the simulated pasture yield generated for year 2006 from the historical dataset was removed from the analysis. Table 3.1 summarizes the sources and methods used to arrive at a complete historical time series for the five weather variables required by IFSM.

Table 3.1: Sources of historical weather datasets with respective time steps and derivation method

Variable	Period	Sources (timestep)	Derivation Method
Temperature (Maximum, Mean, Minimum)	2000 – 2007	ShoalLake CS station (daily)	DR ¹
	2008 – 2019	Birtle station (hourly)	DA ²
Wind Speed	2000 – 2007	ShoalLake CS station (hourly)	DR, DA, SD ³
	2008 – 2019	Birtle station (hourly)	DA
Precipitation	2000 – 2007	ShoalLake CS and Rossburn 4 North stations (daily)	DR
	2008 – 2016 (non-winter months)	Birtle station (hourly)	DA
	2008 – 2016 (winter months)	ShoalLake CS and Rossburn 4 North stations (daily)	DR
	2017 – 2019	Birtle station (hourly)	DA
Solar Radiation	2000 – 2007	ShoalLake CS station (daily)	TR ⁵ , HS ⁵ , DA
	2008 – 2016	Birtle station (hourly)	DT ⁶ , HS, DA
	2017 – 2019	Birtle station (hourly)	DA

¹ DA = Data aggregation from hourly to a daily timestep; ² DR = Data were retrieved from nearby stations; ³ SD = Synthetic data from NASA Power database for Year 2006 (National Aeronautics and Space Administration. 2023); ⁴ TR = Maximum and minimum daily temperature retrieved from nearby stations; ⁵ HS = Hargreaves and Samani model; ⁶ DT = Determination of maximum and minimum temperature at a daily timestep from hourly data

3.3.2.2. Future Climate Data

Climate data for the near and distant future periods were retrieved for two Representative Concentration Pathways (RCP), which are a set of future scenarios that capture trends of climate change based on the land-use trajectory, and the emission and concentration of greenhouse gases in the atmosphere (van Vuuren et al., 2011). The stabilization scenario (RCP 4.5) and the high emission scenario (RCP 8.5) were examined to assess the impact of climate change on pasture

yield. Daily data were acquired from the North American component of the international Coordinated Regional Downscaling Experiment (NA-CORDEX; Mearns et al., 2017) database for three regional climate models (RCMs) driven by various global climate models (GCMs) from the Coupled Model Intercomparison Project Phase 5 (CMIP5; Taylor et al., 2012): CanESM2.CanRCM4, CanESM2.CRCM5-UQAM, and MPI-ESM-LR.CRCM5-UQAM. The typical scale of the GCM grids span approximately 100-km, whereas these GCMs-driven RCM projections have finer resolution with 25-km projected grid spacings (Mahoney et al., 2021). The inherent variability among climate models was considered by employing an ensemble approach, with three climate models used for each RCP. Such approach helps to capture the range of potential outcomes and reveal the underlying uncertainties associated with climate projections.

3.3.3. Integrated Farm System Model

The IFSM model (version 4.7; Rotz et al., 2022) was used to simulate pasture yield in this study. It is a whole-farm model that mimics the operations of an actual farm with nine major modules: crop and soil, grazing, machinery, tillage and planting, harvest, storage management for harvested crops, herd and feeding, manure handling, and economics. Parameterization of these process-based modules allows users to create customized operations throughout the simulation period. Since investigating the change in pasture yield under climate scenarios was the main focus of this study, the machinery, tillage and planting, harvesting, storage of harvested crops, manure handling, and economics were not parameterized. An input file containing meteorological variables at a daily time-step between 2000 and 2019 was prepared to force IFSM. These variables included incoming short wave radiation (MJ m^{-2}), mean temperature ($^{\circ}\text{C}$), maximum temperature ($^{\circ}\text{C}$), minimum temperature ($^{\circ}\text{C}$), precipitation (mm), and average wind speed (m s^{-1}).

IFSM simulates the process of photosynthesis which transforms light energy into photosynthates (e.g., carbohydrates; Johnson, 2016). Structural carbohydrates are associated with plant growth (i.e., root and shoot) whereas non-structural carbohydrates are utilized for plant metabolism (Slewinski, 2012). According to Rotz et al. (2022), these carbohydrates are allocated to two pools: storage and structure. The above-ground biomass, or dry matter (DM), is estimated in IFSM by multiplying the sum of carbohydrates in the storage and structure pools by 2.5, assuming 40% of the total DM are carbohydrates.

IFSM simulates the amount of manure generated by the herd, but the manure nutrient content is determined based on the user-defined pasture quality (i.e., N and P content). By default, IFSM automatically estimates external procurement of hay required to feed the livestock if needed in order to meet its nutritional demands. Equation (3.3) is used in this study, which estimates the N content in pasture biomass.

$$MN_p = N_t \times \frac{N_p \times C_p}{(N_p \times C_p + N_h \times C_h)} \quad (3.3)$$

where with N_p , N_h , N_t , C_p , C_h , and MN_p represent the N content in pasture (%), the N content in purchased hay (%), the total excreted N (kg), the grazed pasture (kg DM), the consumed hay (kg DM), and the manure N originating from pasture (kg), respectively. A similar calculation is applied for the estimation of manure P from pasture.

3.3.4. Assumptions

To construct a representative model that encapsulates the characteristics of the study area, a series of assumptions was incorporated into the model configuration. Firstly, the herd size was comprised of 373 lactating cows (i.e., Black Angus) with 20% first lactation cows, and they were placed on pasture for continuous grazing each year from May through September. Cow-calf pairs

were assumed to be grazed throughout the growing months, with source with no additional supplement offered. Other farming operations, including tillage, pasture harvesting and storage were not considered, resulting in minimal land management. Secondly, the simulation did not incorporate the collection and storage of manure. Instead, all excreted manure from beef cattle was directly deposited on the ground and left exposed. Thirdly, the pasture was solely dependent on rainfall for its water supply. The model did not consider irrigation or alternative water sources. In addition, IFSM did not account for temporal variation in pasture quality. Cattle have a tendency to be selective in their consumption, favoring plant parts with higher nutritional values (Meyer et al., 1957). Consequently, the values assigned to pasture quality were assumed to be constant during specific seasonal intervals: early spring (April and May), late spring (June), summer (July and August), early fall (September), and late fall and winter (October to next March), respectively. These values were obtained from a recent study that reported nutrient composition of clipped pasture east of Brandon, Manitoba (Appleyard, 2023).

3.3.5. Model Assessment

Evaluation of the model performance was conducted by comparing the simulated pasture yield with the data reported in the Manitoba Forage Benchmarking Project (Agriculture and Agri-Food Canada, 2019). This survey project collected forage DM yield data in four of the nine ecoregions and eight of the 21 ecosites in Manitoba between 2004 and 2009. The sampling protocol consisted of placing 1 m² cages in various locations across the province. In order to emulate realistic grazing scenarios, the forages samples were clipped twice a year (i.e., June and August). The yield data were classified by distinct vegetation types (e.g., Upland grassland, Transitional grassland, and Open woodland) and ecosites (e.g., Sandy Loam, Wet Meadow, and Shallow Marsh). Given the location of our study area, which is in the Aspen Parkland ecoregion

characterized by sandy loam as the dominant soil type, an average forage DM yield of 220.9 tonnes km⁻² was used in our study for model calibration. To assess the model performance, the percent bias (PBIAS) metrics was employed. Calculations of PBIAS was carried out according to Equation 3.4 by Wu et al. (1995).

$$PBIAS = \frac{\sum_{i=1}^n O_i - P_i}{\sum_{i=1}^n O_i} \times 100\% \quad (3.4)$$

where i as the i^{th} term, O stands for observations, and P as predictions.

The amount of manure excreted simulated by IFSM varies with breed, growth stage, health condition, feed consumption, and feed digestibility. Statistics Canada (2006) reported that cattle manure excretion ranges from 12 (for calves) to 62 (for lactating cows) kg each day on a wet basis. Despite the significant variation caused by variation in growth stage and the associated body mass, these values were utilized to verify the simulation of manure production by IFSM.

The Mann-Kendall test, a non-parametric test that has been widely employed to statistically examines the presence of a monotonic trend of time series data (Yue and Wang, 2004), was used in this study for climate projections of temperature and precipitation. The null hypothesis for the Mann-Kendall test was that there is no statistical significance in the temperature and precipitation trends in the future.

In addition, it was necessary to compare the simulations with the climate modelled data during the reference period against the observations, as well as the historical simulation. This analysis would elucidate the influence of climate modelled data on the model performance.

3.4 Results

3.4.1. Future Climate Trends

Analysis of the climate projections indicated a prevailing trend of increasing trend of increasing temperatures for both RCP 4.5 and RCP 8.5, which resulted in an increasing trend in heat unit accumulation (Fig. 3.1). The two-sided Mann-Kendall test provides evidence that this trend was statistically significant. Monotonically increasing trends ($p < 0.05$) in temperature were observed across the near future and distant future, as well as the entire simulation period spanning from 2000 to 2079. For the reference period under RCP 4.5, there was no evidence that the trend was significant. GDD also exhibited a significant tendency to increase ($p < 0.01$) in all simulation periods, as well as the overall simulation duration, with the exception of the GDD in the reference period under RCP 4.5 ($p = 0.38$).

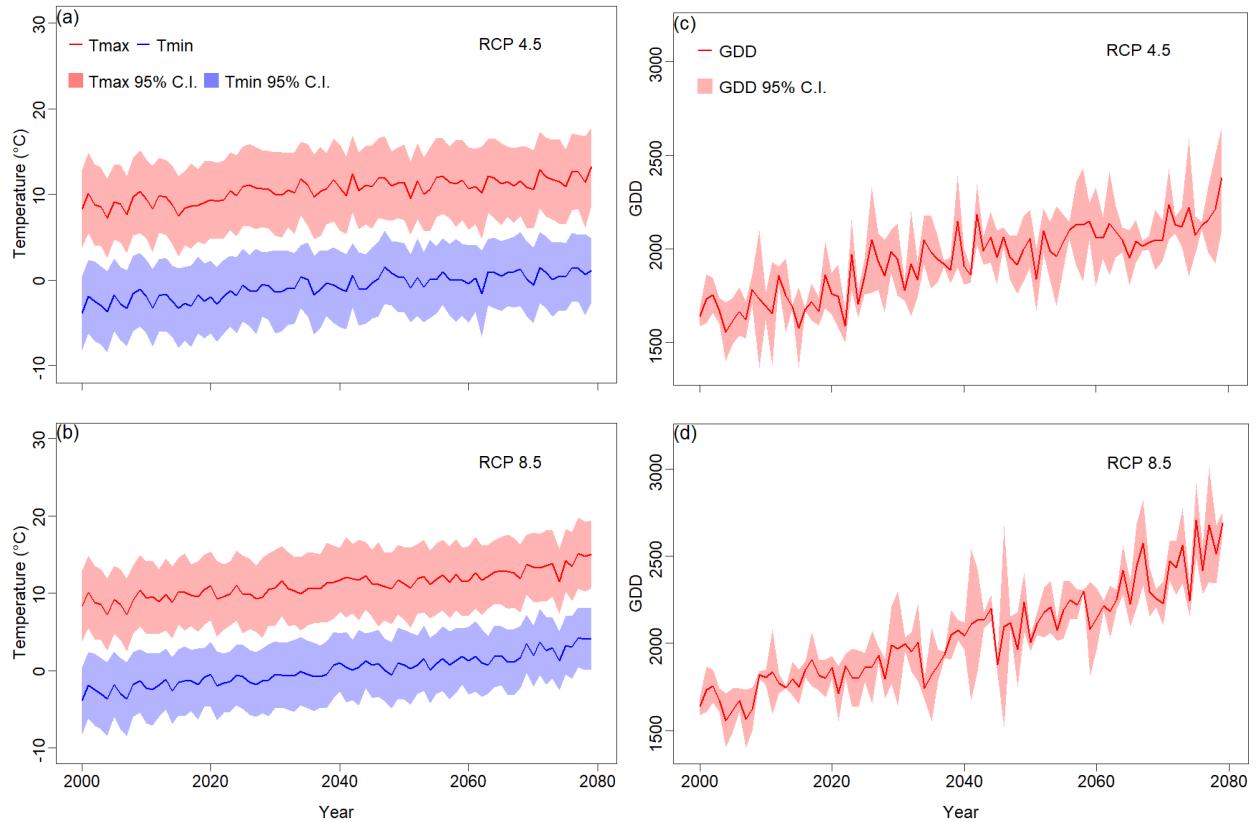


Figure 3.1: Long-term trends of maximum (Tmax) and minimum (Tmin) daily temperature (a & b) and growing degree days (GDD) for growing season from April to September (c & d) under RCP 4.5 and RCP 8.5 for the reference period (2000 – 2019), near future (2020 – 2049), and distant future (2050 – 2079). Solid lines represent the annual averages for maximum and minimum temperature and accumulation of growing degree days calculated from the model ensemble. Shaded areas represent the 95% confidence interval.

The multi-decadal long-term average annual precipitation were the greatest in the distant future period, which was caused by a substantial rise in spring precipitation, increasing from 172 mm in the reference period to 191 mm in the near future under RCP 8.5 (Fig. 3.2). Similar patterns of seasonal variation were observed for both RCP, where winter precipitation increased roughly by 4 to 7.6 mm in the near future, followed by an additional increase of 10 to 15 mm in the distant future under RCP 4.5 and RCP 8.5, respectively. Meanwhile, although summer precipitation decreased in both scenarios, the reduction was evident under RCP 8.5, which declined from 120 mm in the reference period to 106 mm in the near future, and further to 97

mm in the distant future. The decline in summer precipitation bears significance as it could severely impact the agronomic performance (i.e., yield) of pastureland.

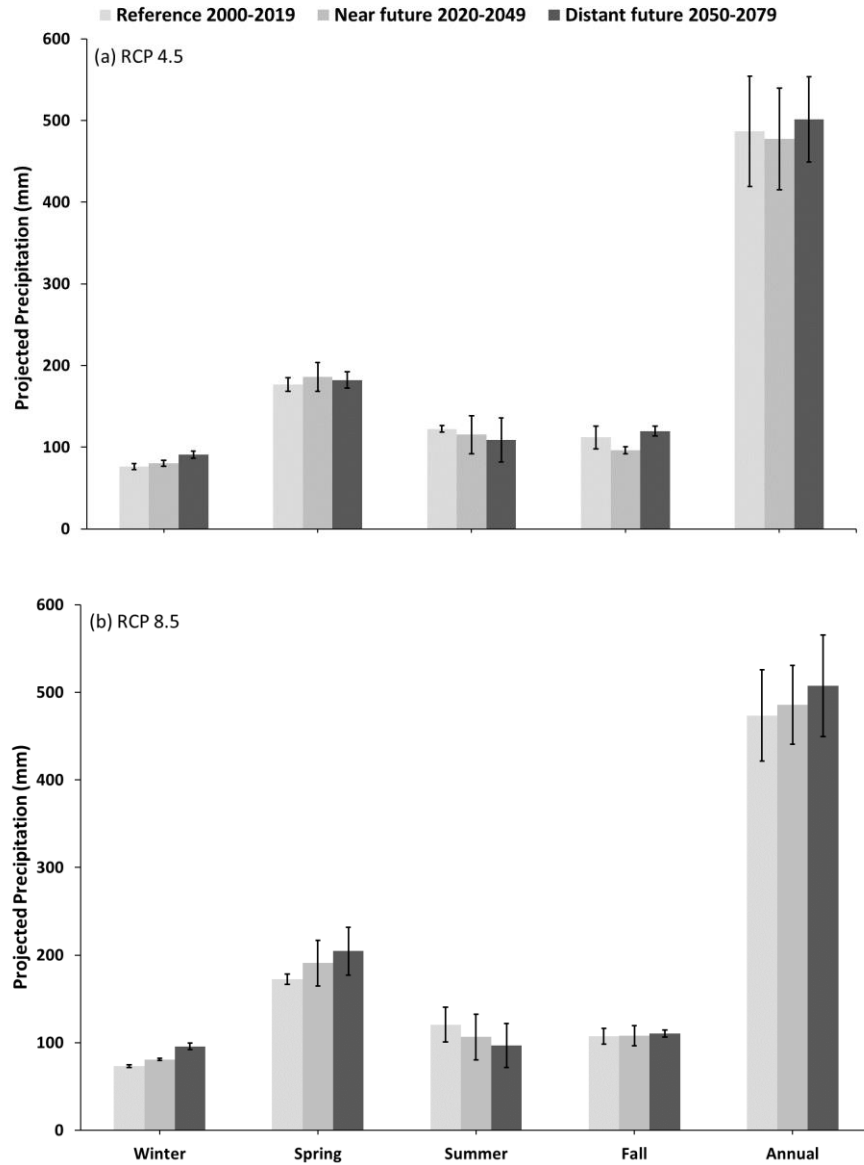


Figure 3.2: Long-term average seasonal and annual precipitation for the reference, near future, and distant future periods under RCP 4.5 (a) and RCP 8.5 (b). Error bars represent the standard deviation of precipitation data.

3.4.2. Model Assessment

Model simulations during the historical period resulted in an average pasture yield of 219.9 t DM km⁻², which was only 0.45% lower than the benchmark value (220.9 t DM km⁻²) with a

PBIAS of -0.4%. The simulated manure production averaged $752,050 \pm 4780$ kg DM per year, equivalent to 13.3 kg DM head⁻¹ day⁻¹. This value is at the lower end of the range ($12 - 62$ kg day⁻¹) suggested by Statistics Canada (2006). However, the range was reported on a wet basis, accounting for the combination of urine and feces, so that a considerable portion of manure consisted of moisture. This range only serves as a reference, since the reported values are for cattle in confinement, which have a different diet compared to cattle grazing on pastureland.

3.4.3. Model Hindcast

Prior to predicting pasture yield and manure production in the near and distant future, a comparison was made between yield simulated with climate modelled data against the benchmark value during the historical period. The simulated pasture yields during the reference period were 222.7 t DM km⁻² and 220.5 t DM km⁻² for RCP 4.5 and RCP 8.5, corresponding to a PBIAS of +0.8% and -0.2% compared to the benchmark value, respectively. Meanwhile, yield simulated with historical weather data was the lowest (i.e., 219.9 t DM km⁻²), which was likely caused by the lowest average GDD (Fig. 3.3) with slightly higher precipitation than the RCP 8.5 during the same period (Table 3.2).

Table 3.2: Annual and seasonal precipitation during the reference period for the historical, and the future dataset under RCP 4.5 and RCP 8.5 scenarios, expressed in mm.

Season	Reference Period		
	Historical	RCP 4.5	RCP 8.5
Spring	160	177	173
Summer	131	122	120
Fall	96	112	107
Winter	93	76	73
Annual	480	487 ± 67	473 ± 52

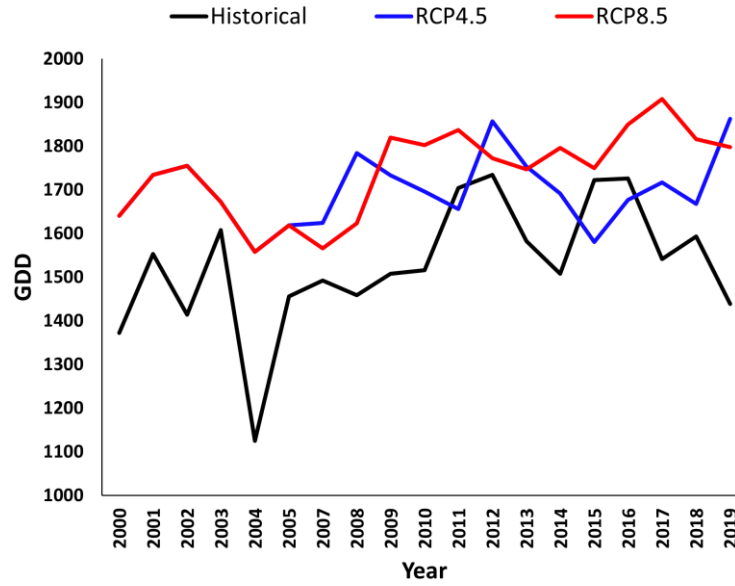


Figure 3.3: Comparison of growing degree days of the historical dataset and the future climate datasets under RCP 4.5 and RCP 8.5

3.4.4. Model Forecast

3.4.4.1. Agronomic Performance

Simulated pasture yield in the near future under RCP 4.5 increases by 2.2% from 222.7 to 227.5 t DM km⁻² compared to the reference period, then decreased to 217.9 t DM km⁻² in the distant future. In contrast, the projected yield under RCP 8.5 was consistently reduced by 2.4% by the mid-century, and then by another 4.6% by 2070 (Fig. 3.4). In general, the outputs suggested that during the same period, pasture yield under RCP 4.5 was greater than that of RCP 8.5. Additionally, it was observed that the uncertainties of the predicted yields in the distant future were more pronounced with 17.7 (RCP 4.5) and 25.1 t DM km⁻² (RCP 8.5). Those uncertainties were substantially larger than those in the near future (RCP 4.5: 4.7 t DM km⁻²; RCP 8.5: 9.9 t DM km⁻²).

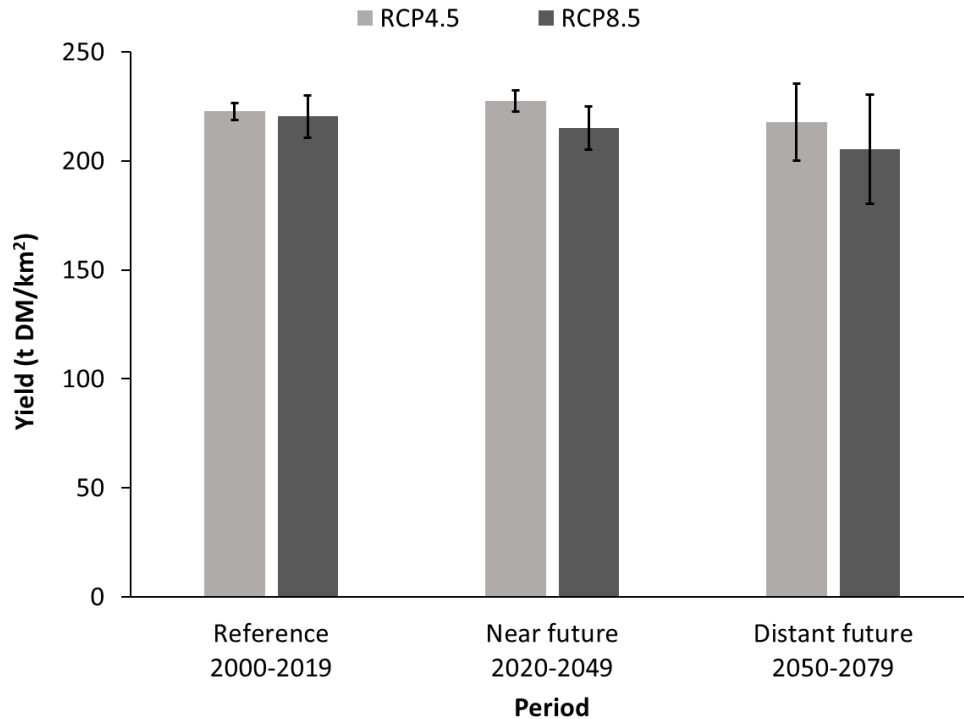


Figure 3.4: Long-term average pasture yield for the reference, near future, and distant future periods under RCP 4.5 and RCP 8.5. Standard deviation of the predicted yields are represented by error bars.

Considering the influence of climate change on pasture production, yield remained relatively constant with a $\pm 2\%$ change, except for a 6.8% reduction in the distant future period under RCP 8.5.

3.4.4.2. Manure Production

The estimated manure production for the reference period were $750,867 \pm 1953$ and $750,467 \pm 1447$ kg DM per year under RCP 4.5 and RCP 8.5, respectively; which were 0.16% and 0.21% greater than simulations obtained with the historical dataset. The largest difference of (-0.39%) was observed for the distant future under RCP 8.5 (Fig. 3.5a), indicating climate change would have minimal impact on manure excretion.

Fig. 5b-c illustrates the manure N and P that originated from pasture only, after isolating the contribution from hay. Based on the climate projections, both N and P did not show significant variations when subject to climate change in the long term, given the highest projected manure N and P values on an annual basis in the distant future under RCP 8.5, were only 213 kg and 16 kg greater than the values in the reference period (N: 15714 kg; P: 1215 kg).

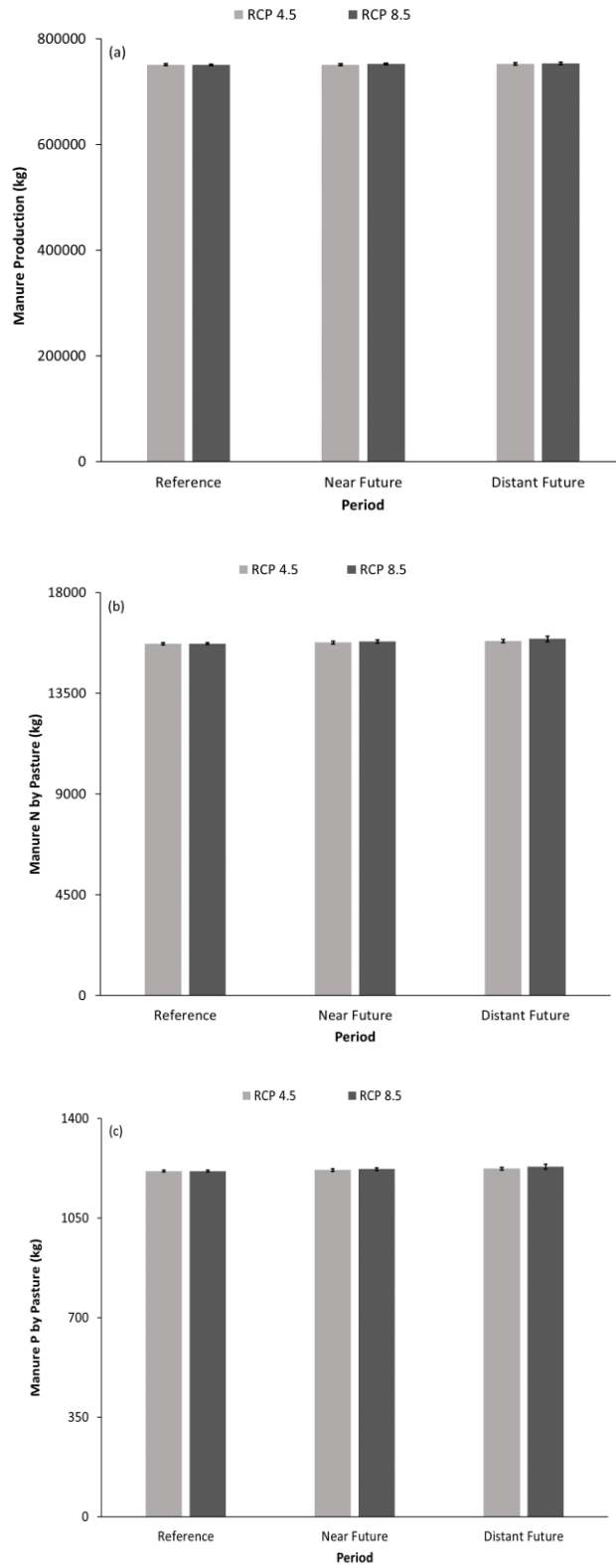


Figure 3.5: Long-term average manure production (a), nitrogen (b) and phosphorus (c) content in manure for the reference, near future, and distant future periods under RCP 4.5 and RCP 8.5.

3.4.5. Relationship between Yield and Precipitation

The relationship between annual pasture yield and precipitation prior to, and during the growing season was assessed using linear regression. Precipitation in spring and summer was found the most pronounced under RCP 4.5 and RCP 8.5 compared to other seasons (Fig. 3.6). Although precipitation in all seasons was positively correlated to pasture yield, this relationship was generally weak, with the highest R^2 values in both scenarios being 0.2932 under RCP 4.5 and 0.3492 under RCP 8.5.

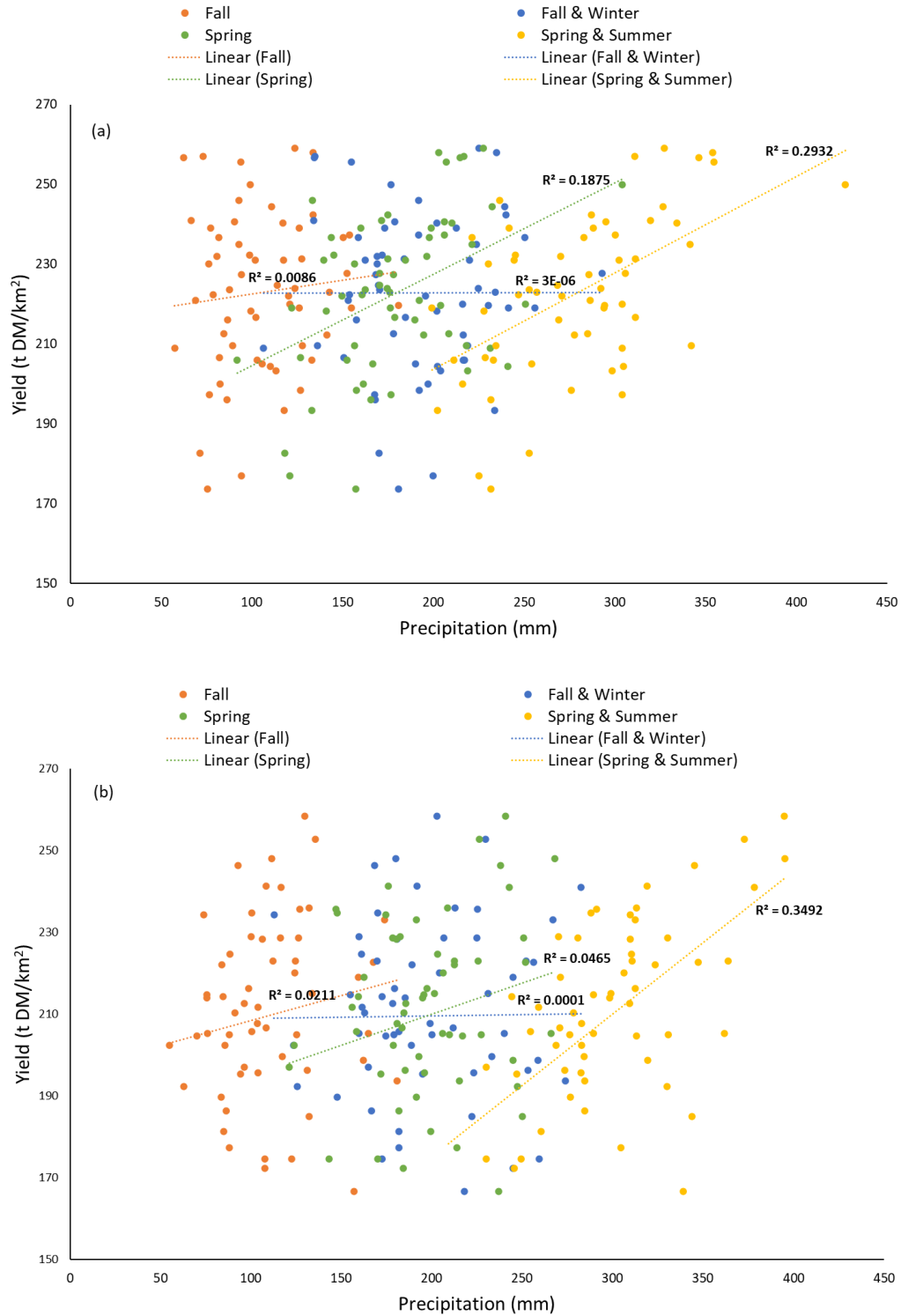


Figure 3.6: Relationship between pasture yield and seasonal precipitation under RCP 4.5 (a) and RCP 8.5 (b), whereas Fall represents the months of September, October, and November from previous year, Fall & Winter spans from September in the previous year to March in the next year, Spring represents the months of April, May, and June in the upcoming year, and Spring & Summer is the timespan from April to August in the same year.

3.5 Discussion

With a warmer climate, the annual precipitation is anticipated to increase as a result of the intensification of hydrological cycle due to a higher evapotranspiration rate (Pratap and Markonis, 2022). However, the decline in summer precipitation expected for the study area could have detrimental effects on pasture growth depending on species, and could have implications for future water resource management and agricultural practices within the region.

The projected pasture yield had a decreasing trend, except for the 2.2% projected increase during the near future period under RCP 4.5. Considering the substantial variability due to different geographic locations, climate conditions, and plant species, yield results predicted in other studies are not suitable for direct comparison. However, some practical insights can still be linked to the current study. For example, Thivierge et al. (2017) used IFSM and predicted a +30% to +62% increase in alfalfa yield in a virtual farm in Central Alberta for the near future and distant future periods, respectively. The yield increase was likely attributed to the change in projected precipitation, with an average annual precipitation of 531 and 529 mm in the near future and distant future periods under RCP 4.5, and 517 and 560 mm under RCP 8.5. These are significantly higher than the projected precipitations in the Beaver Creek watershed. Moreover, the warming climate would favor those N-fixing grass species with elevated CO₂ levels (Thivierge et al., 2016). Furthermore, the yield of cool-season grasses are likely to be impacted by a warmer climate (Thivierge et al., 2017; Payant et al., 2021). Cool-season grasses, which comprise the majority of grass species in the study area, typically reaches peak growth in spring (Putnam and Orloff, 2014), but this might not always be the case. Sharpe and Rayburn (2019) have highlighted the possibility of delayed peak growth in late spring or early summer in regions characterized by higher latitude, attributable to prolonged winter in colder regions. Nevertheless,

the overall increase in annual precipitation in the processed climate dataset did not result in a higher pasture yield. Although spring precipitation increased considerably, it failed to compensate for the heat stress which likely impaired pasture growth, ultimately resulting in a lower pasture yield. This was verified by the coefficient of determination shown in Fig. 3.6, in which a very weak relationship was observed between spring precipitation and pasture yield under both CO₂ emission scenarios ($R^2 = 0.1875$ and $R^2 = 0.0465$ for RCP 4.5 and RCP 8.5, respectively). Although the configured model assumed no irrigation, relying exclusively on natural precipitation as the only water source for pasture growth, it is worth noting that the antecedent conditions (e.g., soil moisture content at the end of the previous growing season) could theoretically supply moisture for pasture growth in the following year. Soil moisture freezes up during winter months, and becomes available for pasture growth when thawing (Bo et al., 2021). However, this was not reflected in the simulation results as the R^2 values were very low for the combined precipitation of fall in the previous year to March in the next year. This affirms that the precipitation during the growing season plays an important role as the primary water source, outweighing the significance of antecedent soil conditions.

The optimal growing temperature for cool-season grass is around 18 – 24 °C, and 30 – 35 °C for warm-season grass (Fry and Huang, 2004). Once the ambient temperature surpasses the threshold of heat tolerance by 5 to 10 °C, plants would suffer irreversible functional and structural damages that hinders growth performance, resulting in lower yield (Xu et al., 2011). The growth inhibition due to heat stress, coupled with the reduced summer precipitation, is likely the reason that led to the projected reduction in pasture yield in the simulations (Agriculture and Agri-Food Canada, 2020).

In terms of pasture quality, IFSM used average values to represent the nutrient content in pasture by season. This simplified approach constrains changes in pasture quality simulation along the growth phases, within each season, and between years. Because of the interactions and combinations of multiple factors (e.g., temperature, CO₂ level, precipitation), studies have indicated the complexity of forage quality quantification under climate change. For example, a reduction in precipitation can lead to early maturity (March-Salas and Fitze, 2019), increased acid detergent fiber (ADF) and neutral detergent fiber (NDF; Khorasani et al., 1997), while elevated CO₂ levels can increase the water soluble carbohydrates in the laminae, thereby increase pasture digestibility (Picon-Cochard et al., 2004), increase water soluble carbohydrates, and decrease the crude protein content (Dumont et al., 2015). The increase in temperature can lead to increased maturity, which lowers the crude protein content (Izaurrealde et al., 2011), the leaf-to-stem ratio, and the digestibility (Dumont et al., 2015). Therefore, it is evident that the effects of climate change on pasture quality cannot be accurately ascertained by isolated consideration of a single climatic factor. The intricate interplay and synergistic influences of these multifaceted factors necessitate a holistic approach to better understand the associated impact of climate change on pasture quality.

Failing to dynamically capture the response in pasture quality due to climate effect poses a challenge for the analysis of nutrient dynamics in the present study. Due to the complex interactions affecting pasture quality, historical values of pasture quality were used for future scenarios. While this approach is acknowledgedly not ideal, it allowed for an assessment of nutrient changes based on manure production and composition.

Analyzing the manure production and nutrient content in manure is an alternative to examine the nutrient cycling on grassland. Reduced manure inputs can lead to reduced pasture quality,

which can compromise cattle performance. To address this issue, protein supplementation that improves digestibility of organic matter and neutral detergent fiber can be applied (Bargo et al., 2003). Manure N and P in this study, was governed by the user-defined nutritive content in feed and the feed consumption [Equation (3.3)]. Since manure production is expected to remain stable and nutrient content was assumed to remain constant, the simulations indicated that nutrient inputs would not change in the future. However, this result is very uncertain, as explained above.

On the other hand, it is also imperative to not neglect the uncertainties associated with the future climate ensembles as indicated by the 95% confidence interval (Fig. 3.1a-b). The uncertainties are mostly attributed by three major sources: model uncertainty, emission scenario uncertainty, and natural internal climate variability (Wu et al., 2022). The importance of internal variability and model uncertainty in the context of global air temperature, is particularly pronounced over the first half of the century, while the emission scenario becomes the dominant factor in the subsequent periods (Kirtman et al., 2013). When considering precipitation in western Canada, the key contributor to uncertainty in climate projections for the entirety of the 21st century is identified as the natural internal variability (Barrow and Sauchyn, 2019).

3.6 Conclusion

The assessment of climate change effect on pasture yield and quality was conducted for a 33.92 km² grasslands located in Manitoba using the IFSM model under two emission scenarios (i.e., RCP 4.5 and RCP 8.5). The analysis of weather trend revealed the projected ambient temperature to significantly increase in both near and distant future periods. Despite the increases in average annual precipitation, a reduction in summer precipitation was observed. These alterations in climatic factors implied a progressively warmer climate with an augmented likelihood of drought conditions during the summer, indicating a potential reduction in pasture

yield. With the only exception that the yield increased by 2% in the near future period under RCP 4.5, IFSM simulations generally supported this outcome by simulating a 2% to 6.8% decline in the yield of cool-season grass, which is prevalent in the study area. This decline was more pronounced during the distant future under RCP 8.5 scenario. In contrast, minimal impact was observed on manure production. An adaptation strategy to counteract the adverse effects of climate change is the transition to grass species that are more heat and drought tolerant.

BRIDGE TO CHAPTER 4

Upon the completion of simulating pasture yield and manure production using IFSM, the analysis revealed crucial insights about the nutrient content in the vegetation and manure nutrient pools, indicating the nutrient content in the vegetation and manure pools that can potentially contribute to eutrophication. Subsequently, a hydrological simulation specific to the study area within Beaver Creek was performed, recognizing the pivotal role of water movement in influencing nutrient dynamics.

CHAPTER 4: IMPACT ASSESSMENT OF CLIMATE CHANGE ON THE HYDROLOGY OF A PASTURE-DOMINATED UNGAUGED WATERSHED IN MANITOBA USING A MULTI-MODEL APPROACH

4.1 Abstract

To address concerns regarding the risk of ecosystem services loss, the climate change impact on the hydrology of grasslands in the Canadian Prairies has yet to be assessed. The objectives of this study were to simulate the changes in hydrology due to climate change within a 46.6 km² ungauged basin in Manitoba predominantly characterized by pastures using the Cold Regions Hydrological Model (CRHM) platform and the Hydrological Predictions for the Environment (HYPE) model, and to assess how the simulations from both models complement each other. Both models were set up for an ungauged study area within the Beaver Creek watershed and forced with historical meteorological data from 2000 – 2019. The performance of the CRHM model was deemed satisfactory with a Nash-Sutcliffe efficiency (NSE) of 0.503 and a percent bias (PBIAS) of +7.8% using water yield as the assessment variable, and a PBIAS of 14.1% using annual evapotranspiration (ET) as a second assessment metric. HYPE had a comparable performance with a NSE of 0.529 and a PBIAS of +0.4% for water yield, and a +7.8% PBIAS for annual ET. The impact associated with climate change was assessed by extending the simulation to near future (2020 – 2049) and distant future (2050 – 2079) periods under two representative concentration pathways (RCP 4.5 and RCP 8.5). Both models suggested a reduction in annual stream discharge in the near future under RCP 4.5, followed by a subsequent recovery in the distant future. Conversely, both models predicted an increase in annual stream discharge for both periods under the higher emission scenario (RCP 8.5). Furthermore, across all scenarios, a shift in the timing of peak discharge was observed, taking place from 6 to 21 days

earlier except for the near future period under RCP 4.5 with a modest 2-day delay. This implies an earlier onset of snowmelt, potentially leading to a longer growing season. CRHM and HYPE models showed similar performance, and were considered adequate tools to simulate the hydrology of pasture landscapes in cold climates.

4.2 Introduction

Agricultural development in the Northern Great Plains took place at the expense of converting perennial grasslands to annual cropland. According to the World Wildlife Fund (2016), over 214,500 km² of grasslands have been converted to cropland across the Great Plains since 2009, averaging 1 - 5% conversion rate annually (Gage et al., 2016). As home to nearly 89% of the tame and native pasture in Canada, the Canadian Prairies region, part of the Northern Great Plains, is no exception to this land cover change (Statistics Canada, 2022c). Croplands in Canada accounted for 250,000 km² prior 1960 (Statistics Canada, 2006), but drastically increased to 378,000 km² in 2016 (Statistics Canada, 2017). During the later period of this expansion, it was observed that the coverage of tame and native grasslands decreased from 202,360 km² in 2011 to 193,430 km² in 2016 nationally (Statistics Canada, 2017). Manitoba, one of the three Prairie provinces, had a 7% grassland loss between 2011 and 2016 (Statistics Canada, 2017).

The loss of grasslands poses a threat to ecosystem services, such as habitat maintenance, carbon sequestration, forage production, soil stability, and water regulation (Bengtsson et al., 2019; Ceballos et al., 2010; Huber et al., 2022). To address those issues, there has been renewed interest in restoring perennial grasslands by reversing the conversion (Gage et al., 2016; Laforge et al., 2021; Kharel et al., 2016). Despite this interest, only a few studies addressed the associated hydrological implications on land use conversion in Manitoba. Cordeiro et al. (2022) used modeling approach to compare the major components of hydrological cycle when planting

canola versus smooth brome grass in a subbasin of the Red River Valley. By converting land cover back to perennial forage, the annual cumulative discharge and peak discharge were found reduced by 36.6% and 29.9%, respectively, while the evapotranspiration (ET) increased by 34.5% due to greater canopy coverage. The significant reduction in discharge was attributed by perennial forage enhanced soil infiltration, resulting in a reduced surface runoff (van der Kamp et al., 2003).

Another factor complicating the hydrological assessment of grasslands is climate change. Climate models projected annual mean temperature increases of 1.8°C in Canada by 2050 under a low greenhouse gas (GHG) emission scenario (Representative Concentration Pathway, RCP 2.6), while increases by 6°C by 2100 are expected under a high GHG emission scenario (RCP 8.5; Zhang et al., 2019). Temperature increases will be more pronounced in winter than in summer, implying a longer growing season. Precipitation, on the other hand, is projected to increase in Canada by 6.8% by the end of the century under RCP 2.6, and by 24.2% under RCP 8.5, respectively (Zhang et al., 2019). Although with lower confidence, an overall lower summer precipitation was predicted for Canada, leading to more frequent and severe drought events. For Manitoba, the trend of streamflow is projected to increase (Bonsal et al., 2019). Yet, the investigation on the hydrological responses under the profound variation in seasonal precipitation with a warmer climate, has been lacking for grassland landscape, especially in cold regions like Manitoba with a more complex hydrological cycle (i.e., cold-region processes).

Given the complex interactions among hydrological processes, hydrological model is typically a practical alternative for impact assessment as they are cost-effective, robust, and offer forecasting capabilities (Idrissou et al., 2020; Parra et al., 2018). A well-configured and calibrated hydrological model can provide insights about the interactions among regional

hydrological processes. Among various hydrological models, such as the Soil and Water Assessment Tool (SWAT; Arnold et al., 1998), the Variable Infiltration Capacity model (VIC; Cherkauer et al., 2003), the Arctic Hydrological and Thermal Process Model (ARHYTHM; Zhang et al., 2000), and HYDRUS (Šimůnek et al., 2012), the Cold Regions Hydrological Model (CRHM; Pomeroy et al., 2007) has been widely used in Canada. This model is able to simulate a suite of hydrological processes that are unique to cold regions, including snow transport, snow sublimation, infiltration through unsaturated frozen soil layers, and snowmelt. Moreover, the capability of CRHM to simulate snow redistribution by wind, featuring a more realistic representation over other models (Fang and Pomeroy, 2009; Pomeroy et al., 1993), facilitates a comprehensive assessment for hydrological simulations.

The CRHM platform has been implemented in multiple studies that were related to hydrological simulations under climate change. Recent research has shown that, with a 6°C warming and a 30% increase in annual precipitation by 2100 under the assumption of a high emission scenario, the annual runoff would decrease by 40% in western Prairie and increase by 55% in eastern Prairie (Spence et al., 2022). For grassland landscapes, every 1°C of warming would induce an 8% reduction in the maximum snow water equivalent (SWE) in spring, highlighting the sensitivity of hydrological components in response to climate change (Spence et al., 2022). Simulations of the magnitude and timing of spring snowmelt is critical because it is the major facilitator of annual stream discharge (Pavlovskii et al., 2019), contributing more than 70% of the annual surface runoff in the region (Glozier et al., 2006; Shrestha et al., 2012). Fang and Pomeroy (2020) predicted an 18% increase in the annual stream discharge in the Marmot Creek in Alberta using CRHM, assuming local temperature increases by 4.7°C under RCP 8.5. It was found that the increased rainfall failed to offset the escalated ET, substantially advancing the

onset of snowmelt by at least 1.5 months. Similar findings were reported for the Elbow River Basin and the Bow River Basin in Alberta, where shorter snow-covered durations were observed for both basins at the end of the 21st century under RCP 8.5 (Fang and Pomeroy, 2023). Despite having a comparable increase in projected temperature and annual precipitation, the Bow River Basin had a 43 mm increment in annual snowmelt volume, contrasting a 55 mm decrease in the Elbow River Basin. The fact that the Bow River Basin has a higher capacity of water storage, further reinforcing that landscape characteristics plays a significant role in hydrological analysis (Fang and Pomeroy, 2023).

The Hydrological Predictions for the Environment (HYPE) is another robust model that has been proven reliable in both short-term and long-term hydrological forecasts (Arheimer et al., 2020). Processes that are unique in cold regions, such as snow ablation, snow melt, frozen soil, surface runoff, subsurface runoff, limited infiltration through frozen soil, aquifer recharge and groundwater fluctuation are available in HYPE (Lindström et al., 2010). By forcing 19 climate models from the Coupled Model Intercomparison Project Phase 5 (CMIP5; Taylor et al., 2012) with the Arctic-HYPE model, the streamflow in the Hudson Bay Complex has been projected to increase by 2070 (Gelfan et al., 2017). The trend was more pronounced in response to a 2°C warming, in contrast to a 1.5°C warming, underscoring the sensitivity of the forecast to variations in temperature. Furthermore, spatial heterogeneity was observed, with the greatest increase in discharge occurring in regions situated further north. Notably, an underlying phenomenon of climate projection was revealed, namely that low-precipitation and warm regions, such as the Western Hudson Bay, are inherently more susceptible to greater uncertainties in forecasting stream discharge. This is affirmed by the findings of Stadnyk et al. (2019).

The objective of this research was to comprehensively assess the impact of climate change on grassland hydrology in Manitoba using a multi-model framework consists of the CRHM platform and the HYPE model. This approach is recommended to achieve a more comprehensive hydrological assessment (Srivastava et al., 2019). The models were used to represent the hydrological processes of an ungauged pasture watershed within the Beaver Creek watershed. The simulations from CRHM and HYPE were contrasted by focusing on the changes in evapotranspiration, streamflow, and the timing of peak discharge. This study does not assert a high degree of confidence in the accuracy of the hydrological response predictions, nor does it make definitive remarks on the superior hydrological model for application. Instead, its ultimate goal is to offer preliminary simulation results, emphasizing the general trend of hydrological behavior in response to climate change.

4.3 Materials and Methods

4.3.1. Study Area

Spanning across 46.6 km², the study area (50°23'36" N, 101°21'27" W) is within the Beaver Creek watershed (Fig. 4.1), a tributary of the Assiniboine River located at the southeast of St. Lazare, Manitoba, Canada. Land cover in this area consists of pasturelands (72%), forest (19%), and agricultural lands (8%) with other covers (i.e., barren, urban, and wetland; 1%; Agriculture and Agri-Food Canada, 2023). This region is relatively flat with a slope ranging from 2-5% (U.S. Geological Survey, 2014). Soils in the area are characterized as loamy sand with moderate to excessive drainage. As a result, the region is prone to drought and wind erosion (Hamel and Reimer, 2004). The average soil composition in the study area is 8% silt, 6% clay, and 86% sand (Cordeiro et al., 2018).

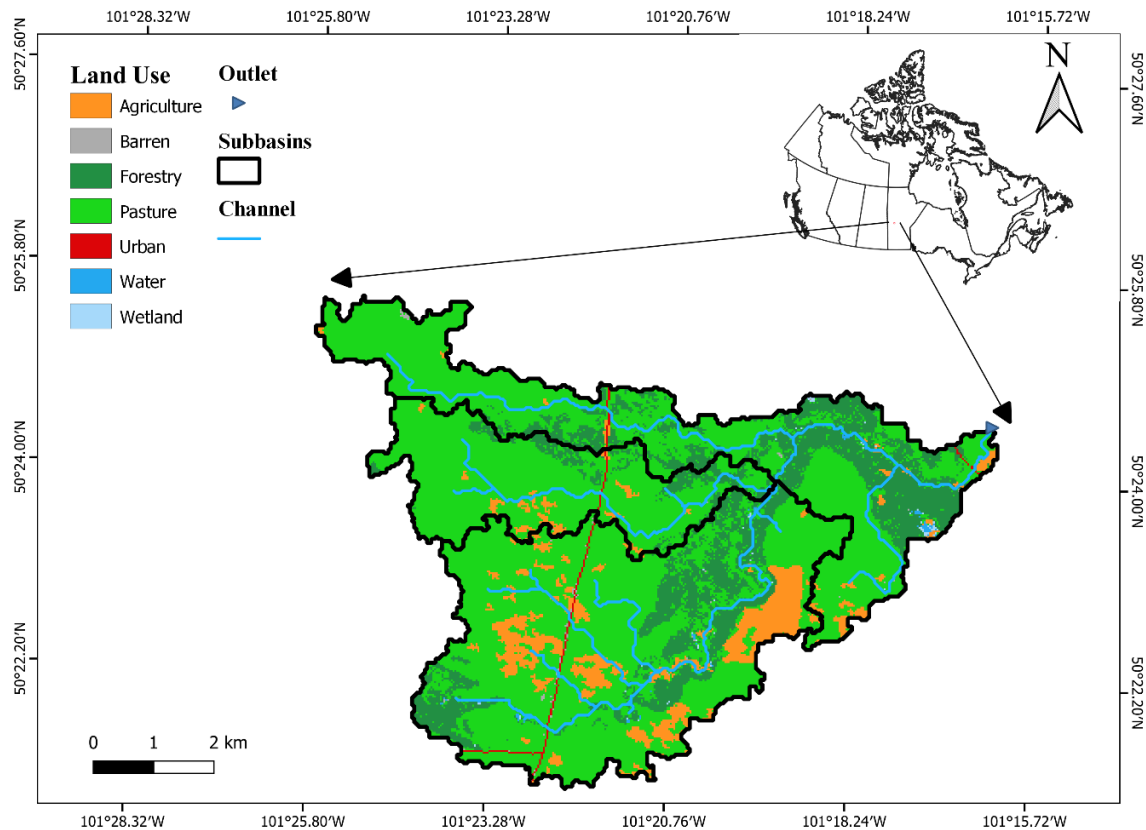


Figure 4.1: Location and land cover in the study area in the Beaver Creek watershed

The long-term mean annual temperature is 2°C (from 2000 to 2020) derived from the meteorological records at the Birtle station (Manitoba Agriculture, 2022). During the same period, Beaver Creek watershed received 470 mm of precipitation per year on average, with snowfall accounting for 5 - 33% of the total precipitation (Manitoba Agriculture, 2022; Environment and Climate Change Canada, 2023a). Recorded wind speed averaged 10.5 – 16.7 km/hr at the Birtle station over the period.

4.3.2. Input Datasets

4.3.2.1. Historical Weather Data

The same weather variables were used as input for both CRHM and HYPE models, although in different time steps. CRHM was forced in an hourly timestep, while HYPE was forced in a

daily timestep. Therefore, hourly and daily weather data were acquired. Historical weather data collection consisted of: (1) retrieving hourly data from a parent station, and (2) obtaining both hourly (if available) and daily from close-by stations for gap-filling. Hourly data was used for CRHM, while this data was aggregated to a daily time step for HYPE.

Mandatory weather variables for CRHM include air temperature ($^{\circ}\text{C}$), relative humidity (%), wind speed (m s^{-1}), precipitation (mm h^{-1}), and incoming short wave radiation (W m^{-2} ; Pomeroy et al., 2007). The historical dataset was mainly collected from the Birtle station ($50^{\circ}24'39''\text{N}$, $100^{\circ}53'36''\text{W}$), which is the closest to the study area and provided hourly measurements (Manitoba Agriculture, 2022). However, only data from 2008 and onward was available for that station. Also, only rainfall was recorded through a tipping bucket rain gauge prior to 2017. The total precipitation in the input file required segmentation into rainfall and snowfall component. The physically-based method described by Harder and Pomeroy (2013) was used to estimate precipitation in liquid and solid phases. This method estimates the phase transition of falling hydrometeor using the psychrometric energy balance. To overcome the missing values in the record, data were also gathered from other stations nearby. Thereafter, various strategies were implemented to address remaining gaps. Linear interpolation was used for non-consecutive short gaps. For any retrieved data at a daily timestep, temporal downscaling techniques were applied for different variables before filling the data gaps. The hyperbolic tangent fitting algorithm estimates hourly temperature based on the daily maximum and minimum temperature, and the estimation depends on the hour of the day. The HyetosMinute is a R package that used the Bartlett-Lewis rainfall model, a stochastic model in order to generate hourly or sub-hourly data from daily precipitation data. The collected daily maximum and minimum temperature, together with the estimated hourly extraterrestrial radiation according to Allen et al. (1998), were used to

estimate hourly solar radiation using the Hargreaves and Samani model, which is a temperature-based empirical model. Table 4.1 shows an overview of the historical dataset, encompassing the data sources, record period, and the implemented downscaling strategies.

Table 4.1: Description of the historical dataset variables, sources, and gap filling method.

Variable	Data use	Data Availability	Source	Method
Temperature	Parent station	2008 – 2019	Birtle station	-
	Gap-filling	1998 – 2019	Nearby stations ¹	HT ²
	Gap-filling	2006	NASA Power ³	-
Relative humidity	Parent station	2008 – 2019	Birtle station	-
	Gap-filling	1998 – 2019	Nearby stations	-
	Gap-filling	2006	NASA Power	-
Wind speed	Parent station	2008 – 2019	Birtle station	-
	Gap-filling	1998 – 2019	Nearby stations	-
	Gap-filling	2006	NASA Power	-
Precipitation	Parent station	2017 – 2019	Birtle station	-
	Gap-filling	2008 – 2016 (non-winter months)	Birtle station	-
	Gap-filling	1998 – 2019	Nearby station	HM ⁴
	Gap-filling	2006	NASA Power	-
Incoming shortwave radiation	Parent station	2017 – 2019	Birtle station	-
	Gap-filling	2008 – 2016	Birtle station	HS ⁵
	Gap-filling	1998 – 2007	Nearby stations	HS

¹Nearby stations include ShoalLake CS station, Rossburn 4 North stations, and Roblin station, which are 53.9, 55, and 87.8km away from the study area, respectively (Environment and Climate Change Canada, 2023 a); ² HT = Hyperbolic tangent fitting algorithm; ³ NASA Power = Synthetic data from NASA Power database for Year 2006 (National Aeronautics and Space Administration. 2023); ⁴ HM = HyetosMinute; ⁵ HS = Hargreaves and Samani model

The preparation of weather data for HYPE followed a similar approach, except that a different set of variables was required, such as daily mean, maximum, and minimum temperature, relative humidity, wind speed, precipitation, and shortwave radiation. Also, no disaggregation was performed and the values were kept at a daily time step. For the year of 2006, synthetic data from the NASA Power database was obtained to create a complete historical dataset, but simulation results from this year were removed during model assessment of both models due to high uncertainty.

4.3.2.2. Future Climate Data

Hydrological projections were carried out using climate data for the near future (2020 – 2049) and distant future (2050 – 2079) periods. In this study, future climate data were prepared for Representative Concentration Pathways (RCP) 4.5 and 8.5, which represent the radiative forcing at 4.5 and 8.5 W m⁻², respectively, based on the level of anthropogenic emission of greenhouse gases (GHG; Baek et al. 2013). Bias-corrected daily data from 1998 to 2079 were downloaded from the North American component of the international Coordinated Regional Downscaling Experiment (NA-CORDEX) database for three regional climate models (RCMs), namely CMIP5: CanESM2.CanRCM4, CanESM2.CRRCM5-UQAM, and MPI-ESM-LR.CRRCM5-UQAM (Mearns et al., 2017). These GCM-driven RCMs have a grid size of 25-km (Mearns et al., 2017). These daily data were acquired as the future climate datasets for HYPE. Since the historical dataset consists of hourly values for CRHM, the future climate data were downscaled from a daily to an hourly timestep with different approaches depending on the variables. The downscaling methods are summarized in Table 4.2.

Table 4.2: Methods used for disaggregation of daily weather data to a hourly time step for CRHM.

Variable	Method
Temperature	Hyperbolic tangent fitting algorithm (USAF, 1991)
Relative humidity	Safeeq and Fares (2011)
Wind speed	Guo et al. (2016)
Precipitation	HyetosMinute (Kossieris et al., 2016)
Incoming shortwave radiation	Hargreaves and Samani model (Aladenola and Madramootoo, 2014)

4.3.3. Watershed Delineation and Hydrological Response Unit Definition

Topography, soil, and land use datasets (Table 4.3) were used to delineate the watershed using the Quantum Geographic Information System (QGIS) interface for the Soil and Water Assessment Tool (SWAT) model (QSWAT, Dile et al., 2015). SWAT is a process-based model

that is often used to assess the impact of management practices on water and nutrients (Arnold et al., 1998). The 46.6 km² large study area was divided into 3 subbasins (Fig. 4.1). Once the watershed was delineated, hydrological response units (HRUs) were defined, which are the fundamental spatial unit in hydrological models that represents a discrete combination of land use, soil, and topographic characteristics (Kalcic et al., 2015). Both CRHM and HYPE models are capable of computing water balance in each subbasin (Pomeroy et al., 2007; Lindström et al., 2010). Table 4.4 outlines the details of the defined HRUs, where the sequence of the HRUs is ranked based on the aerodynamic roughness of the stubble height of crops.

Table 4.3: Input data for watershed delineation.

Type	Data	Data Source
Topography	30m SRTM Digital Elevation Model (DEM)	USGS Earth ¹
Land use	Annual Crop Inventory	Agriculture and Agri-Food Canada ²
Soil	Soil Landscapes of Canada database processed by Cordeiro et al. (2018)	Soil Landscapes of Canada ³ ; Soil and Water Assessment Tool (SWAT)

¹: U.S. Geological Survey, 2014; ²: Agriculture and Agri-Food Canada, 2023; ³: Soil Landscapes of Canada Working Group, 2010

Table 4.4: Lists of hydrological response units (HRUs) defined in the study area

HRU ID	HRU acronym	Land use	Soil texture	Occurrence		
				SB* 1	SB 2	SB 3
1	PAST/LoSa	Pasture	Loamy sand	Yes	Yes	Yes
2	PAST/CiLo	Pasture	Clay loam	Yes	No	Yes
3	BARL/LoSa	Barley	Loamy sand	Yes	No	Yes
4	OATS/LoSa	Oats	Loamy sand	No	No	Yes
5	OATS/CiLo	Oats	Clay loam	Yes	No	No
6	SOYB/LoSa	Soybean	Loamy sand	No	No	Yes
7	SWHT/LoSa	Spring wheat	Loamy sand	Yes	Yes	Yes
8	SWHT/CiLo	Spring wheat	Clay loam	Yes	No	No
9	WWHT/LoSa	Winter wheat	Loamy sand	Yes	Yes	Yes
10	CANP/LoSa	Canola	Loamy sand	Yes	No	Yes
11	CANP/CiLo	Canola	Clay loam	Yes	No	No
12	BARR/LoSa	Barren	Loamy sand	Yes	Yes	Yes
13	BARR/CiLo	Barren	Clay loam	Yes	No	No
14	FRST/LoSa	Forest	Loamy sand	Yes	Yes	Yes
15	FRST/CiLo	Forest	Clay loam	Yes	No	Yes
16	URLD/LoSa	Urban (low density)	Loamy sand	Yes	Yes	Yes
17	URLD/CiLo	Urban (low density)	Clay loam	Yes	No	No
18	WETL/WA	Wetland	-	Yes	No	Yes
19	WETL/WA	Wetland	-	Yes	No	No
20	WATR/WA	Water bodies	-	Yes	No	Yes
21	WATR/WA	Water bodies	-	Yes	No	No
22	River Channel	River	-	Yes	Yes	yes

*SB = subbasin

4.3.4. Hydrological Model Configuration

4.3.4.1. Cold Regions Hydrological Model

The CRHM platform, has been developed by the Centre for Hydrology at the University of Saskatchewan, a modular and semi-distributed model that encompasses a set of physically-based algorithms for hydrological simulations (Pomeroy et al., 2007). The model structure is customizable with several modules corresponding to different hydrological processes. The CRHM model used in this study was adapted from Spence et al. (2022), who grouped all basins

in Canadian Parries into seven categories based on physio-geographic characteristics (e.g., geology, climate, topography, land use, and hydrology), and created generalized models to represent each of these basin types. The Beaver Creek watershed is within the major river valley region. Therefore, the model for this region was used. The model was further adapted through parameterization in order to create a more representative model for the study area. The modules used in the major river valley model are described in Table 4.5.

Table 4.5: CRHM modules used in the major river valley model (adapted from Cordeiro et al. 2017)

Sequence	Module	Description
1	basin	Contain shared parameters of land characteristics.
2	global	Calculate short-wave direct and diffuse solar radiation, ground slope, aspect, and maximum number of daily sunshine hours.
3	obs	Transfer climate data from the meteorological file and proceed with requested corrections before assigning to HRUs.
4	Grow_Crop	Simulate crop growth based on the daily growth rate, the start and end day of the growing season.
5	Annandale#1	Estimate incoming shortwave radiation from observed daily maximum and minimum temperatures (Annandale et al., 2002).
6	walmsley_wind	Estimate wind speed variation due to topographic features such as ridges, 3D hills, rolling terrain, and flat terrain.
7	longVt#2	Calculate long-wave radiation using either measured or estimated shortwave.
8	netall	Calculate interval net all-wave radiation from short- and long-wave radiation.
9	evap_Resist#1	Consider constant stomatal and aerodynamic resistance, interval evapotranspiration from unsaturated surfaces can be estimated by the Penman-Monteith method (Monteith, 1965).
10	CanopyClearing#3	Based on the type of land use (e.g., crops), adjust precipitation, short- and long-wave radiation due to canopy interception. No adjustments for open environment.
11	pbsm#1	Prairie blowing snow module that models processes of snow drifting and sublimation (Pomeroy and Li, 2000).
12	albedo	Estimate the snow albedo for winter months, as well as the onset of freshet (Gray and Landine, 1987)
13	ebsm#1	Energy-budget snowmelt model that estimates daily and cumulative snowmelt for regions in the Canadian Prairies (Gray and Landine, 1988)
14	PrairieInfiltration	Estimate the rate and the amount of infiltration from snowmelt into frozen soil (Gray et al., 1985), and from rainfall into unfrozen soil (Ayers, 1959).
15	Prevent_Refreeze	Customized function for users to determine whether or not refreezing is allowed outside of winter months.
16	Soil	Calculate several water components, such as soil moisture balance, groundwater storage, subsurface and groundwater discharge, depression storage, surface depression, subsurface runoff, and groundwater (Leavesley et al., 1983; Dornes et al., 2008; Fang et al., 2010).
17	Volumetric	Calculate volumetric soil moisture content.
18	Netroute M D	Routing between HRUs within subbasin (Chow, 1964).
19	REW_route	Model routing from representative basins.

Typically, calibration is a customary procedure in hydrological modeling. Nevertheless, CRHM was developed with no provision for calibration due to the need for predicting hydrology in ungauged basins (Pomeroy et al., 2007). To reduce the reliance on calibration data, CRHM utilizes parameters that are defined based on an understanding of the characteristics of the area, or borrowed from analogous ecoregions sharing similarities in climate, hydrology, and landscape features with the target watershed (Pomeroy, 2022). Such a modelling approach has shown promising performance for ungauged basins (Pomeroy et al., 2013). Therefore, most of the parameters from the major river valley model from Spence et al. (2022) were used in this study for comparable HRUs. Physically identifiable parameters from published literature were utilized for default settings, accommodating situations when the major river valley model did not represent local practice or distinct HRU types.

Physio-geographic attributes required during CRHM parameterization (e.g., area, aspect, elevation, and ground slope) were acquired either through processing the DEM in QGIS, or from the output files generated during watershed delineation in QSWAT. The dominant soil type in the area, namely loamy sand, encompasses 95.7% of the watershed with the rest being clay loam. The porosity of loamy sand and clay loam generally ranges from 0.363 to 0.506, and from 0.409 to 0.519 $\text{cm}^3 \text{cm}^{-3}$, respectively (Rawls et al., 1983). For each texture, the mean values within these ranges were used.

In this study, a linear crop growth was assumed, postulating a consistent daily growth rate starting from the start date of crop growth to maturity. The majority of these growth stage dates were sourced from Cordeiro et al. (2017) in the La Salle River watershed located in Manitoba. The remainder crops were based on local reports (Manitoba Agricultural Services Corporation, 2023; Manitoba Agriculture, n.d.b.). Stem diameters for various crops were defined based on

values reported by SMAP Validation Experiment 2012 (Kim et al., 2014), a field campaign that measured diverse properties of major crops, including stalk diameter.

Estimation of evapotranspiration was carried out in CRHM using the Penmen-Monteith method for non-water HRUs, and the Priestley-Taylor method for wetlands and open water. The values of albedo varied between HRUs from 0.11 for saturated surface (e.g., wetlands, water), to 0.145 for forest HRUs, and 0.17 or 0.18 for agricultural lands. Notably, blowing snow was disabled for forest HRUs, permitting snow interception by the forest canopy. This is a crucial consideration given the substantial forest cover spanning approximately 9 km² within the study watershed. The maximum snow interception load was set to 6.6 kg m⁻², the upper end of the range (5.9 – 6.6 kg m⁻²) reported by Pomeroy et al. (2002). Snow drift was simulated from low aerodynamic resistance HRU to greater roughness HRU, followed by wetlands and waterbodies in depressions in each subbasin (Fang and Pomeroy, 2009).

4.3.4.2. Hydrological Predictions for the Environment (HYPE) Model

HYPE is a semi-distributed, dynamic, integrated and conceptual rainfall-runoff model that has been widely implemented at catchment and continent scale for hydrological and nutrient fluxes simulations (Donnelly et al., 2013; Du et al., 2020; Ghaffar et al., 2021). Runoff generation in HYPE is based on the fill-and-spill mechanism, also known as the bucket model, which is a simplified expression that has been widely implemented to track water fluxes in soil layers (Romano et al., 2011). HYPE can handle a maximum of three soil layers (Fig. 4.2). Soil water will first replenish the unsaturated layers to reach field capacity, and surface and subsurface runoff will be formed if excess water is available. Rainfall and snowmelt water supply the potential of water availability for infiltration, which could end up as either surface runoff, infiltration into the upper most soil layer, or percolation into layers further down through

macropores. The actual amount of infiltration is estimated after removing macropore flow and surface runoff from the total available water for infiltration. Similar to CRHM, HYPE also takes ice layer formation into consideration, which is formed if the minimum daily temperature and the infiltration rate reaches specific thresholds of $< 10^{\circ}\text{C}$ and $> 5 \text{ mm d}^{-1}$, respectively. If an ice lens forms, all infiltration is diverted to surface runoff and macropore flow. Even without ice layers, infiltrability would be hindered if soil temperature in the uppermost layer is below 0°C . For simulating snowmelt, a temperature-index model was used, in which the amount of snowmelt generated is linearly correlated with the difference between the ambient temperature and a threshold temperature (typically 0°C ; Hock, 2003). Evapotranspiration, one of the major components of the water balance, was estimated using the Food and Agriculture Organization (FAO) Penman-Monteith method. This method accounted for both energy balance and mass transfer mechanisms, and the evapotranspiration from the top two soil layers can be determined based on the net downward radiation, ambient temperature, wind speed, saturation and actual vapor pressure (Allen et al., 1998).

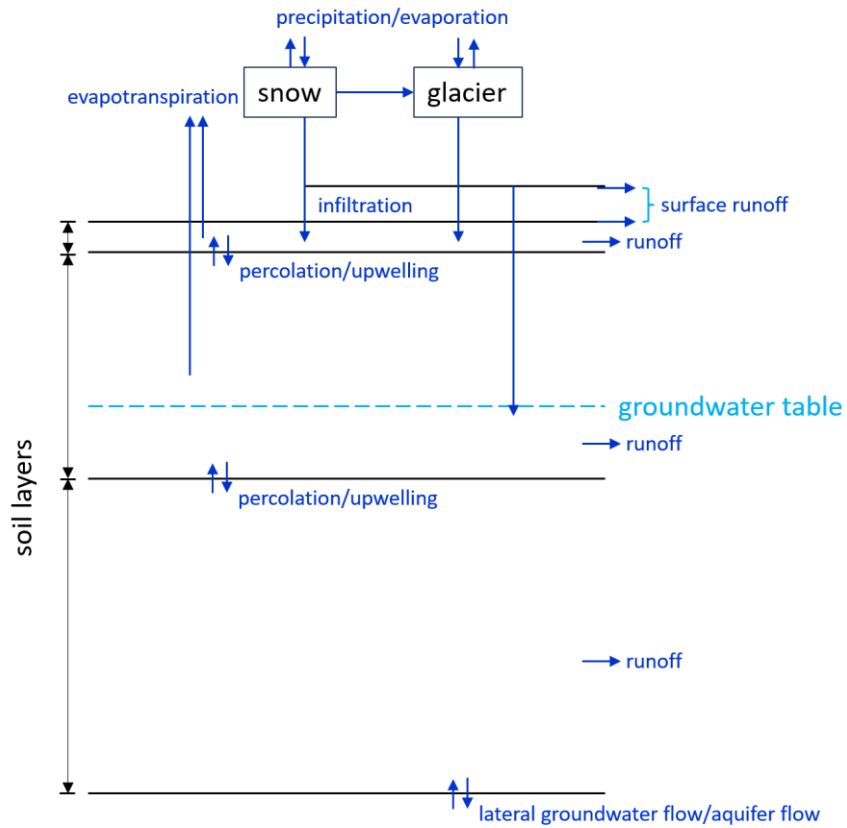


Figure 4.2: Flowpaths in the soil from one land class assuming no drainage tile (adapted from Swedish Meteorological and Hydrological Institute, n.d.)

HYPE parameters are either watershed-, land use-, or soil type-dependent. Table 4.6 summarizes some of the sensitive parameters for streamflow simulation and their values after calibration.

Table 4.6: HYPE model parameters description, dependency, and values

Parameters (Units)	Description	Dependency	Calibrated values
lp (-)	factor for calculating the soil water limit for potential evapotranspiration	General	0.8
rrcs3 (ts ⁻¹ % ⁻¹)	recession coefficient for slope dependence (upper layer)	General	0.002
epotdist (m ⁻¹)	coefficient in exponential function for potential evapotranspiration's depth dependency	General	4.5
cmlt (mm °C ⁻¹ ts ⁻¹)	melting parameter for snow	Land use	[1, 4] ¹
surfmem (d)	upper soil layer soil temperature memory	Land use	[8, 13]
alb (-)	albedo for petmodels	Land use	[0.11, 0.17]
kc (-)	crop coefficient for petmodels	Land use	[0.9, 1.2]
treda (-)	soil temperature control on soil evapotranspiration	Land use	0.7
srrcs (ts ⁻¹)	recession coefficient for surface runoff (fraction)	Land use	[0.01, 0.2]
rrcs1(ts ⁻¹)	recession coefficient for uppermost soil layer	Soil type	[0.05, 0.49]
rrcs2 (ts ⁻¹)	recession coefficient for lowest soil layer	Soil type	0.03
macrate (-)	fraction for macro-pore flow	Soil type	[0.05, 0.4]
mactrinf (mm ts ⁻¹)	threshold for macro-pore flow	Soil type	0
srrate (-)	fraction for surface runoff	Soil type	[0.05, 0.1]
wcwp (-)	wilting point as a fraction, same for all soil layers	Soil type	0.11
wcep1(-)	effective porosity as a fraction, for uppermost soil layer	Soil type	0.01
mactrsm (-)	threshold soil water for macro-pore flow and surface runoff (fraction of wilting and field capacity in uppermost layer)	Soil type	[0.1, 1]

¹: values were within this range depending on the land use and soil type.

4.3.5. Model Assessment

Lack of hydrometric data has been hampering hydrological studies in data-sparse regions and ungauged basins, rendering model calibration and performance assessment challenging (Tsegaw et al., 2020). To evaluate the modeled output generated for the ungauged basin in this study, two alternative variables were used: evapotranspiration (ET) and water yield. The mean annual

evapotranspiration for the Prairie derived from a 30-year average (1979 – 2008) dataset of ET at a 1 km resolution was used. This dataset was estimated by integrating remote sensing land surface data and gridded climate data (Wang et al., 2013). Similarly, annual water yield reported by ecoprovinces with data availability from 1971 to 2019 was also acquired (Statistics Canada, 2023a). To assess the performance of model simulations, the percent bias (PBIAS; Equation 4.1), Nash Sutcliffe efficiency (NSE; Equation 4.2), and mean absolute error (MAE; Equation 4.3) were used.

$$PBIAS = \frac{\sum_{i=1}^n O_i - P_i}{\sum_{i=1}^n O_i} \times 100\% \quad (4.1)$$

$$NSE = 1 - \frac{\sum_{i=1}^n (O_i - P_i)^2}{\sum_{i=1}^n (O_i - \bar{O})^2} \quad (4.2)$$

$$MAE = \frac{1}{n} \sum_{i=1}^n |O_i - P_i| \quad (4.3)$$

Where i is the i^{th} term, O_i is the observation value, P_i is the simulated value, and \bar{O} represents the mean of the observation values (Wu et al., 1995). When calculating the PBIAS of ET, the mean was the long-term average ET value (i.e., 380; Wang et al., 2013). NSE determines the goodness-of-fit between the regional estimates of annual water yield and the simulated water yields generated from the historical dataset, by quantifying the residual variance (Moriassi et al., 2007). Lastly, the MAE quantifies the errors between the observation data and simulation results, which helped to assess the effect of climate modelled data on stream discharge predictions for the reference period.

To capture the general trend of any future projections, including annual temperature, annual precipitation, and annual cumulative stream discharge, the Mann-Kendall trend test (Mann, 1945; Kendall 1975) was used to detect the presence of monotonic trend.

4.3.6. Relationship between Variables

Precipitation is one of the major water components continuously cycled within the hydrological cycle. Understanding how varying amounts of precipitation impact stream discharge is essential. In addition, given that antecedent soil moisture conditions play a critical role in water storage, precipitation from previous fall was also taken into consideration. The relationship between seasonal precipitation and stream discharge was investigated through the coefficient of determination (R^2).

4.4 Results

4.4.1. Future Climate in the Study Area

The long-term trend of ambient temperature at the Beaver Creek watershed is projected to increase, and it is especially pronounced in the distant future period under RCP 8.5 (Fig. 4.3). Monotonic trends ($p < 0.05$) were observed for maximum and minimum temperatures across the near future, and for the distant future period under both RCP scenarios. A warmer climate was generally observed under RCP 8.5 with all average mean temperatures exceeding those under RCP 4.5 in the same period. Using the modelled temperature of the reference period as the baseline, Fig. 4.4 (left) and Fig. 4.5 (left) panels depict the percentage change of the long-term average daily mean temperature of the near and distant future under RCP 4.5 and 8.5, respectively. Over the same period, the increase in temperature was more pronounced under the higher emission scenario (RCP 8.5). For example, the mean multi-decadal temperature under RCP 8.5 in the distant future, was 1.34 °C greater than that under RCP 4.5.

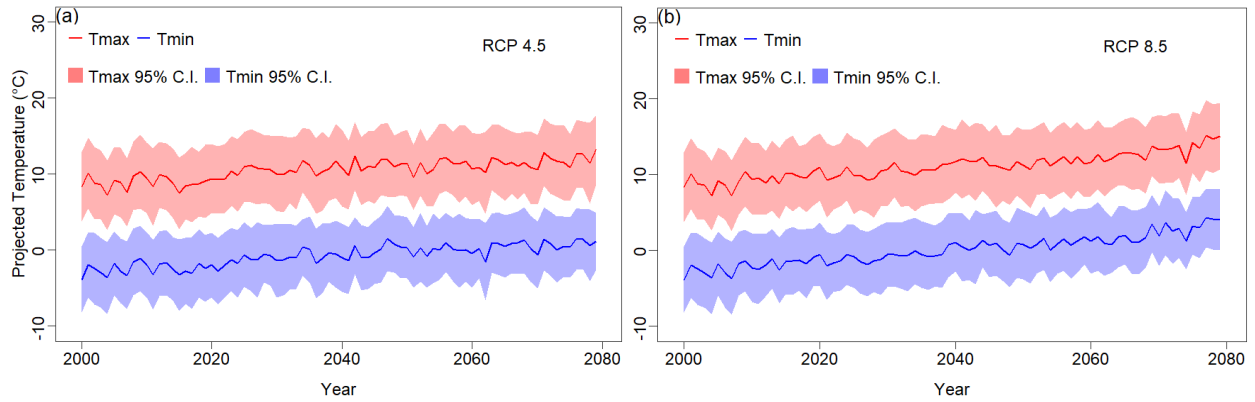


Figure 4.3: Long-term trends of the projected maximum (Tmax) and minimum (Tmin) daily temperature under RCP 4.5 (a) and RCP 8.5 (b) from 2000 to 2079. Solid lines represent the annual averages of maximum and minimum temperature. Shaded areas represent the 95% confidence interval.

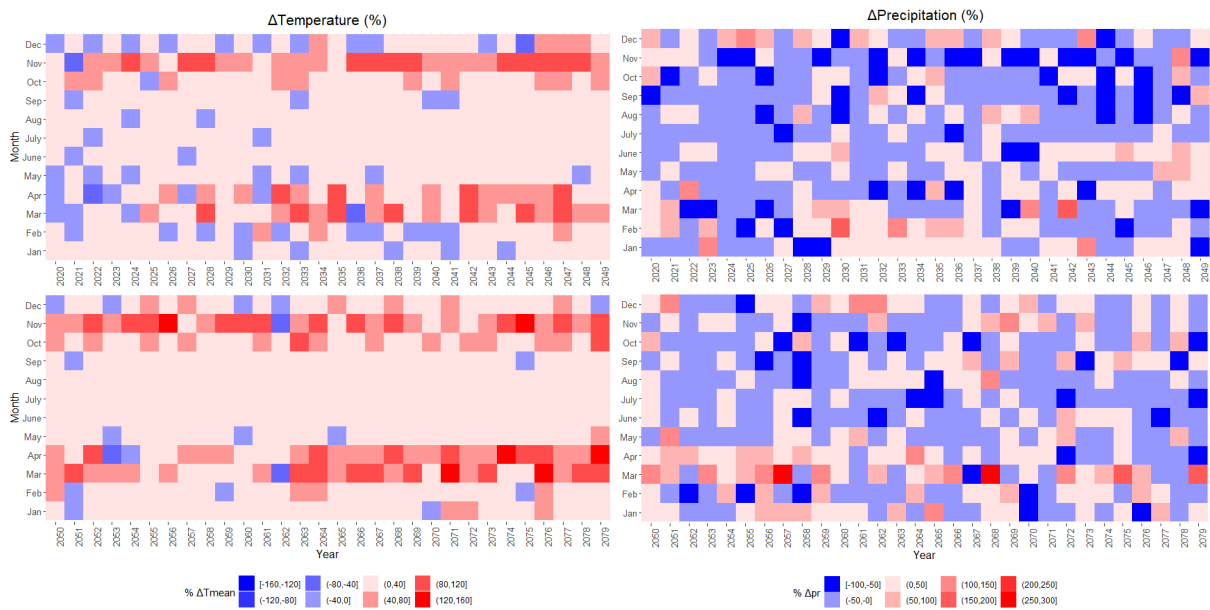


Figure 4.4: Percentage change of ensemble daily mean temperature and total precipitation of each month during the near future (top) and distant future (bottom) under RCP 4.5. Percent change calculated using monthly averages during reference period under RCP 4.5 as the baseline.

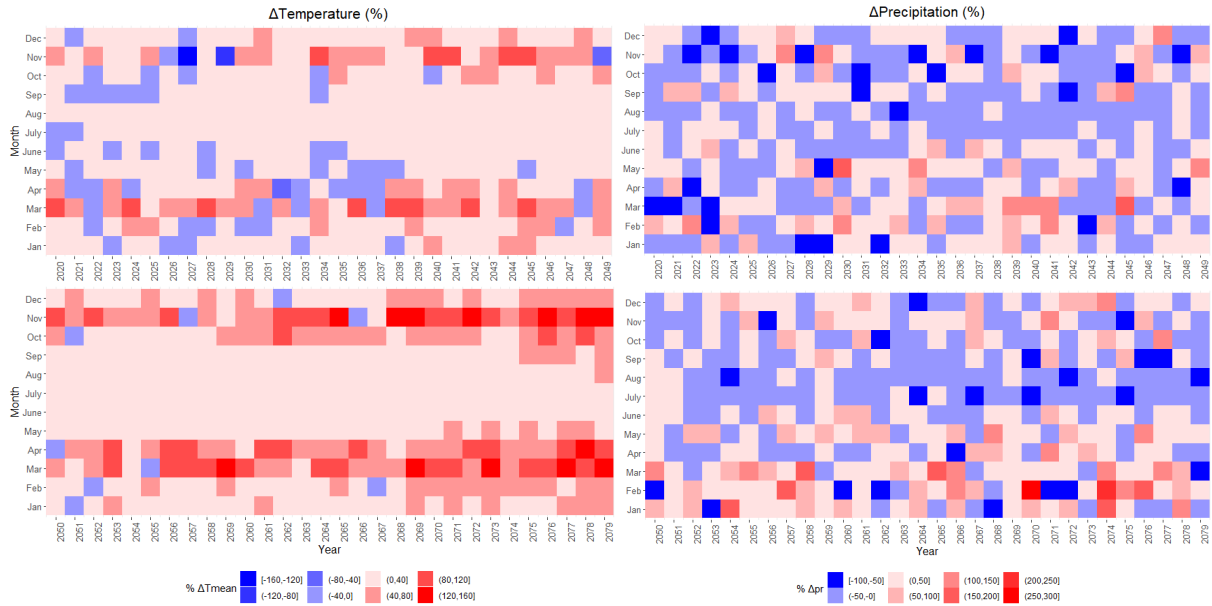


Figure 4.5: Percentage change of ensemble daily mean temperature and total precipitation of each month during the near future (top) and distant future (bottom) under RCP 8.5. Percent change calculated using the monthly average during reference period under RCP 8.5 as the baseline.

In contrast to temperature, there was no evidence to indicate a monotonic increasing trend in precipitation for all simulation periods (Fig. 4.6), except for RCP 8.5 over the entire timespan ($p < 0.05$). The long-term averages of annual precipitation were 487, 477, and 501 mm for the reference, near future and distant future periods under RCP 4.5, respectively. On the other hand, the long-term averages under RCP 8.5 gradually increased from 474 mm for the reference period, to 486 and 508 mm for the near and distant future, respectively. By further segmenting the annual precipitation to a monthly scale (Fig. 4.4 right and Fig. 4.5 right panels), the changes in precipitation distribution can be visually inspected. Despite the fluctuations due to temporal variability, it is still clear that the projected precipitation mostly reduce during summer and fall seasons, particularly for the near future period under RCP 4.5.

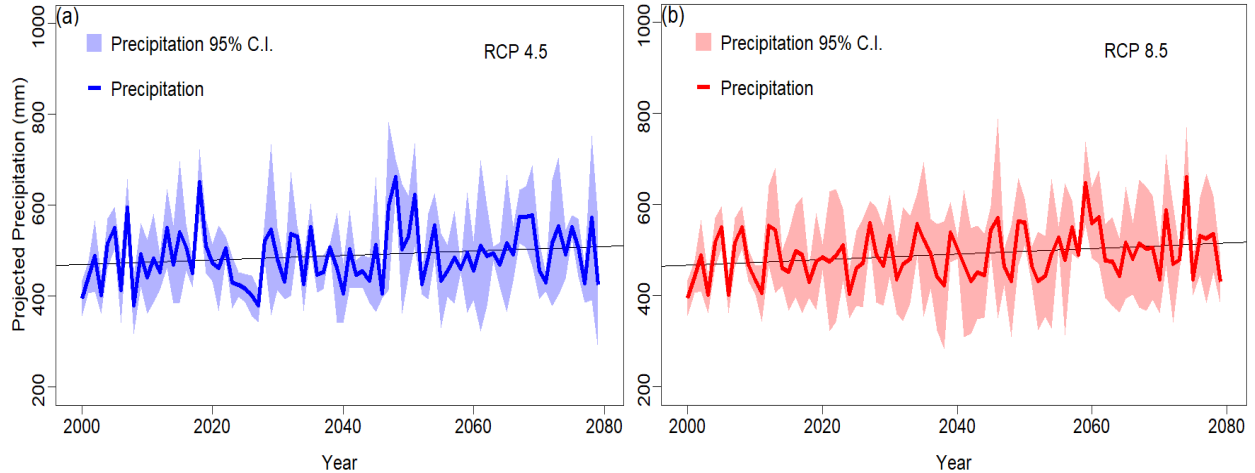


Figure 4.6: Long-term trends of precipitation under RCP 4.5 (a) and RCP 8.5(b). Solid lines represent the annual averages of precipitation. Shaded areas represent the 95% confidence interval.

4.4.2. Model Assessment

For simulations using historical weather data, both CRHM and HYPE were able to capture 10 out of 19 years (52.6%) of ET values within the range of long-term average ET (Fig. 4.7a). Both models overestimated ET between 2010 and 2016. Over the entire reference period, CRHM consistently overestimated ET in comparison to the average ET. On the other hand, HYPE exhibited greater variability and a lower degree of overestimation, as indicated by a PBIAS of +7.2%, in contrast to that of CRHM (+14.1%) in simulating ET.

For the water yield simulation, CRHM achieved a NSE of 0.503 and a PBIAS of +7.8%, whereas HYPE had a NSE of 0.529 and a PBIAS of +0.4%. According to Moriasi et al. (2015), flow simulation is satisfactory if $0.50 < \text{NSE} < 0.60$, while it can be considered good performance with $\pm 2.5 \leq \text{PBIAS} \leq \pm 15$, and very good performance if the $\text{PBIAS} < \pm 2.5$.

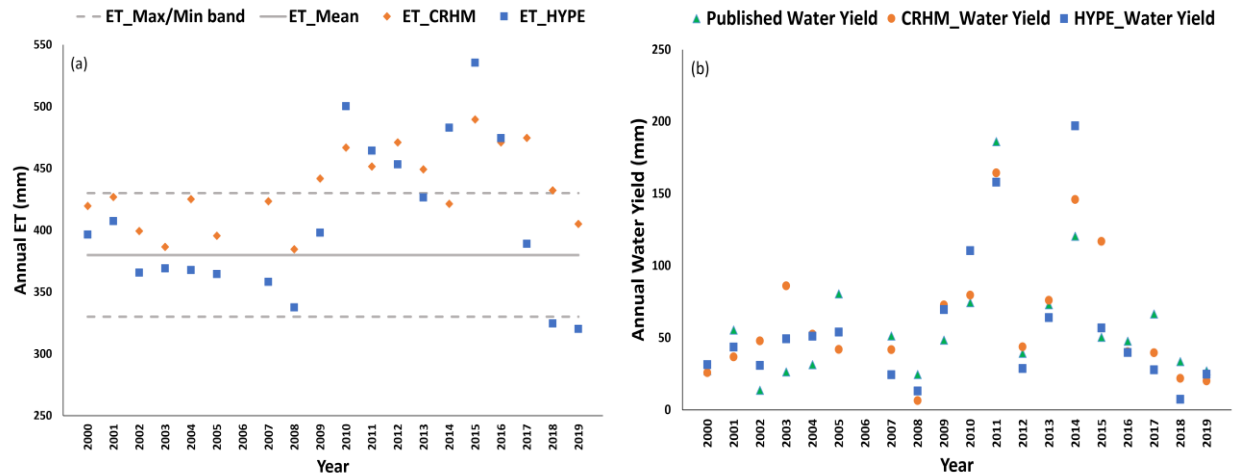


Figure 4.7: Comparisons of evapotranspiration (ET) simulated by CRHM and HYPE models against the long-term average evapotranspiration (ET) range in the Prairies ecozone (a), and the simulated water yield (WY) against the published annual WY reported for the Eastern Prairies and Parkland Prairies ecoprovince (b).

4.4.3. Effect of Climate Modelled Data on Hydrological Simulations

In the realm of climate modeling, hindcasting compares simulated model outputs obtained from the climate modelled data against the observations for the same period (Farjad et al., 2019). This helps to examine the effect of the climate modelled data on the model performance. Both CRHM and HYPE had comparable performance when predicting water yield (Fig.4.8 and Fig. 4.9). On average, the predictions can be explained by the weather pattern (Fig. 4.10) because the interaction between water components is climate-driven. Comparatively, the annual water yield simulated by CRHM was generally greater than the simulations by HYPE with the same forcing data.

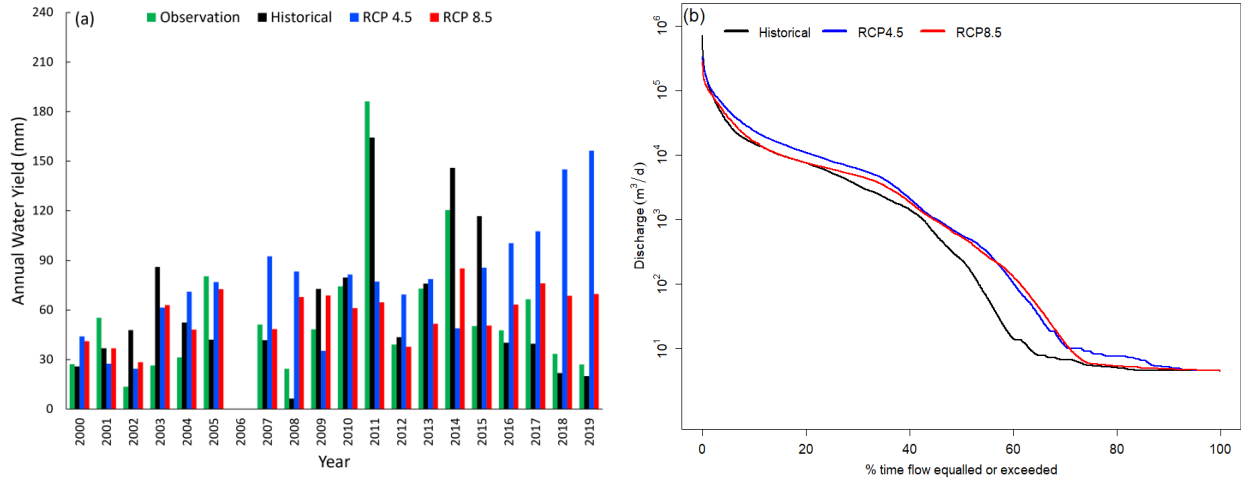


Figure 4.8: Comparison of CRHM simulated water yield (a) and flow duration curve in logarithmic scale (b) using historical dataset and climate modelled data for RCP 4.5 and 8.5

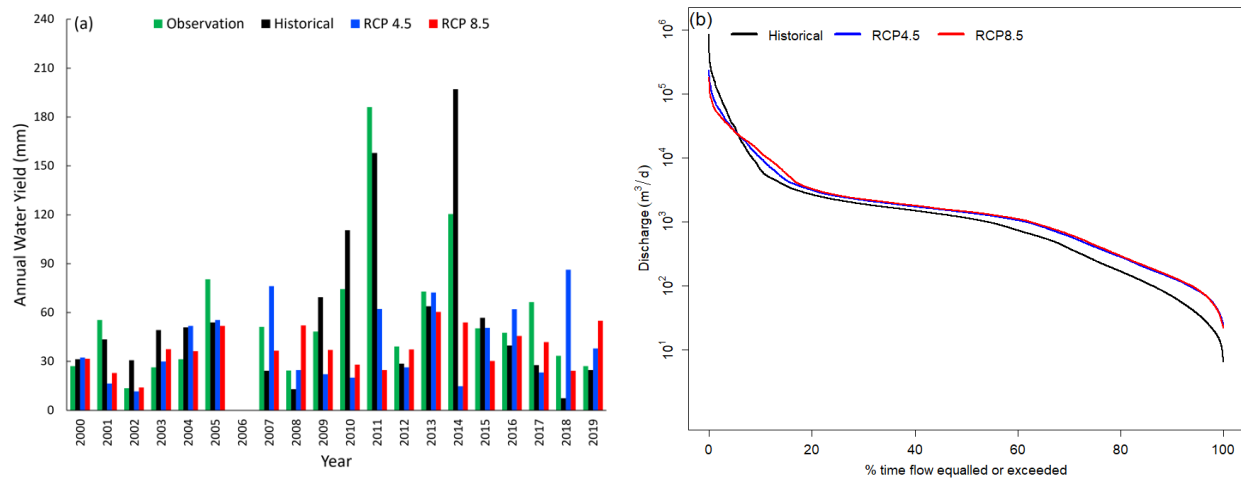


Figure 4.9: Comparison of HYPE simulated water yield (a) and flow duration curve in logarithmic scale (b) using historical dataset and climate modelled data for RCP 4.5 and 8.5

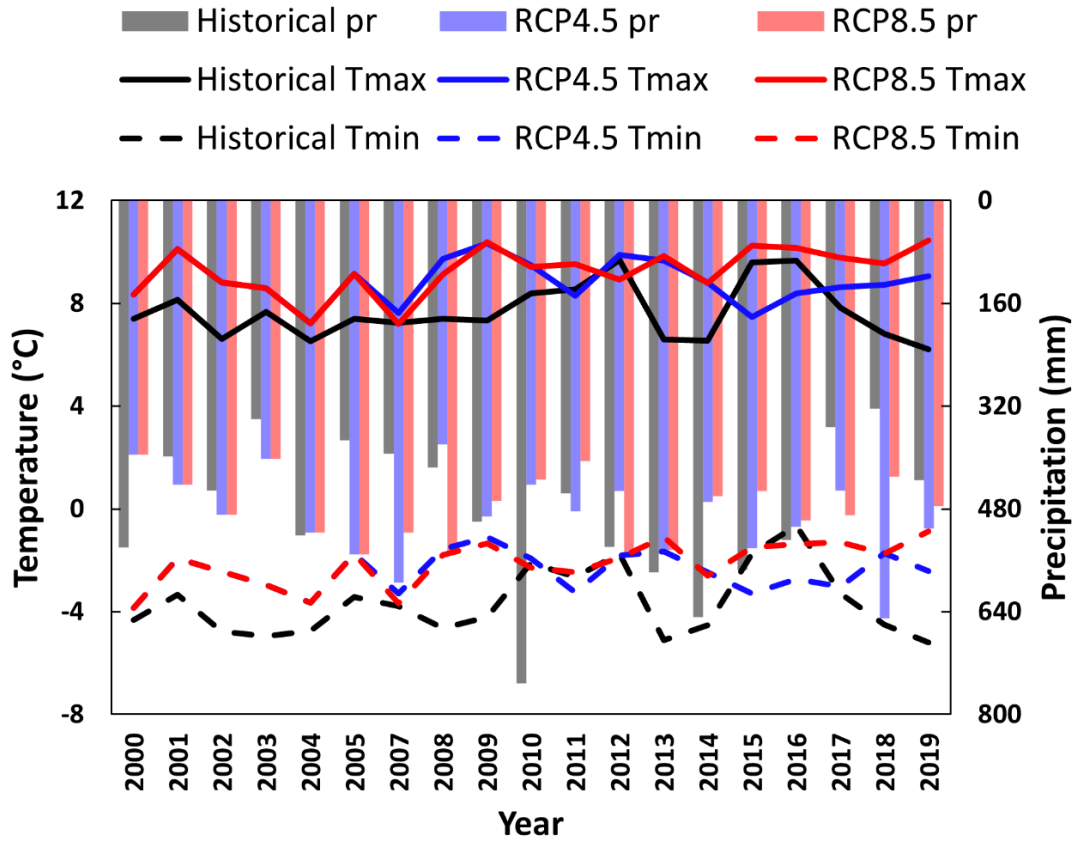


Figure 4.10: Comparison of historical measurement of daily maximum and minimum temperature and annual total precipitation against climate modelled data (RCP 4.5 and 8.5) for the reference period from 2000 to 2019 (except 2006). In the legend, pr, Tmax, and Tmin represent precipitation, maximum temperature, and minimum temperature, respectively.

Despite the numeric similarity between the CRHM and HYPE simulations of water yield (Fig. 4.8a and Fig. 4.9a), the water yield simulated with climate modelled data disagreed with the observation with a substantial bias regardless of the model used (Table 4.7). Only the CRHM model under RCP 8.5 yielded moderate performance in comparison to that of the historical simulation, with a MAE and PBIAS of 24.8 mm and +2.6% for water yield, respectively. For annual ET, the MAE and PBIAS were 57.5 mm and +15.1%, respectively. Significant discrepancies were observed in other scenarios, which were caused by the extreme flow events,

as the majority of the flow events were in agreement between weather datasets according to the flow duration curves (Fig. 4.8b and Fig. 4.9b).

Table 4.7: Assessment metrics for simulated water yield and annual ET during the reference period (2000 – 2019) obtained from climate modelled data (RCP 4.5 and 8.5) against the observations

Model	Scenario	MAE of water yield (mm)	MAE of annual ET (mm)	PBIAS of water yield (%)	PBIAS of annual ET (%)
CRHM	Historical simulation	21.3	53.5	+7.8	+14.1
	RCP 4.5	44.3	56.2	+36.3	+14.7
	RCP 8.5	24.8	57.5	+2.6	+15.1
HYPE	Historical simulation	21.3	51.6	+0.4	+7.2
	RCP 4.5	29.8	66.9	-27.8	+16.6
	RCP 8.5	26.7	46.9	-33	+12.2

4.4.4. Model Forecast

Utilizing the simulated ET for the reference period of the climate modelled dataset as the baseline, CRHM predicted a gradually increased trend in ET (Fig. 4.11), with an exception that ET remained relatively the same in near future under RCP 4.5. Under RCP 8.5, the annual ET gradually increased by 1.3% and 8.2% in the near and distant future, respectively. For HYPE, a 5.4% reduction (i.e., 24 mm) was observed in the multi-decadal average annual ET during the near future period under RCP 4.5. In the distant future period, it increased to the same level (i.e., 443 mm) as the reference period. A similar trend was captured under RCP 8.5 (Fig. 4.12), in which the long-term average annual ET increased by 2.3% in the near future, and 8% in the distant future. Comparatively, the largest interquartile ranges (IQR) produced by CRHM was between 436.2 and 476.6 mm, which were lower than that of HYPE (412.5 – 477.1 mm), indicating the predictions were less variable.

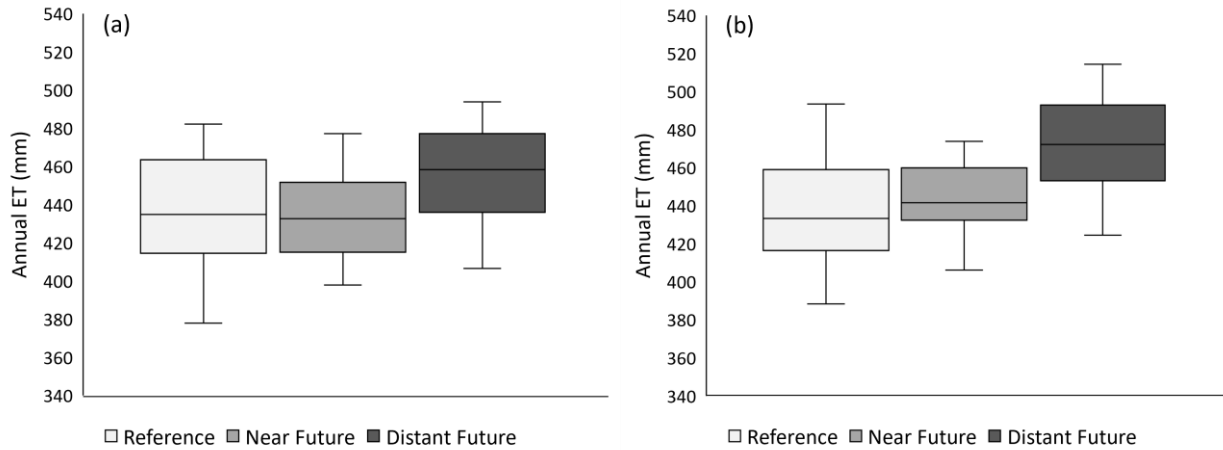


Figure 4.11: Comparison between evapotranspiration (ET) projected by CRHM under RCP 4.5 (a) and RCP 8.5 (b).

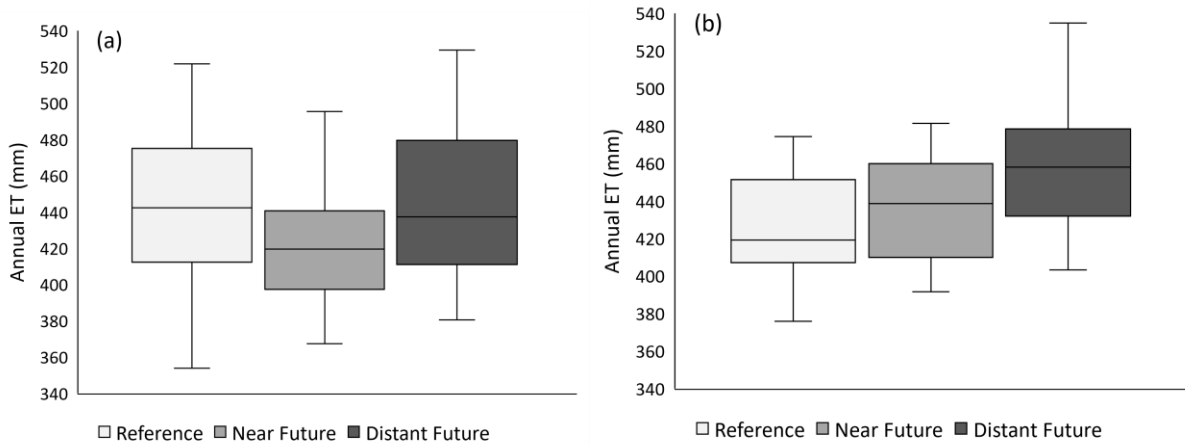


Figure 4.12: Comparison between evapotranspiration (ET) projected by HYPE under RCP 4.5 (a) and RCP 8.5 (b).

According to the Mann-Kendall trend analysis, the monotonic increasing trajectory in stream discharge was only observed under RCP 8.5 ($p < 0.05$; Fig. 4.13) when CRHM was employed. This suggests that streamflow generation is mainly governed by the precipitation pattern, as the only monotonic increasing trend in projected precipitation was observed for RCP 8.5 over the entire simulation period (2000 – 2079; Fig. 4.6). This was further reinforced with the multi-decadal averages of the annual streamflow shown in Table 4.8, in which RCP 8.5 was the only scenario that stream discharge both increased in the near future (+25.7%) and distant future

(+39.4%) periods. Although the average values of stream discharges by HYPE under RCP 8.5 also increased (Table 4.8), the p value from the Mann-Kendall test of 0.67 implied there was no evidence indicating that the trend was statistically significant (Fig. 4.14). The uncertainties in RCP 8.5 were greater than that in RCP 4.5, particularly in the CRHM outputs. Also, the stream discharge generated by CRHM was much greater in magnitude than that of HYPE over the same simulation period. The effect of climate variability on hydrological response, in terms of the pattern of cumulative stream discharge and its associated uncertainties, was amplified in CRHM. Despite these differences, both models independently forecasted a decline in annual stream discharge in the near future under RCP 4.5, followed by a recovery in the distant future. For the higher emission scenario (RCP 8.5), the simulation outcomes from both models consistently indicated an increment in the projected stream discharge.

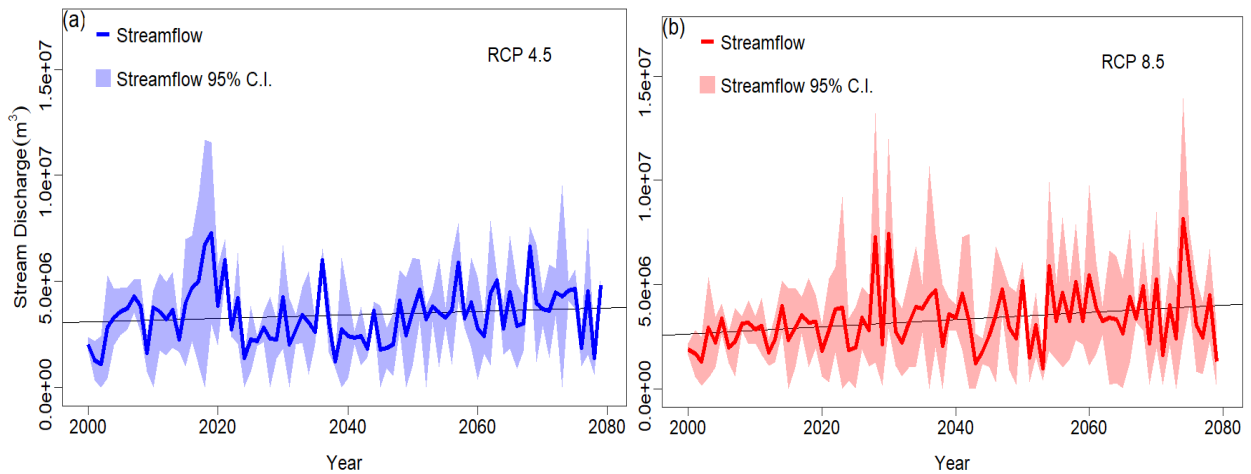


Figure 4.13: Long-term trends of annual stream discharge using CRHM under RCP 4.5 (a) and RCP 8.5 (b). Solid lines represent the average cumulative stream discharge on a yearly basis. Shaded areas represent the 95% confidence interval.

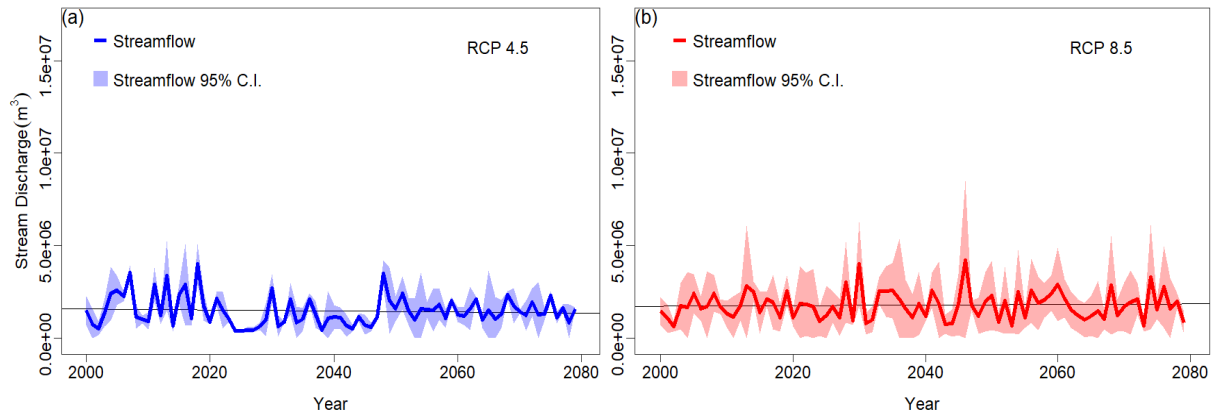


Figure 4.14: Long-term trends of annual stream discharge using HYPE under RCP 4.5 (a) and RCP 8.5(b). Solid lines represent the average cumulative stream discharge on a yearly basis. Shaded areas represent the 95% confidence interval.

Both CRHM and HYPE indicated that the predicted time of peak discharge would shift to an earlier date in the future (Table 4.8), except for the near future period under RCP 8.5 using CRHM with a 2-day delay. Although not necessarily to the same extent, the onset of snowmelt was mostly projected to occur on an earlier date. This implies the duration of snow-covered period will be shortened, potentially leading to a longer growing season. The results also reinforced that snowmelt runoff was the dominant contributor to stream discharge, with the time of peak discharge taking place between early April and mid-May. Noteworthy, the predicted peak discharge occurred at a much earlier date in CRHM than in HYPE, with at least a 25 – 41 day gap in between for the same simulation period.

Table 4.8: Long-term average of ET, streamflow, and time of peak discharge CRHM and HYPE simulations for RCP 4.5 and RCP 8.5 scenarios, respectively. Percentage of change is calculated based on simulated values of the reference period.

		Climate Scenario					
		RCP 4.5			RCP 8.5		
		REF ¹	NF ¹	DF ¹	REF	NF	DF
CRHM	Annual ET (mm)	435 ²	434 (-0.2%)	454 (+4.4%)	438	443 (+1.1%)	473 (+8.0%)
	Annual stream discharge (m ³)	3.605 × 10 ⁶	2.877 × 10 ⁶ (-20.2%)	3.845 × 10 ⁶ (+6.7%)	2.672 × 10 ⁶	3.358 × 10 ⁶ (+25.7%)	3.726 × 10 ⁶ (+39.4%)
	Timing of peak discharge (Julian day)	111	105 (-5.4%)	103 (-7.2%)	105	107 (+1.9%)	98 (-6.7%)
HYPE	Annual ET (mm)	443	419 (-5.4%)	444 (+0.2%)	426	436 (+2.3%)	460 (+8.0%)
	Annual stream discharge (m ³)	1.923 × 10 ⁶	1.162 × 10 ⁶ (-39.6%)	1.537 × 10 ⁶ (-20.1%)	1.761 × 10 ⁶	1.804 × 10 ⁶ (+2.4%)	1.793 × 10 ⁶ (+1.8%)
	Timing of peak discharge (Julian day)	149	139 (-6.7%)	128 (-14.1%)	146	140 (-4.1%)	131 (-10.3%)

¹: REF = reference period, NF = near future, DF = distant future; ²: Bolded values are baselines using climate modelled data during the reference period

4.4.5. Relationship of Seasonal Precipitation and Annual Discharge

The relationship between precipitation and stream discharge was estimated for RCP 4.5 and RCP 8.5 in both models. While not a remarkably strong relationship, precipitation from previous fall and winter months showed a moderate connection with the annual discharge simulated by CRHM, with a R² of 0.4663 and 0.5781 under RCP 4.5 and RCP 8.5, respectively (Fig. 4.15). Similar findings were observed for HYPE, where the precipitation combining previous fall, winter, and spring months related to the cumulative discharge with a R² of 0.5594 and 0.6405 under RCP 4.5 and RCP 8.5, respectively (Fig. 4.16).

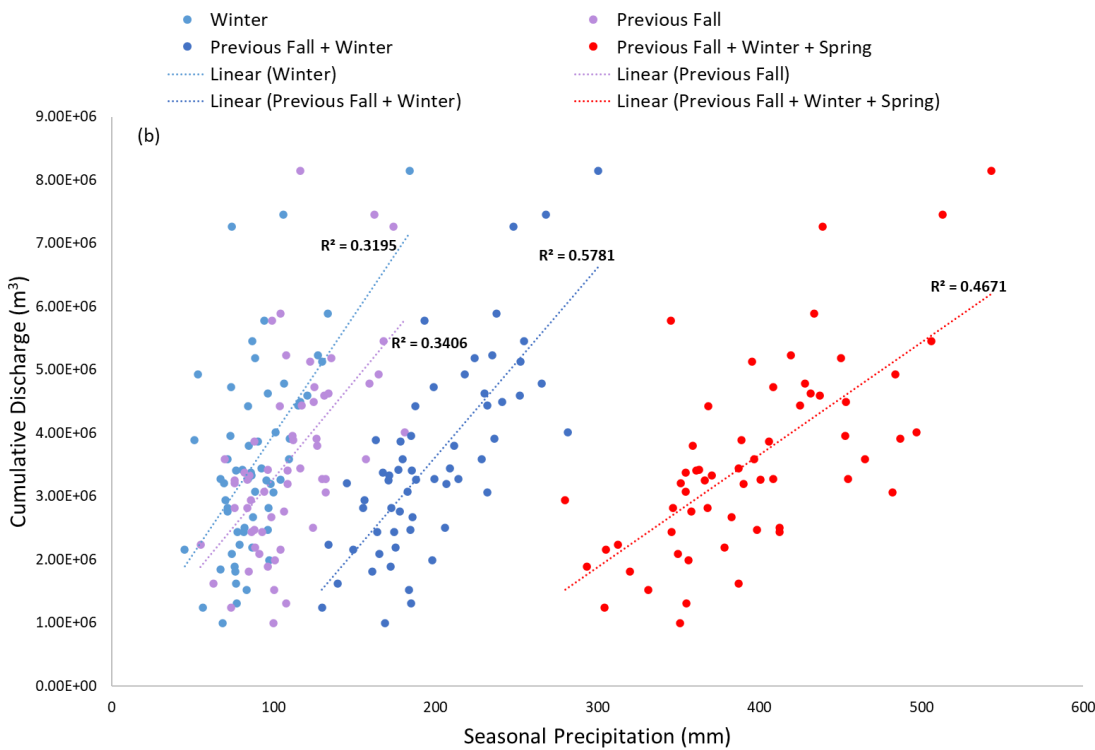
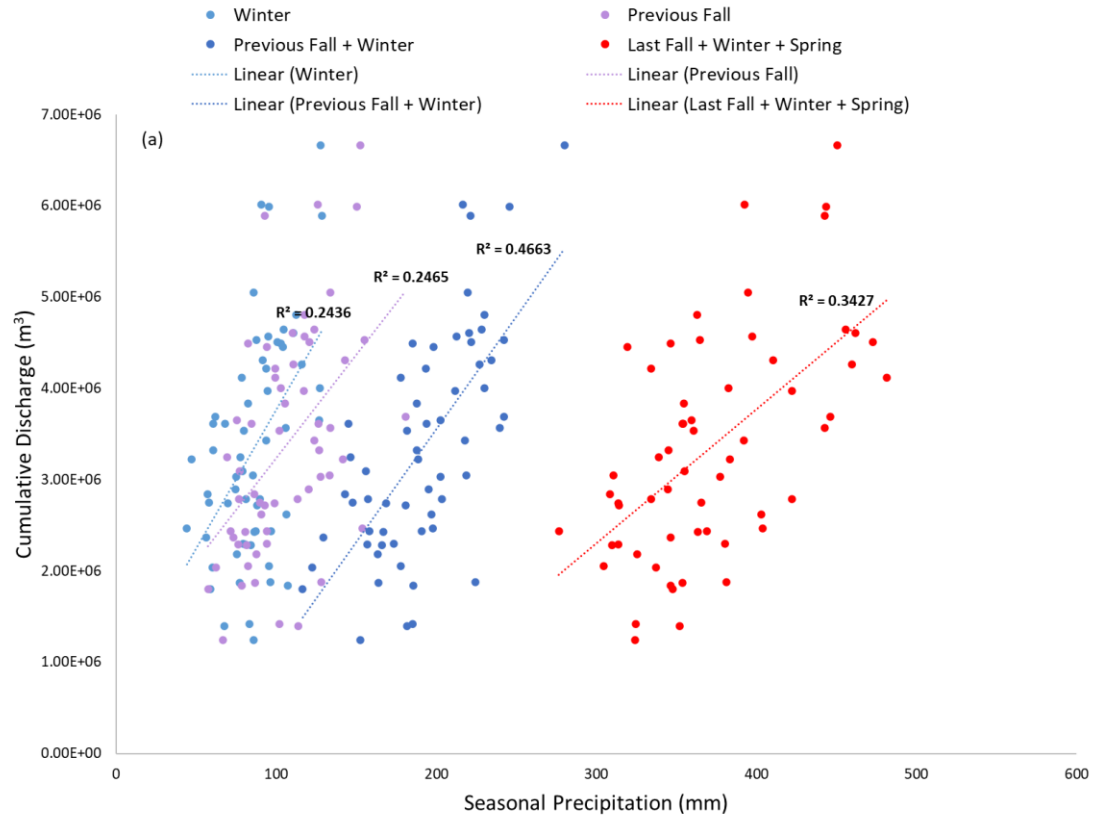


Figure 4.15: Relationship between seasonal precipitation and annual cumulative discharge using CRHM for the near and distant future under RCP 4.5 (a) and RCP 8.5 (b)

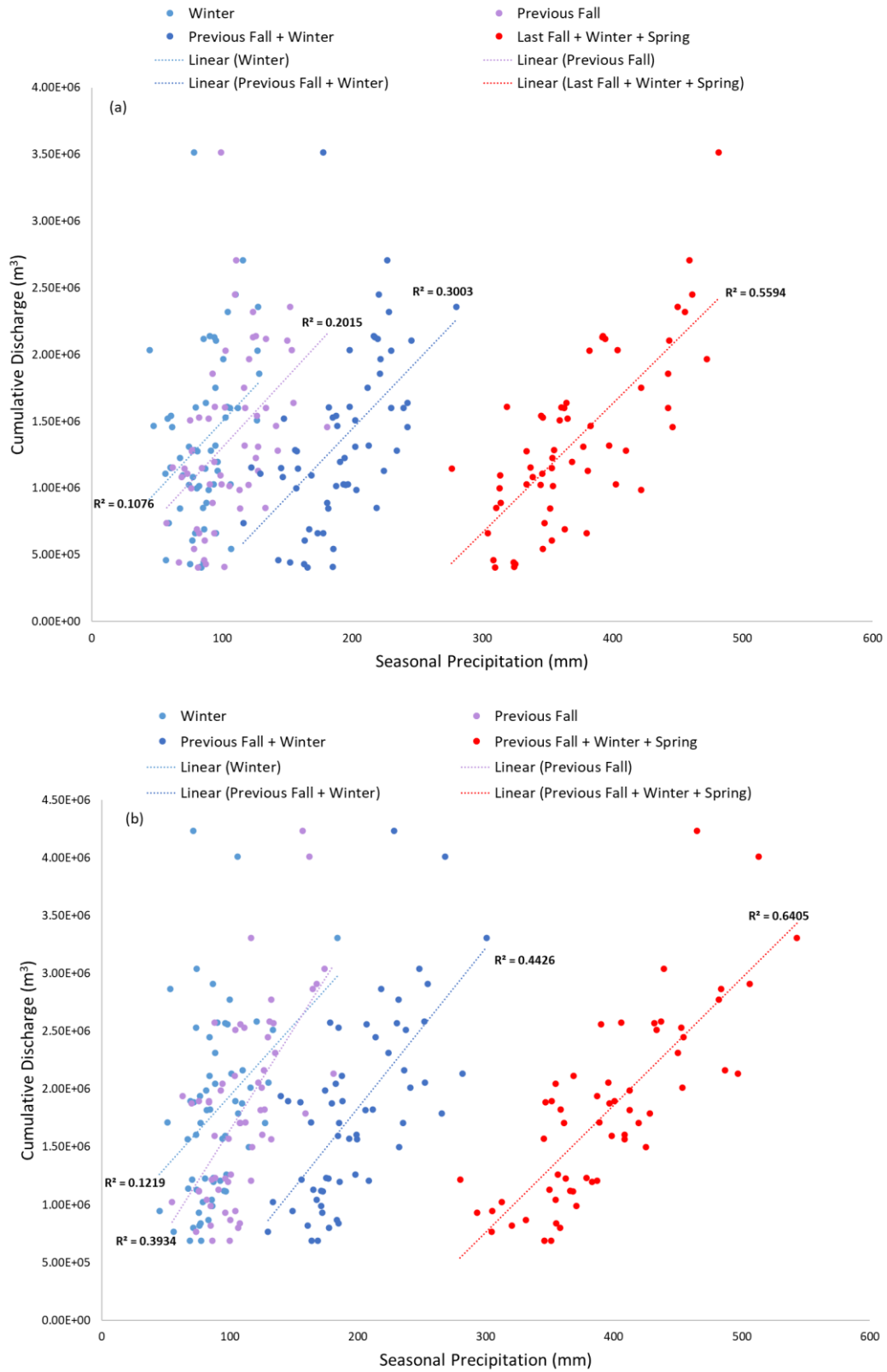


Figure 4.16: Relationship between seasonal precipitation and annual cumulative discharge using HYPE for the near and distant future under RCP 4.5 (a) and RCP 8.5 (b)

4.5 Discussion

As stated in section 4.4.1, the greatest increase in seasonal mean temperatures under both RCP 4.5 and 8.5 was in winter and early spring (November, March, and April). This will shorten the snow-covered duration, leading to early snowmelt events. Meanwhile, coupled with the reduction in projected summer precipitation, it is expected the magnitude and frequency of drought events will increase as well, induced by the warmer climate (Tam et al., 2018).

During model assessment, the water yield simulated by CRHM had a NSE of 0.503, achieved a borderline satisfactory performance ($0.5 < \text{NSE} < 0.6$; Moriasi et al., 2015). This moderate performance could be attributed to the use of regional estimates of water yield for the evaluation of model performance, which was decoupled from precipitation records used for simulation. In 2015, the Beaver Creek watershed received 575 mm precipitation, which above the 75th percentile of all weather stations in the ecoprovince (i.e., Eastern Prairies and Parkland Prairies) that year. This led to a simulated water yield of 116.8 mm in CRHM for 2015, which was twice the published water yield (i.e., 50.3 mm). This highlights the study watershed in 2015 was located in a relatively wetter region compared to other places in the same ecoprovince, and the assessment of water yield simulation was significantly impacted by comparing it to the much lower value reported at a coarser scale. Significant improvements in model performance were observed if 2015 was excluded, with the NSE of water yield assessment increasing from 0.503 to 0.653, and the PBIAS decreasing from 7.8% to 1.7%. This would be classified as very good performance according to the range suggested by Moriasi et al. (2015), especially for an ungauged basin, in which model performance is usually poor (Pomeroy et al., 2013).

HYPE had a satisfactory model performance for water yield with a NSE of 0.529, or a very good performance with a PBIAS of +0.4% during model assessment. However, it was identified

throughout the simulations (including projections) that the outcomes in HYPE were generally lower than that of CRHM, specifically for ET, stream discharge, and the time of peak discharge. Technically, CRHM overestimated the stream discharge with a PBIAS of 7.8%. Also, the much earlier timing of peak discharge (at least 6 days in advance) captured in CRHM and HYPE, could plausibly be one of the reasons that led to the much greater volume of cumulative streamflow than that of HYPE. This has yet remained inconclusive because the outcomes could be affected by many factors, such as weather conditions, land use, soil conditions, drainage, magnitude of individual peaks, and flashiness of the basin. For example, hydrological models have a better predictability in watersheds characterized with steady flood, than flashy basins with high variability in streamflow (Sazib et al., 2020; Haruna et al., 2022). Despite this difference between CRHM and HYPE, both models performed satisfactory in simulating the hydrology of ungauged pasture watersheds in cold climates.

Although both CRHM and HYPE had a satisfactory performance at the assessment phase, weak agreement with substantial biases were found during model hindcast when comparing the water yield simulated by the climate modelled data of the reference period against the observations (Table 4.7). As Duethmann et al. (2020) pointed out, one of the leading causes that hydrological models performed poorly in new climate conditions than those seen in the calibration, was the omission of changes in vegetation dynamics (e.g., length of growing season) in a transient climate. Furthermore, it is possible that the poor performance was attributed to extreme weather events which have been inadequately represented in climate projections (Clarke et al., 2022). Thus, it is not a surprise for hydrological models to perform poorly in low flow events (Deb and Kiem, 2020). Typically, several techniques are often employed to improve hydrological simulations, such as bias correction (Soriano et al., 2019). However, the decision

was made to refrain from employing bias correction strategy in this study due to the high uncertainties arising from the observations used for model assessment (i.e., regional estimates of water yield) at a very coarse spatial scale, which may not be representative of the study area (e.g., year 2015). In fact, hindcast is only effective with a model with strong performance (Chiang et al., 2017), which was not this case because of the high level of uncertainties associated with our models.

Simulation results indicated the timing of peak discharge would take place by 6 – 21 days earlier. This is in agreement with most of studies that also predicted an earlier snowmelt in Canada (Fang and Pomeroy, 2020; Grillakis et al., 2011; Kuo et al., 2017). While the shift of the snowmelt occurrence to an earlier date is driven by the warmer climate in snowmelt-dominant watersheds, an increase in streamflow is not necessarily guaranteed (Byun et al., 2019; Mahat and Anderson, 2013; Jenicek et al., 2021). Kuo et al. (2017) predicted an earlier onset of snowmelt for three river basins within the Lake Simcoe watershed in Ontario, and the projected winter streamflow increased at the expense of a reduction in spring streamflow. It was found that a reduction in streamflow volume was associated with a slower rate of snowmelt, even with an earlier onset of freshet (Barnhart et al., 2016; Chen et al., 2022). Hence, given the complex interaction between water components and the countereffect of climate change (e.g., change in precipitation), further investigation is required to determine the rate of snowmelt, or the depletion rate of snowpack before drawing the conclusion whether an earlier onset increase or decrease the streamflow.

Other sources that introduced uncertainties were also identified, including climate models, emission scenario, natural internal climate variability, and temporal downscaling the projected meteorological data from a daily to an hourly timestep (Cordeiro et al., 2019; Wu et al., 2022).

Among them, the uncertainties associated with emission scenarios can be visualized, as the variation of precipitation under RCP 8.5 is greater than that under RCP 4.5 (Fig. 4.6), resulting in an amplified variations in streamflow projection (Fig. 4.13 and Fig. 4.14). Moreover, the major river valley CRHM model developed by Spence et al. (2022) was used as the template for the Beaver Creek watershed. Utilizing a generalized model could impact the model performance if the governing hydrological processes are no longer applicable or sufficient to represent the local watershed, leading to incomplete or model misrepresentation (Martina and Todini, 2009).

Lastly, the simulated multi-decadal long-term averages in Table 4.8 should be interpreted with caution. The extent of variability associated with this multi-model approach is substantial between CRHM and HYPE. From the model structure perspective, heterogeneity originated from the implementation of different sub-models to handle the same hydrological process in CRHM and HYPE could explain this variability. For instance, the Penman-Monteith model was used for agricultural lands and the Priestley-Taylor model was used for HRUs related to wetland, water, and river channel in CRHM. In contrast, HYPE utilized a more generalization approach with only one potential ET model (petmodel) for the entire basin. Another example was the snowmelt model, in which the temperature index model was applied in HYPE (Hock, 2003). This differs from the energy-budget snowmelt model used in CRHM, which estimates the changes in internal energy of snowpack (Gray and Landine, 1988). With different sub-models, the model representations are anticipated to vary as well, potentially leading to simulation outputs in different scale of magnitude. In terms of parameterization, HYPE assigns parameters predicated upon dependency classification, differentiating between general parameters, those tailored to land use, and those specific to soil types. Conversely, CRHM adopts a more granular approach, whereby a distinct parameter is allocated to each individual HRU, corresponding to a unique

combination of land use and soil type attributes. In addition, CRHM used a finer temporal resolution (i.e., hourly timestep), which would result in differences in model structure and complexity compared to the input data for HYPE (i.e., daily time step; Mouelhi et al., 2006; Ficchi et al., 2019). Calibrated parameters could vary substantially with forcing data at different timesteps (Littlewood and Croke, 2008).

4.6 Conclusion

The implementation of a multi-model approach was used to assess the implications of climate change to hydrological response within a 46.6 km² pasture-dominated ungauged watershed located in Manitoba, Canada. During model assessment, CRHM achieved a satisfactory performance with a NSE of 0.503 and a PBIAS of +7.8% for water yield, while registering a +14.1% PBIAS for ET. HYPE had a similar performance, boasting a NSE of 0.529 and a PBIAS of +0.4% for water yield, along with a +7.8% PBIAS for ET. Simulations performed with future climate datasets under RCP 4.5 and RCP 8.5, indicated that both models forecasted a reduction in annual stream discharge in the near future under RCP 4.5, followed by a recovery in the distant future. Meanwhile, both models concurred in predicting an increase in the multi-decadal stream discharge increased under RCP 8.5. Regardless of the simulation period, the emission scenario, and the model applied, an earlier onset of peak discharge was consistently captured, ranging from 6 to 21 days. The only exception was found in the simulations by CRHM for the near future period under RCP 4.5, with a marginal 2-day delay. To improve the model performance, future work should include more climate models to provide a more comprehensive insight on the hydrological response on the prairies. Most importantly, collecting hydrometric data by field monitoring would be ideal to refine the model for a better representation of this ungauged basin.

BRIDGE TO CHAPTER 5

Given the comparable performance of CRHM and HYPE during model assessment, and considering that HYPE allows for water quality simulation, which is not yet available in CRHM, the subsequent simulation of water quality was exclusively conducted using the HYPE model. Nutrient inputs were derived from the simulation results presented in Chapter 3, while the hydrological behaviors observed in Chapter 4 offered valuable insights into the changes in hydrology induced by climate change. The objective of the water quality simulation was to estimate nutrient export from pasturelands to streams, accounting for the intricate interactions between nutrient pools and hydrological processes.

CHAPTER 5: PREDICTING NUTRIENT EXPORT FROM A PASTURE-DOMINATED UNGAUGED WATERSHED IN MANITOBA UNDER CLIMATE CHANGE

5.1 Abstract

Eutrophication has been identified as one of the potential environmental issues caused by cattle grazing. The objective of this study was to assess the impact of climate change on nutrient export from pasturelands in Canadian Prairies. To achieve this, the Hydrological Predictions for the Environment (HYPE) model was used for hydrological and water quality simulations in a 46.6 km² pasture-dominated watershed in Manitoba, characterized by seasonal cattle grazing. During the historical period between 2000 and 2019, the model demonstrated a good model performance on predicting total nitrogen and phosphorus loading with a Nash-Sutcliffe efficiency (NSE) of 0.586 and 0.544, respectively. Meanwhile, a percent bias (PBIAS) of -11.5% and -3.8% was also achieved for total nitrogen and phosphorus loading, respectively, underscoring the predictive capabilities of the baseline model. Projections with the future climate datasets suggested a reduction in total nitrogen and phosphorus loading under both RCP 4.5 and RCP 8.5. Because nutrients redistribution and export are contingent upon water movement, it was observed that the general trend of water quality closely followed that of the stream discharge, which also showed a reduction or insignificant increase in the future.

5.2 Introduction

Grazing, a common practice in the cow-calf stage of the Canadian beef production system, has been widely used in the Canadian Prairies. Manitoba, one of the Prairie provinces with a large proportion of cow-calf operations, relies on grazing to support its beef industry (Statistics Canada, 2022b). Manitoba generated nearly \$530 million annually in revenue by selling cattle and calves from 2000 – 2020, averaging 27% of the total livestock products traded in the

province (Statistics Canada, 2023b). While generating significant economic benefits, grazing has been under scrutiny due to nutrient export from grazed pastureland, which is one of the prevalent causes of eutrophication (Bourke et al., 2008). Vegetation, manure, and soil have been identified as the predominant sources of nutrients in pasturelands that contribute to the nutrient buildup in downstream water bodies (Beetz, 2002; Khan and Mohammad, 2013).

Nutrient loss from the vegetation pool is attributed by plant residues, and it is closely related to cold regions like Manitoba. Due to sub-zero temperatures in the winter season, the moisture in the plant tissues of ungrazed pastures freezes. Subsequently, during freeze-thaw cycles (FTC) in the spring season, plant tissues suffer mechanical damage induced by the phase change of water, resulting in the rupture of plant tissues and release of solutes in dissolved form (Cober et al., 2018). The amount of nutrient released is influenced by several factors, including plant species (Elliott, 2013; Liu et al., 2014), stage of plant development (Roberson et al., 2007), the degree of FTC temperatures (Øgaard, 2015), residue composition (Liu et al., 2013a), and the number of FTC (Costa et al., 2019; Øgaard, 2015). Among them, studies have revealed that the number of FTC can significantly affect the release of plant nutrients. Comparatively, the nutrients released from plant residues after repeated FTC are greater than those after a single FTC, followed by treatments without freezing involved (Liu et al., 2013a).

Nutrient in the manure pool depends on both manure production and its nutrient content. The quantity of manure produced can vary significantly depending on the type of cattle, ranging from 12 kg day⁻¹ for calves to 62 kg day⁻¹ for lactating cows, which is much higher than other livestock species (Statistics Canada, 2006). Quantifying the nutrient composition of cattle manure is challenging due to its susceptibility to several influencing factors, including dietary composition, digestibility of the feed, the stage of growth the cattle are in, the type of storage method

employed, and the prevailing weather conditions (Government of Manitoba, 2015). As summarized by Pagliari et al. (2020), the majority of manure nitrogen is from urine, whereas feces are the main contributor to total phosphorus excreted.

Nutrient loss from the soil pool is difficult to monitor because soil serves as an intermediate sink where part of the nutrients from the vegetation and manure pools would be trapped upon contact. Besides the interaction between the other two pools, atmospheric deposition is a major input to the soil pool (Gaudio et al., 2015; Chiwa, 2020). Dry deposition, the spreading of particulate matter, originates from industrialization and anthropological activities (Osada et al., 2014). Conversely, wet deposition brings in nitrogen- and phosphorus-containing substances through precipitation, which can be measured by analyzing the precipitation concentrations (Wu et al., 2018). Notably, the uncertainties in nutrient inputs from both types of deposition could have substantial spatiotemporal variability. For instance, Köchy and Wilson (2001) recorded the atmospheric deposition of nitrogen at a rate of 22 kg/ha/yr in Elk Island, Manitoba, between 1994 and 1996. This measurement surpassed the long-term average reported in Manitoba (0.8 – 3.4 kg N/ha/yr) during the 1990s by at least 6-fold. In addition to atmospheric deposition, biological nitrogen fixation, a biochemical process that converts the atmospheric nitrogen gas (N_2) into ammonia (NH_3) for plant growth, is another input of the nutrient cycle (Mus et al., 2016). According to Yang et al. (2010), the nitrogen fixation rate in Manitoba ranged from 16 to 27 kg N ha⁻¹. Those authors observed a higher fixation rate correlated with the expansion of legume coverage.

It is worth noting that a portion of the nutrients from these pools serves as a valuable resource as fertilizer (Lessmann et al., 2023), despite the potential loss to the environment. There are various mechanisms that facilitate nutrient loss. The pathways of nitrogen export can take place

through denitrification, volatilization, leaching, erosion and runoff, and removal of harvested crops (Whetton et al., 2022). In contrast, the loss of phosphorus occurs exclusively in particulate and dissolved form via pathways intertwined with water, namely leaching, erosion and runoff. This is primarily due to the fact that phosphorus cannot be transformed into gaseous form (i.e., phosphine) under the conditions on pasturelands (Mackey and Paytan, 2009). Nutrients in dissolved form have been found the most prominent during spring snowmelt or intense rainfall-induced runoff events, indicating that leaching, erosion and runoff are the governing pathways of nutrient loss in cold regions (Wilson et al., 2019). A long-term study conducted at the South Tobacco watershed in Manitoba between 1993 and 2010, reported that 91% of total nitrogen and 73% of total phosphorus exported were in dissolved form during spring snowmelts, implying that eutrophication in the Canadian Prairies region is driven by the accumulation of dissolved nutrients (Liu et al., 2013b).

Besides the nutrient pools, accounting for the hydrological processes is critical when investigating nutrient export, as nutrient transport is intrinsically linked to water movement (Bogunovic et al., 2022). Analyzing the interaction of hydrological processes and the corresponding response in nutrient loss can be achieved by employing a hydrological model and a water quality model. The Hydrological Predictions for the Environment (HYPE) is an integrated and conceptual model developed by the Swedish Meteorological and Hydrological Institute (SMHI), featuring the capability of nutrient fluxes simulation that vary dynamically along the hydrological processes generated from a semi-distributed hydrological model (Lindström et al., 2010). By default, HYPE allows for the incorporation of up to three soil layers with user-defined soil depth and texture, and performs simulations at a daily time step. Similar to other hydrological models, runoff generation in HYPE follows the concept of fill-and-spill

mechanism, assuming any infiltration would presumably saturate the lowest unsaturated soil layer until fully saturation, before diverting any excess water into surface runoff (Ahmed et al., 2023). Compared to other models, HYPE stands out with its complete integration of hydrological and nutrient dynamics to simulate the overall water balance and the soil nutrient balance that some water quality models are not capable of (Lindström et al., 2010). Transformation and transport of inorganic and organic nitrogen, dissolved and particulate phosphorus through multiple pathways, such as erosion, denitrification, primary production, sedimentation, resuspension, and mineralization, are simulated by HYPE. Moreover, HYPE has proven its ability to assess impacts of climate change on nutrient discharge. Donnelly et al. (2011) used HYPE to evaluate the change in water and nutrient fluxes under climate change in the Baltic Sea basin. Compared to the simulations during 1971 and 2000, they found the projected stream discharge during 2071 and 2100 increased by 3% to 14%, the total phosphorus loads increased by 14 to 23%, and the total nitrogen loads decreased by 3% in one climate scenario, but increased ranging from 1 to 4% in other scenarios. These findings reinforced that model simulation is subjected to spatial variability.

Hydrological and water quality simulations in data-sparse regions has been a generally acknowledged challenge in hydrological modeling (Qi et al., 2020). A frequently employed strategy in the context of ungauged basins that lack gauging stations to monitor and collect hydrometric data, is parameter transferability, which adopts calibrated parameters for regions that share similar landscape characteristics from gauged basins (Pomeroy et al., 2014). This approach can be used to achieve reliable model performance in ungauged basins with HYPE (Lindström et al., 2010; Strömqvist et al., 2012).

The objective of this study was to use the HYPE model to assess nutrient export from a pasture-dominated watershed under climate change. Specifically, the analysis focused on the load of total nitrogen and total phosphorus.

5.3 Materials and Methods

5.3.1. Study Area

The study area (50°23'36" N, 101°21'27" W) is a 46.6 km² basin located within the Beaver Creek watershed, Manitoba. Up to 72% of the area is occupied by pasturelands, followed by 19% forest, 8% farmlands, and 1% other land covers, such as barren land, urban areas, and wetlands (Fig. 5.1; Agriculture and Agri-Food Canada, 2023). The pasturelands within the study area have been managed by the Association of Manitoba Community Pasture (AMCP), with a 10-year average carrying capacity around 2600 animal unit months (AUMs), equivalent to 77 AUMs km⁻² as the stocking rate (Association of Manitoba Community Pasture, 2021). The study area has a flat topography, featuring gentle slopes ranging from 2% to 5% (U.S. Geological Survey, 2014). The dominant soil type (95% of the area) is characterized as loamy sand, with a composition comprising 8% silt, 6% clay, and 86% sand (Cordeiro et al., 2018).

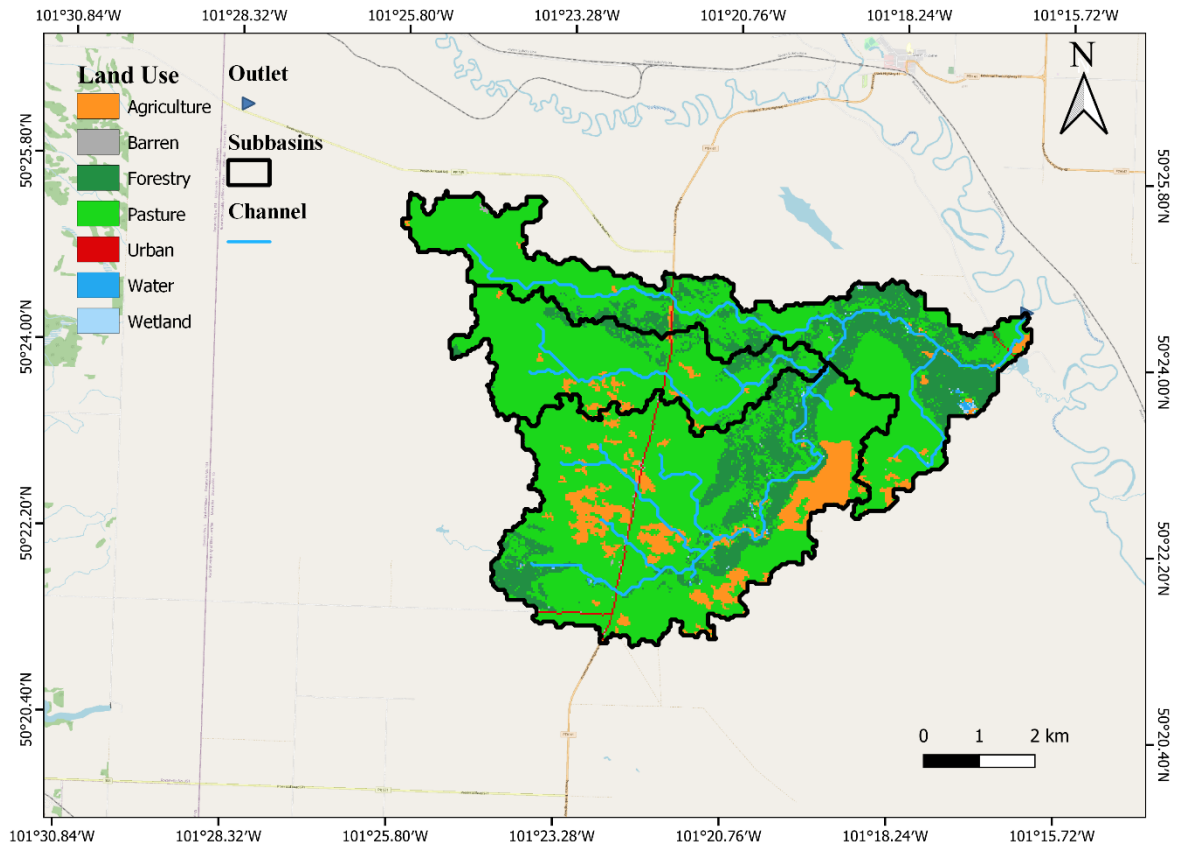


Figure 5.1: Land use in of the study area within the Beaver Creek watershed in Manitoba

Due to its cold continental climate, Manitoba generally has a cold and extended winter season (Delos Reyes et al., 2016). Based on the historical weather data collected from multiple stations near this region, the long-term (2000 – 2020) annual temperature ranged from -3°C to 7°C , with an annual precipitation ranging from 320 to 750 mm (Manitoba Agriculture, 2022; Environment and Climate Change Canada, 2023a). The Birtle weather station, which is the closest to the study area, recorded an annual average wind speed of 13.7 km per hour. This plays a pivotal role in promoting the blowing snow phenomenon, thereby facilitating the redistribution of snow during winter months (Taylor, 1998).

5.3.2. Input Datasets

5.3.2.1. Historical Climate Data

To assemble a historical dataset, meteorological records from 1998 to 2019 were prepared. The dataset consisted of average temperature (°C), maximum temperature (°C), minimum temperature (°C), wind speed (m s⁻¹), precipitation (mm), and relative humidity (%) at a daily time step. Birtle station (50°24'39"N, 100°53'36"W) was the station which the majority of the weather data was obtained (Manitoba Agriculture, 2022). Supplemental data from other stations in close proximity were also obtained to fill data gaps. Table 5.1 lists the sources of each climate variables with the methods applied for gap filling.

Table 5.1: Composition of the historical dataset at a daily timestep.

Variable	Period	Sources (timestep)	Gap-filling Method
Temperature (Maximum, Mean, Minimum)	1998 – 2007	ShoalLake CS station (hourly)	DR ¹ , DA ² , SD ³
	2008 – 2019	Birtle station (hourly)	DR, DA
Wind Speed	1998 – 2007	ShoalLake CS station (hourly)	DR, DA, SD
	2008 – 2019	Birtle station (hourly)	DA
Precipitation	1998 – 2007	ShoalLake CS and Rossburn 4 North stations (daily)	DR, SD
	2008 – 2016 (non-winter months)	Birtle station (hourly)	DA
	2008 – 2016 (winter months)	ShoalLake CS and Rossburn 4 North stations (daily)	DR
	2017 – 2019	Birtle station (hourly)	DA
Relative humidity	1998 – 2007	ShoalLake CS station (hourly)	DA, SD
	2008 – 2019	Birtle station (hourly)	DA

¹ DA = Data aggregation from hourly to a daily timestep; ² DR = Data retrieved from nearby stations; ³ SD = Synthetic data from NASA Power database for Year 2006 (National Aeronautics and Space Administration. 2023)

Simulation results for year 2006 were excluded from model assessment, given the fact that a considerable amount (i.e., more than half a year) of missing gaps were found. Synthetic data was used to create a complete dataset. In addition, year 1998 and 1999 were not included in model assessment because they are used for model warm-up.

5.3.2.2. Future Climate Data

Future climate data for the near future (2020 – 2049) and distant future (2050 – 2079) periods were prepared for Representative Concentration Pathways 4.5 and 8.5 (RCP 4.5 and RCP 8.5), capturing a spectrum of possible future scenario characterized by varying degrees of greenhouse gases emissions and mitigation policy (Baek et al., 2013). The simulation period spans from 1998 to 2079, and daily data were retrieved from the North American component of the international Coordinated Regional Downscaling Experiment (NA-CORDEX; Mearns et al., 2017) database. In this study, the climate models used were CanESM2.CanRCM4, CanESM2.CRCM5-UQAM, and MPI-ESM-LR.CRCM5-UQAM, which are three regional climate models (RCMs) driven by various global climate models (GCMs) from the Coupled Model Intercomparison Project Phase 5 (CMIP5; Taylor et al., 2012).

5.3.2.3. Datasets for Watershed Delineation and Hydrological Response Unit (HRU)

Definition

Watershed delineation and hydrological response unit (HRU) definition were carried out through the Quantum Geographic Information System (QGIS) interface for the Soil and Water Assessment Tool (SWAT) model (QSWAT, Dile et al., 2015). Inputs used in these procedures include topography, land use, and soil datasets obtained from the digital elevation model (DEM; U.S. Geological Survey, 2014), the annual crop inventory (Agriculture and Agri-Food Canada, 2023), and the soil landscapes of Canada database previously processed by Cordeiro et al.

(2018), respectively. As a result, the Beaver Creek watershed was divided into three subbasins with 13 land uses and 22 distinct HRUs (Table 5.2).

Table 5.2: Information of hydrological response units (HRUs) in the study watershed.

HRU ID	HRU acronym	Land use	Soil texture	Percentage of coverage		
				SB 1*	SB 2	SB 3
1	PAST/LoSa	Pasture	Loamy sand	67.6	84.7	63.9
2	PAST/CiLo	Pasture	Clay loam	0.1	-	4.5
3	BARL/LoSa	Barley	Loamy sand	0.1	-	0.1
4	OATS/LoSa	Oats	Loamy sand	0.1	-	-
5	OATS/CiLo	Oats	Clay loam	-	-	0.3
6	SOYB/LoSa	Soybean	Loamy sand	1.0	-	-
7	SWHT/LoSa	Spring wheat	Loamy sand	1.1	0.3	0.7
8	SWHT/CiLo	Spring wheat	Clay loam	-	-	0.3
9	WWHT/LoSa	Winter wheat	Loamy sand	8.0	3.6	1.0
10	CANP/LoSa	Canola	Loamy sand	2.7	-	0.2
11	CANP/CiLo	Canola	Clay loam	-	-	0.2
12	BARR/LoSa	Barren	Loamy sand	0.3	0.1	0.2
13	BARR/CiLo	Barren	Clay loam	-	-	-
14	FRST/LoSa	Forest	Loamy sand	16.5	10.1	20.8
15	FRST/CiLo	Forest	Clay loam	0.7	-	6.2
16	URLD/LoSa	Urban (low density)	Loamy sand	0.7	0.4	0.2
17	URLD/CiLo	Urban (low density)	Clay loam	-	-	0.1
18	WETL/WA	Wetland	-	0.1	-	0.3
19	WETL/WA	Wetland	-	-	-	0.1
20	WATR/WA	Water bodies	-	0.2	-	0.2
21	WATR/WA	Water bodies	-	-	-	-
22	River Channel	River	-	0.8	0.8	0.7

*SB = subbasin

5.3.3. Water Quality Simulations using the Hydrologic Predictions for the Environment

(HYPE) Model

The results of the hydrological simulations using HYPE were already shown and discussed in Chapter 4, this section only covers the water quality aspect. Briefly, HYPE was set up and calibrated to simulate streamflow discharge and export of total nitrogen and phosphorus for the

reference period. Model performance for hydrological simulations (i.e., water yield) were defined satisfactory based on a Nash-Sutcliffe efficiency (NSE) of 0.529, and a percent bias (PBIAS) of +0.4%.

Three major pools were included as nutrient sources in the model, namely, vegetation, manure, and soil. The initiation and the end of manure application within the HYPE model were contingent upon user-defined inputs, aligning with the grazing season duration in the study area from May to September (Association of Manitoba Community Pasture, 2021). Manure application was reset each year throughout the simulation. For this study, the simulated annual mean values of manure nitrogen and phosphorus from the Integrated Farm System Model (IFSM) described in Chapter 3 were utilized as the amount of manure nutrient being applied during the historical and future periods. Nutrient inputs from the vegetation pool were also simulated by IFSM, where the amount of pasture residues was assumed to be 60% of the above-ground biomass (Legesse et al., 2018). Nutrient composition of the residues was based on a recent study that measured the nutrient content of clipped pasture in fall and spring at the Johnson Farm in Manitoba (Appleyard, 2023). Vegetation nutrient values used in this study were averages of the nutrient content in residues during winter months. Nitrogen and phosphorus content of the residues were 2.036% and 0.15% of dry matter, respectively (Appleyard, 2023). For the soil pool, HYPE simulates the process of atmospheric deposition by considering wet deposition in precipitation as an addition to the inorganic nitrogen and dissolved phosphorus pools, whereas that of dry deposition is included in the inorganic nitrogen and the particulate phosphorus pools in the uppermost soil layer (Lindström et al., 2010). In terms of land management for the community pasture, it was assumed that zero irrigation, no-tillage, and no

fertilizer was used. Lastly, the Food and Agriculture Organization (FAO) Penman-Monteith equation was implemented within HYPE to determine crop evapotranspiration.

HYPE model parameters can be categorized as general parameters applied to the entire watershed, land use parameters, and parameters that are specific for different soil types (Pierong and Takman, 2014). Table 5.3 lists parameters that are relevant to the water quality simulation with their corresponding values.

Table 5.3: HYPE model parameters description, dependency, and values.

Parameters (Unit)	Description	Dependency	Calibrated values
rivvel (m s ⁻¹)	Celerity of flood in watercourse (rivvel>0)	General	0.4
denitrln (d ⁻¹)	parameter for denitrification rate in soil	Land use	0.1
dissolfn (d ⁻¹)	decay of fastN to dissolved organic N	Land use	0.01
dissolhn (d ⁻¹)	decay of humusN to dissolved organic N	Land use	[0.01, 0.7] ¹
minerfn (d ⁻¹)	mineralisation of fastN to inorganic N	Land use	1
degradhp (d ⁻¹)	decay of humus to fastP	Land use	0.1
soilerod (g J ⁻¹)	characteristic of soil for calculation of soil erosion (erodibility)	Soil type	[1.5, 11]
soilcoh (kPa)	characteristic of soil for calculation of soil erosion (cohesion)	Soil type	86
freurate (d ⁻¹)	parameter that steers adsorption/desorption speed	Soil type	0.12
freuc (kg ⁻¹)	parameter in Freundlich equation (coefficient)	Soil type	138.8
freuexp (-)	parameter in Freundlich equation (exponent)	Soil type	1.6

¹: values were within this range depending on the land use or soil type.

5.3.4. Model Assessment

The assessment of hydrology simulations by HYPE has been presented in Chapter 4; therefore, only the simulations related to water quality are presented here.

Since Beaver Creek watershed is an ungauged basin, there is no hydrometric station in close proximity reporting streamflow or water quality data. Therefore, observation data were acquired

from the Swan Creek near Lake Manitoba, an alternative watershed that is physiographically similar to the Beaver Creek watershed, and it is approximately 230 km away from the Beaver Creek watershed. Approximately 76% of land cover within Swan Creek is pastureland, and the dominant soil type is loam with 35% silt, 25% clay, and 40% sand. Based on the basin classification proposed by Spence et al. (2022), both Beaver Creek and Swan Creek are categorized as the same basin type: major river valleys. An existing Water Survey of Canada gauging station at Swan Creek (05LN006; 50°43'14" N, 98°4'32" W) recorded daily flow rate data (m³/s) every year from March to October between 2013 and 2021 (Environment and Climate Change Canada, 2023b). Meanwhile, the seasonal total nitrogen and phosphorus concentration data (mg L⁻¹) has been measured at the Swan Creek drain near the Lunder station (MB05LNS016; 50°40'48" N, 98°8'24" W) since 2011 (Water Quality Management Section, 2023). Because the two stations are not at the same location, the drainage area ratio method was applied to estimate the flow rate data at the water quality station (Archfield and Vogel, 2010). This is a regionalization method that utilized the ratio of drainage area to determine the streamflow at an ungauged catchment based on the streamflow at a gauged site. The relationships were initially established between the discharge volume and the nutrient concentration, but poor R² values were obtained, which was likely attributed to the fact that the hydrometric station and the water quality monitoring site were not at the same location. As a result, the relationships were established using linear regression between the discharge volume (m³) and both the total nitrogen load [kg; Equation (5.1)] and the total phosphorus load [kg; Equation (5.2)], with a R² of 0.964 and 0.870, respectively.

$$N \text{ load} = 1.296 \times 10^{-3} \times \text{discharge volume} \quad (5.1)$$

$$P \text{ load} = 5 \times 10^{-5} \times \text{discharge volume} \quad (5.2)$$

The relationships established at Swan Creek were transferred to the Beaver Creek watershed. Then, regional estimates of the annual water yield (mm) for ecoprovinces between 1971 and 2019 published by Statistics Canada (2023b) were multiplied by the watershed area to determine the corresponding total nitrogen and phosphorus loads. These estimated loads served as observation values to calculate the Nash-Sutcliffe efficiency [NSE; Equation (5.3)] and the percent bias [PBIAS; Equation (5.4)] for model assessment. Additionally, the Mean Absolute Error [MAE; Equation (5.5)] was used in the model hindcast assessment, measuring the absolute difference between the nutrient loads simulated by HYPE with climate modelled data for the reference period versus the estimated loads.

$$NSE = 1 - \frac{\sum_{i=1}^n (O_i - P_i)^2}{\sum_{i=1}^n (O_i - \bar{O})^2} \quad (5.3)$$

$$PBIAS = \frac{\sum_{i=1}^n O_i - P_i}{\sum_{i=1}^n O_i} \times 100\% \quad (5.4)$$

$$MAE = \frac{1}{n} \sum_{i=1}^n |O_i - P_i| \quad (5.5)$$

Where i as the i^{th} term, O_i stands for observation, P_i as the predicted nutrient loads, and \bar{O} represents the average of the observation values (Moriassi et al., 2007).

In order to conduct a trend analysis on model projections for precipitation, temperature, streamflow, and water quality, the Mann-Kendall test was carried out. This analysis aims to identify statistically significant monotonic trends, whether increasing or decreasing (Yue and Wang, 2004).

5.4 Results

5.4.1. Future Climate

The projected daily mean temperature showed a statistically significant monotonically increasing trend ($p < 0.05$) in all simulation periods, as well as in the entire period (2000 – 2079), with the exception of the reference period under RCP 4.5 ($p = 0.9$; Fig. 5.2), indicating a generally warmer climate is expected in the study area. Using the long-term average monthly temperatures during the reference period as the baseline, temperature increases ranged from 0.97 °C to 3.67 °C in the near future, and from 1.57 °C to 3.81 °C in the distant future, respectively, under RCP 4.5 (Fig. 5.3). In contrast, temperature increases ranged between 0.92 °C and 2.73 °C in the near future, and 2.72°C and 4.56 °C in the distant future under RCP 8.5, respectively. For RCP 4.5, the greatest increase occurred in November, followed by March and January, whereas the winter months (December to March of the following year) under RCP 8.5 had the most substantial temperature rise. Overall, the rise in temperature under RCP 8.5 was more pronounced than that under RCP 4.5, owing to the elevated levels of greenhouse gas emissions.

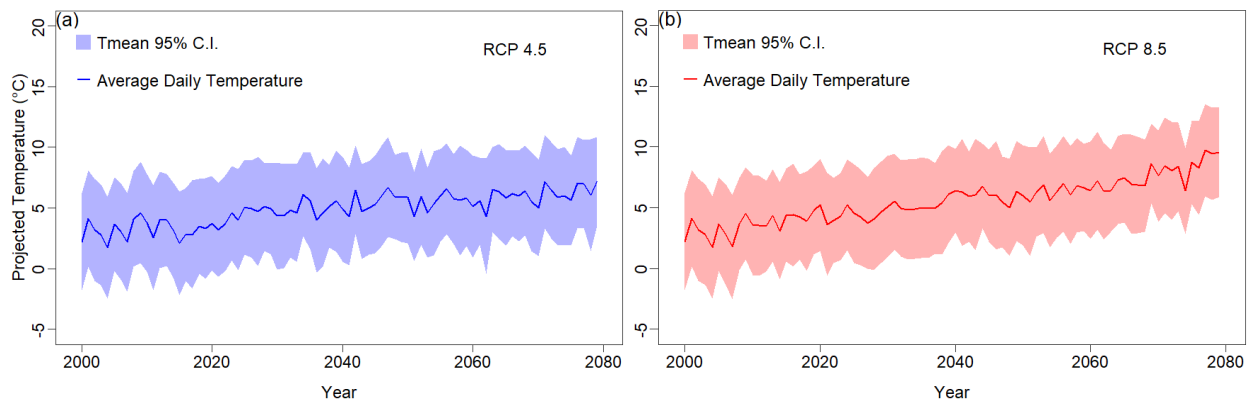


Figure 5.2: Long-term trends of the average daily temperature under RCP 4.5 (a) and RCP 8.5 (b) from 2000 to 2079. Solid lines represent the projected annual averages of daily mean temperature. Shaded areas represent the 95% confidence interval.

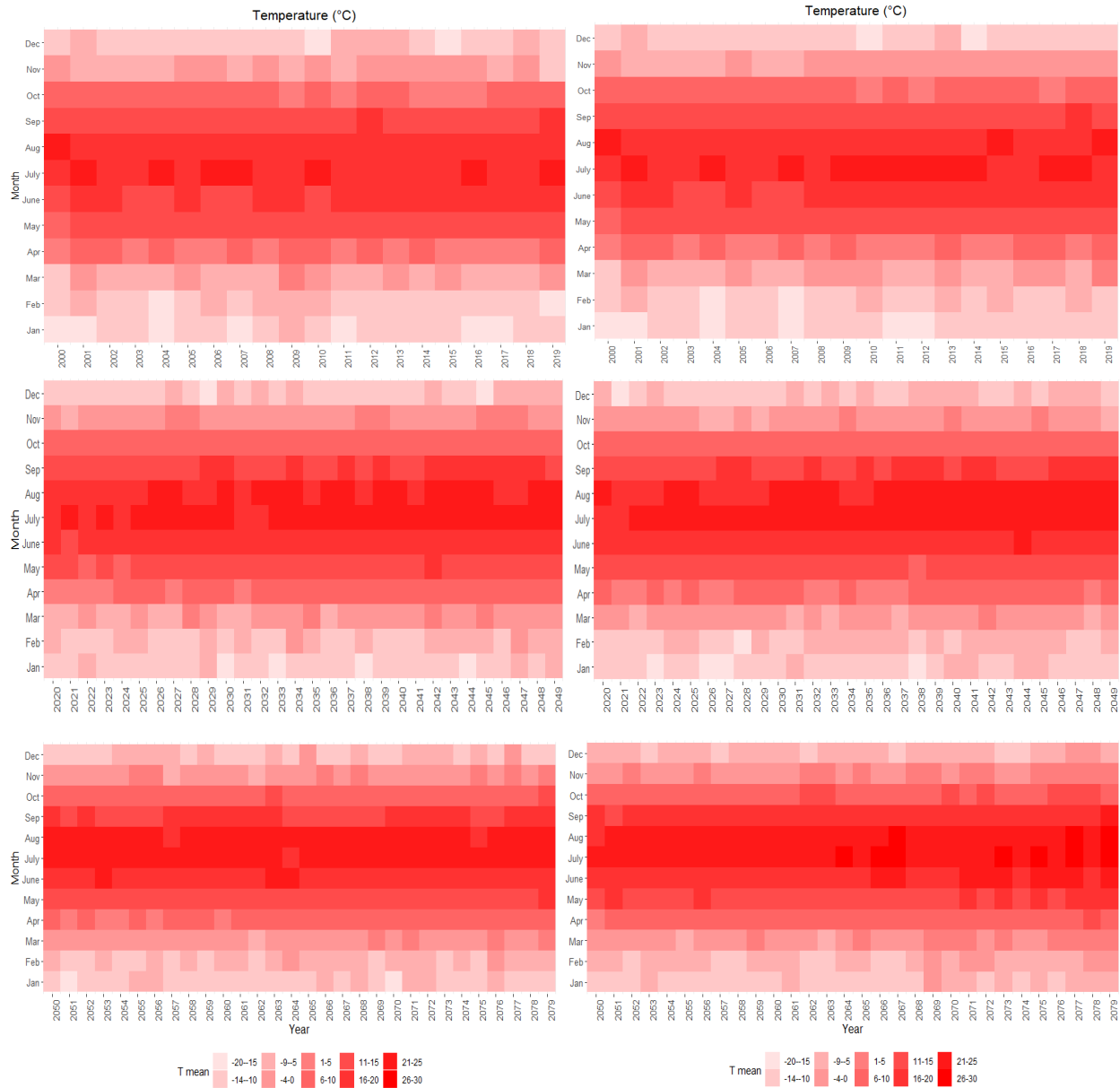


Figure 5.3: Long-term averages of monthly mean for the reference period (top), near future (middle), and distant future (bottom) under RCP 4.5 (left) and RCP 8.5 (right).

On the other hand, a significant monotonic increasing trend was only found for future precipitation for the entire simulation period under RCP 8.5 ($p < 0.05$; Fig. 5.4). Analysis of monthly precipitation (Fig. 5.5) indicated that, for the near future, precipitation was marginally reduced from March to May, whereas a considerable increase in March was predicted in the distant future under RCP 4.5. In contrast, more precipitation was observed from January through

June, of which the most significant increase will occur in May, with an increase ranging from 11.6 to 19.2 mm in the monthly averages under RCP 8.5. In both climate scenarios, higher risk of drought was anticipated during summer because of the substantial reduction in July and August, ranging from 14.1 mm to 23.6 mm.

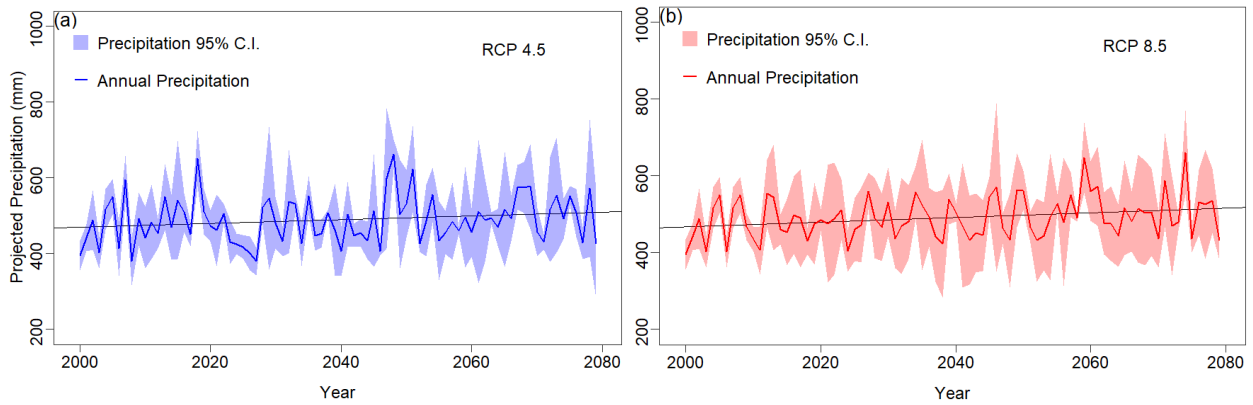


Figure 5.4: Long-term trends of the total precipitation under RCP 4.5 (a) and RCP 8.5 (b) from 2000 to 2079. Solid lines represent the projected annual averages of precipitation. Shaded areas represent the 95% confidence interval.

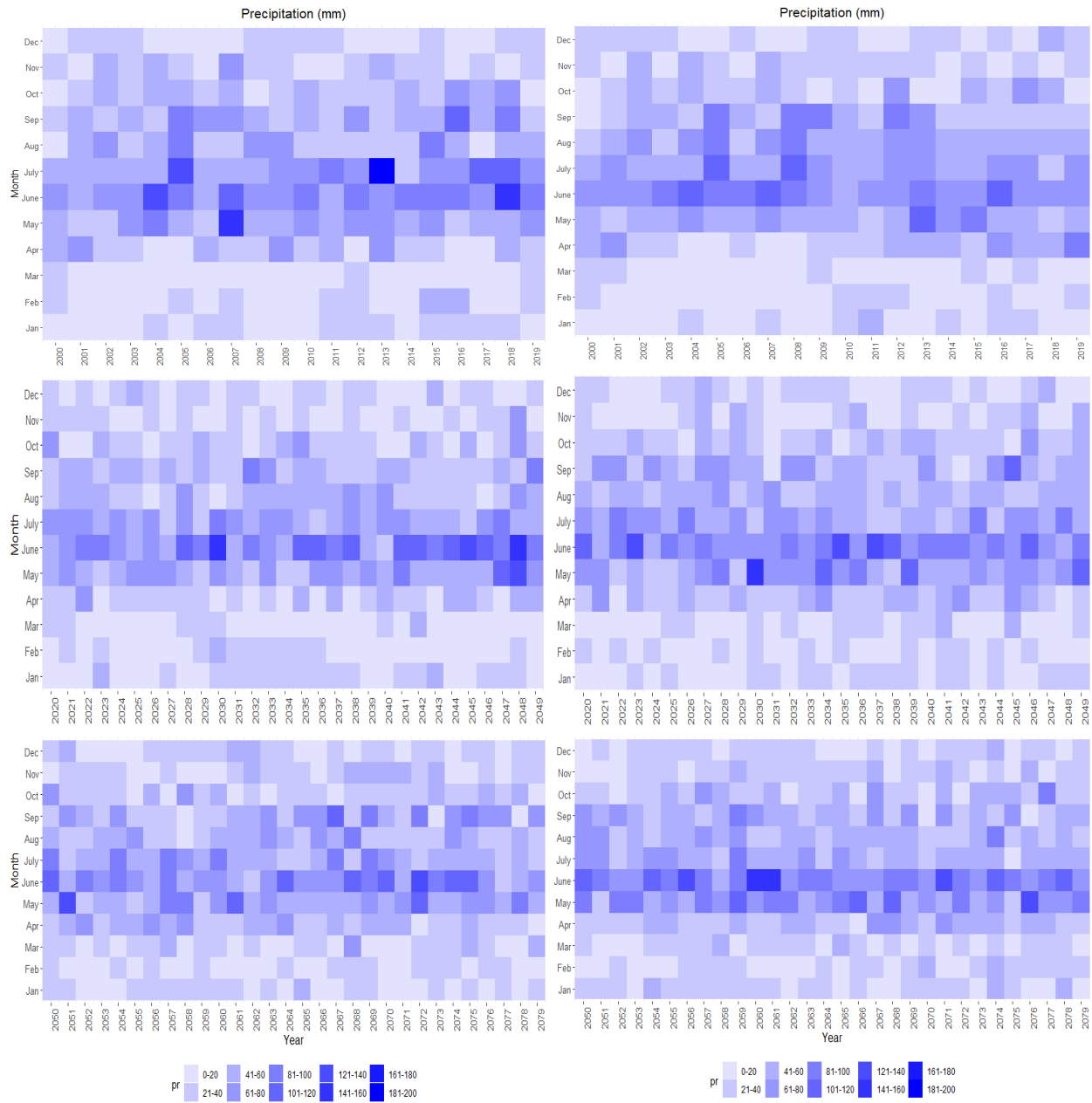


Figure 5.5: Long-term averages of monthly cumulative precipitation for the reference period (top), near future (middle), and distant future (bottom) under RCP 4.5 (left) and RCP 8.5 (right).

5.4.2. Model Assessment

Regional estimates of water yield for the Eastern Prairies and Parkland Prairies ecoprovince were obtained, converted to discharge volume, and proportionally scaled down based on the drainage area of the study watershed. The resulting discharges ranged from $6.36 \times 10^5 \text{ m}^3$ to

$8.67 \times 10^6 \text{ m}^3$ between 2000 and 2019, which were used to calculate the observed nutrient loads. The annual load of total nitrogen and total phosphorus were estimated between 814 to 10966 kg, and 32 to 434 kg, respectively (Fig. 5.6).

After removing the year 2006 from the analysis, the model was capable of achieving a NSE of 0.586 and a PBIAS of -11.5% for total nitrogen, and a NSE of 0.544 and a PBIAS of -3.8% for total phosphorus load. This performance can be classified as good ($0.50 < \text{NSE} \leq 0.65$), and very good ($\text{PBIAS} \leq \pm 15\%$) according to Moriasi et al. (2015).

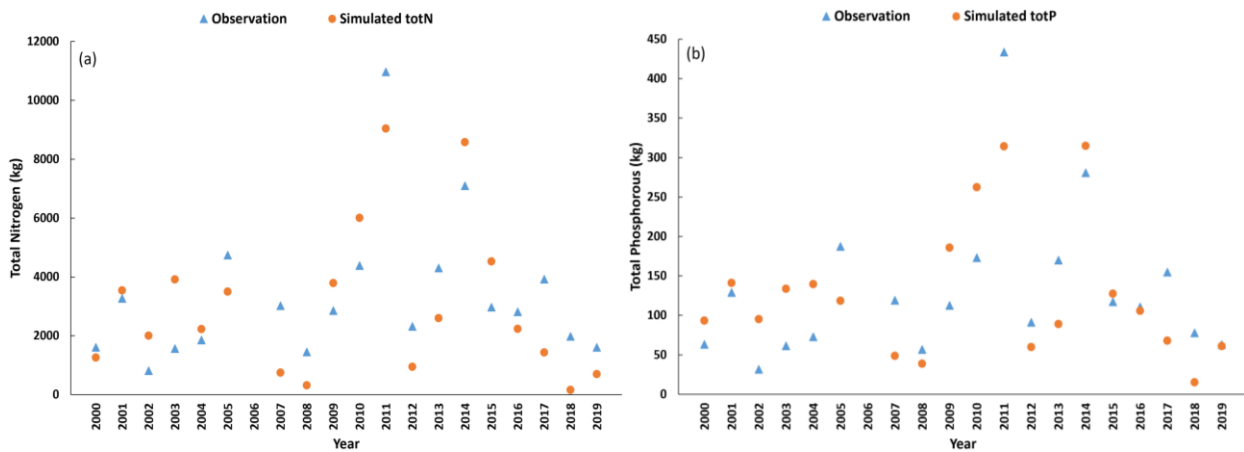


Figure 5.6: Comparisons between estimated observations and simulated total nitrogen (a) and total phosphorus (b) at the study area

5.4.3. Model Hindcast

While acceptable performance was achieved by model forcing with the historical dataset, it is also necessary to compare simulations obtained from climate modelled datasets and the observations for the same time period (2000 – 2019). Given the fact that the accumulation of nutrients is facilitated by water movement, the performance of hydrological simulations was examined first.

Graphical assessment indicated that, in general, trend of the stream discharge was reasonably simulated with modelled data, except for those instances when high flow events occurred, particularly for the year of 2011 and 2014 (Fig. 5.7). In those cases, the model underestimated the stream discharge, with a PBIAS of -27.8% for RCP 4.5, and -33% for RCP 8.5 (Table 5.4). As a result, the model underpredicted total nitrogen and phosphorus loads (Fig. 5.8; Table 5.4), with the PBIAS of total nitrogen equal to -37.6% and -41.5% for RCP 4.5 and RCP 8.5, respectively. Likewise, for total phosphorus, the corresponding PBIAS values were -26.7% and -28% for RCP 4.5 and RCP 8.5, respectively.

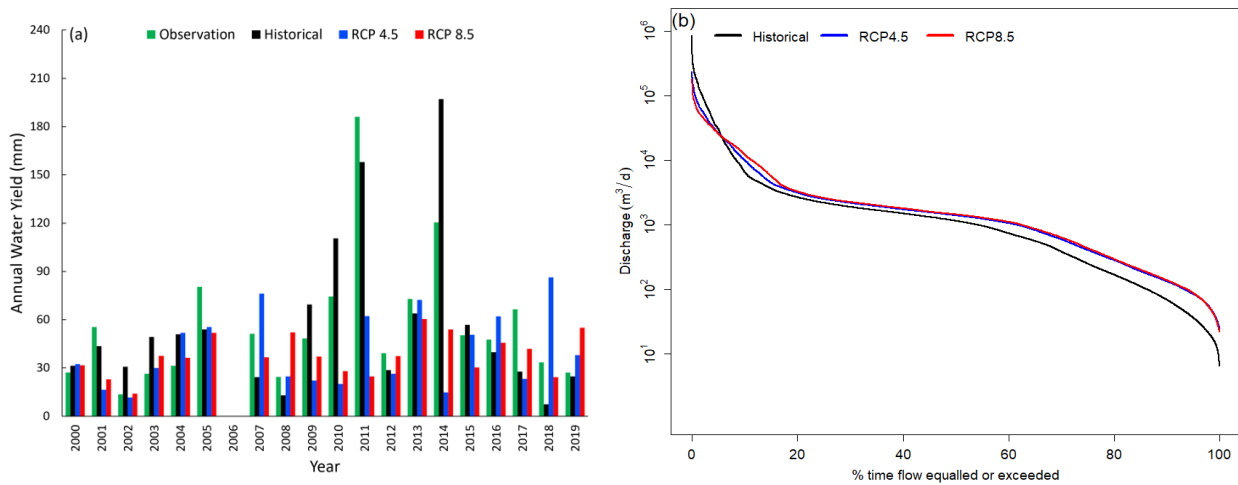


Figure 5.7: Comparison of HYPE simulated water yields (a) and flow duration curves in logarithmic scale (b) using historical dataset and climate modelled data for RCP 4.5 and 8.5

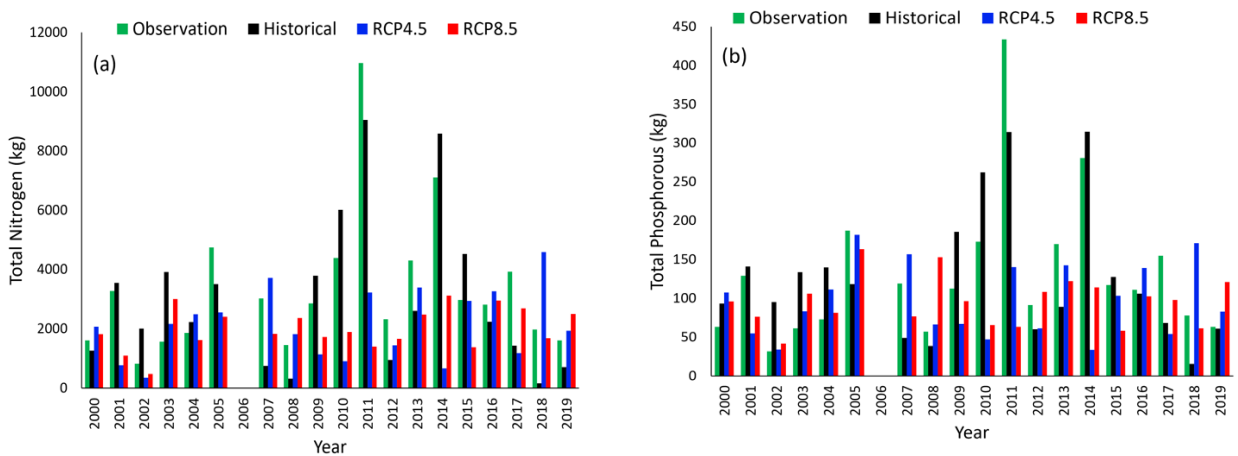


Figure 5.8: Comparison of simulated total nitrogen (a) and total phosphorus (b) using historical dataset and climate modelled data for RCP 4.5 and 8.5

Table 5.4: Assessment metrics for simulated water yield, total nitrogen, and total phosphorus during the reference period (2000 – 2019) obtained from historical weather data and climate modelled data (RCP 4.5 and 8.5)

Scenario	MAE of water yield (mm)	MAE for totN ¹ (kg)	MAE for totP ² (kg)	PBIAS for water yield (%)	PBIAS for totN (%)	PBIAS for totP (%)
Historical simulation	21.3	1346	52.5	+0.4	-11.5	-3.8
RCP 4.5	29.8	1899	66.2	-27.8	-37.6	-26.7
RCP 8.5	26.7	1777	65.0	-33	-41.5	-28

¹:totN = total nitrogen; ²: totP = total phosphorus

5.4.4. Model Forecast

Compared to the reference period, the stream discharge was projected to decrease by approximately 40% and 20% in the near and distant future periods under RCP 4.5, while a marginal increase of 2.4% and 1.8% was observed for those periods under RCP 8.5. The multi-decadal streamflow average ($1.923 \times 10^6 \text{ m}^3$) in the reference period under RCP 4.5, was in fact the greatest among all periods and RCPs, including those produced from the higher emission scenario (Table 5.5). Overall, the majority of the stream discharge (57% – 67%) took place during spring, indicating that annual stream discharge will continue to be governed by snowmelt runoff in cold regions in the future. While the same level of reduction in streamflow did not occur in the summer and fall compared to the spring, there was still a noticeable decrease during these seasons. Overall, the analysis suggested there was no evidence indicating that the trend was statistically significant in streamflow projections (Fig. 5.9). In addition, the timing of peak discharge was advanced by a minimum of 6 days, suggesting an earlier commencement of snowmelt.

Table 5.5: Long-term averages of streamflow, timing of peak discharge, and nutrient loads under RCP 4.5 and 8.5, respectively. Percentage of change was calculated based on simulated values of the reference period.

	Climate Scenario					
	RCP 4.5			RCP 8.5		
	REF ¹	NF ¹	DF ¹	REF	NF	DF
Annual stream discharge (m ³)	1.923 × 10 ⁶	1.162 × 10 ⁶ (-39.6%)	1.537 × 10 ⁶ (-20.1%)	1.761 × 10 ⁶	1.804 × 10 ⁶ (+2.4%)	1.793 × 10 ⁶ (+1.8%)
Timing of peak discharge (Julian day)	149	139 (-6.7%)	128 (-14.1%)	146	140 (-4.1%)	131 (-10.3%)
Total nitrogen load (kg)	2153	1146 (-46.8%)	1754 (-18.5%)	1989	1915 (-3.7%)	1883 (-5.3%)
Total phosphorus load (kg)	99	42.5 (-57.1%)	57.4 (-42.0%)	95	62.6 (-34.1%)	61.2 (-35.6%)

¹: REF = reference period, NF = near future, DF = distant future

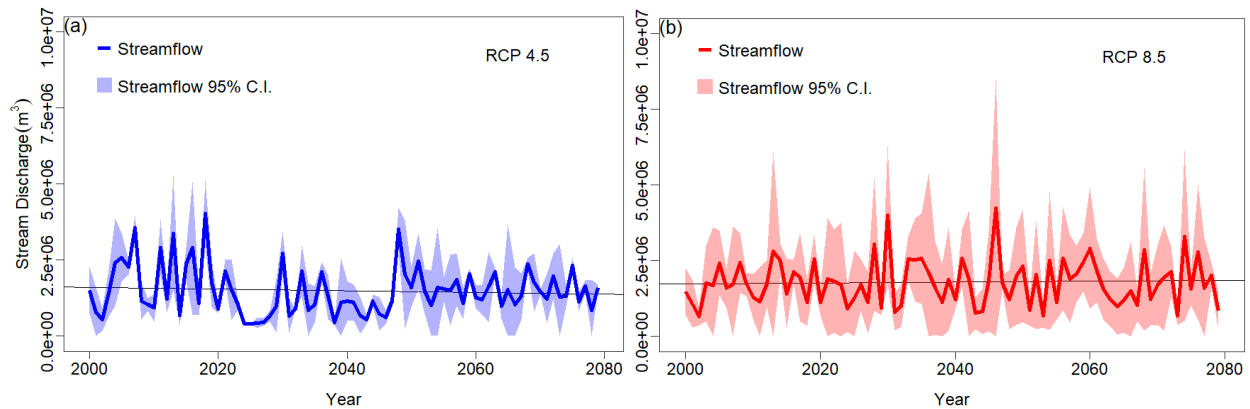


Figure 5.9: Long-term trends of annual cumulative stream discharge under RCP 4.5 (a) and RCP 8.5 (b). Solid lines represent the annual averages of stream discharge. Shaded areas represent the 95% confidence interval.

During the reference period, an annual release of 2153 kg of total nitrogen into the stream was predicted. This figure decreased to 1146 kg in the near future, but then rebounded to 1754 kg in the distant future under RCP 4.5.

Under RCP 8.5, a reduction in streamflow was also anticipated, albeit to a lesser extent compared to RCP 4.5 (Table 5.5). The seasonal distribution of these changes revealed that the majority of total nitrogen discharge occurred during spring snowmelt (data not shown). A similar trend was observed for the total phosphorus load, with decreases ranging from 34% to 57%, with

most export occurring during spring. In comparison, the reduction in phosphorus load under RCP 8.5 was more significant than that of nitrogen, at approximately 35%. Noteworthy, there was no sufficient evidence that statistically significant trend existed in either total nitrogen or phosphorus prediction, as illustrated in Fig. 5.10 and Fig. 5.11.

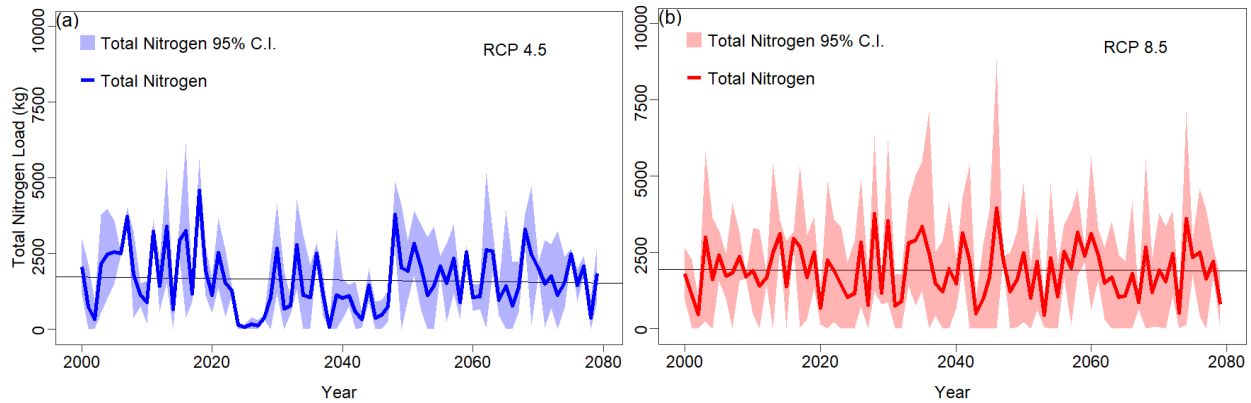


Figure 5.10: Long-term trends of total nitrogen under RCP 4.5 (a) and RCP 8.5 (b). Solid lines represent the annual averages of total nitrogen. Shaded areas represent the 95% confidence interval.

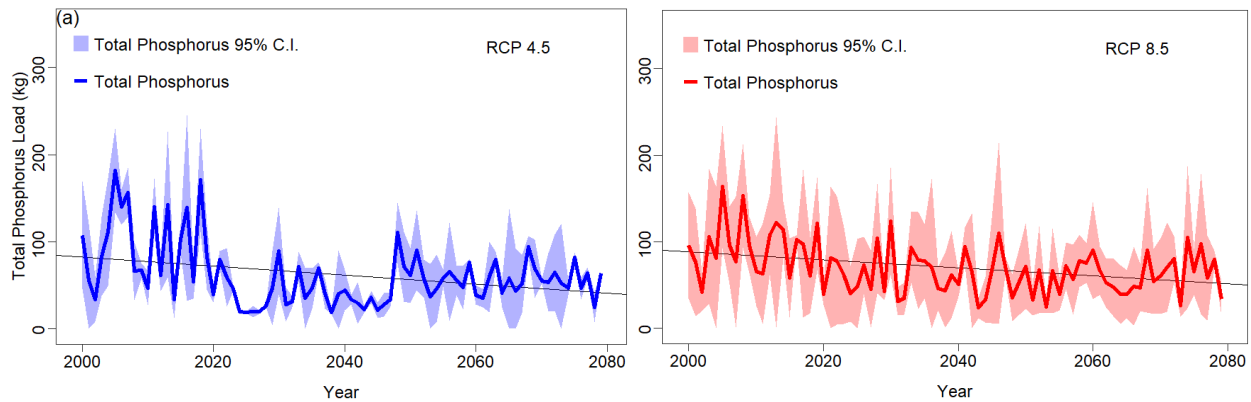


Figure 5.11: Long-term trends of total phosphorus under RCP 4.5 (a) and RCP 8.5 (b). Solid lines represent the annual averages of total phosphorus. Shaded areas represent the 95% confidence interval.

5.4.5. Relationship between Nutrient Loads and Annual Discharge

Nutrient export through water movement is the predominant mechanism responsible for redistributing nutrients spatially and results in their release into streams. Table 5.6 summarizes

the coefficient of determination (R^2) values with all values larger than or equal to 0.75. These values suggest a relationship between stream discharge and the export of total nitrogen and phosphorus for all three climate models under different climate scenarios. Overall, the analysis indicated a strong relationship between stream discharge and nutrient export, with a comparatively stronger association with total nitrogen in contrast to total phosphorus.

Table 5.6: R^2 values of annual discharge and nitrogen and phosphorus loads for three climate models under RCP 4.5 and RCP 8.5

	Climate Scenario			
	RCP 4.5		RCP 8.5	
	totN ¹	totP ²	totN	totP
CanESM2.CanRCM4	0.89	0.85	0.83	0.75
CanESM2.CRCM5-UQAM	0.90	0.85	0.91	0.78
MPI-ESM-LR.CRCM5-UQAM	0.85	0.80	0.84	0.81

¹: totN = total nitrogen; ²: totP = total phosphorus

5.5 Discussion

Model assessment of the simulation with historical weather data demonstrated satisfactory performance in evaluating simulated water yield, as well as loads of total nitrogen and phosphorus when compared to observed values. However, there were notable discrepancies in the model hindcast phase, characterized by significant biases (as indicated by MAE and PBIAS). The inadequate performance in estimating water yield in model hindcast, which subsequently affected the predictions of water quality, was mainly attributed to the lack of predictability of the configured model for extreme flow events (low and peak flow), which was most evident in 2011 and 2014 (Fig. 5.7a and Fig. 5.8). In fact, the streamflow generated by climate modelled data was not substantially different from the historical simulations based on the flow duration curves in Fig. 7b, except for instances of extreme flow events. Climate models have been known for not representing extreme weather conditions satisfactorily (Clarke et al., 2022), resulting in model

simulations that most likely capture the general trend of hydrological response under climate projection, but fails to capture extreme events. The performance deterioration found in the model hindcast stage was recognized and acknowledged, but no attempt (e.g., bias correction; Soriano et al., 2019) was made to address the issue due to the high level of uncertainties associated with the simulations. In fact, it is common that models have poor performance without bias correction during model hindcast, because the calibrated model is forced with a completely new set of climate modelled data for the same time period as the historical weather data (Duethmann, 2020). The uncertainties in this exercise include (1) weather and observation data were not collected in the basin, (2) lack of hydrometric data, and (3) regional estimates of water yield used for model assessment, which would result in low confidence in bias-corrected model outputs.

Determining the impact of climate change on streamflow generation was complicated due to the dynamic interplay among different components of the water budget. Generally in cold regions, more runoff generation is anticipated with increased winter precipitation, as well as a warmer climate that leads to an earlier freshet (Costa et al., 2023). Despite numerous factors affecting streamflow simulation, such as spatial variability, surface albedo feedback (Zhang et al., 2019), and land use change (Sajikumar and Remya, 2015), streamflow generation generally follows the precipitation pattern (Luo et al., 2020), which was also the case in this study (Fig. 5.4; Fig. 5.9).

When analyzing the predicted water quality, it was noticed that the load of total nitrogen and phosphorus exports also followed the trend of streamflow, which was predominantly governed by precipitation patterns. As stated by Liu et al. (2019), nutrient exports from agricultural lands are mostly driven by peak flow events. The underestimation of water yield led to an overall lower load of total nitrogen and phosphorus (Table 5.4). This implies that the factors influencing

streamflow prediction, coupled with their associated uncertainties, inherently impacted the estimation of water quality as well.

Based on the local measurements of water chemistry data for the Assiniboine River in Manitoba, annual total nitrogen loading ranged from 0.17 to 4.28 kg ha⁻¹ for pasture, 0.3 to 6.7 kg ha⁻¹ for cropland, and 0.23 – 3.93 kg ha⁻¹ for forest, respectively, which the total phosphorus loading ranged from 0.02 to 0.51 kg ha⁻¹ for pasture, 0.3 to 1.1 kg ha⁻¹ for cropland, and 0.01 to 0.38 kg ha⁻¹ for forest, respectively (Bourne et al., 2002). Based on the land use of the study area, the values above suggest a range between 898 and 20,551 kg of total nitrogen per year, and 192 and 2485 kg of total phosphorus per year. These ranges agreed with the multi-decadal long-term average values presented in Table 5.5 for total nitrogen loading, but not for total phosphorus. This disagreement for total phosphorus could be explained by overestimated values reported for the Assiniboine River since nutrient uptake by plants was not taken in account (Bourne et al., 2002). In fact, nutrient uptake is a significant factor that could potentially increase in the future due to elevated temperature if plants are not exposed to heat stress (Turner and Lahav, 1985; Geng et al., 2017). Nevertheless, the projected reduction in total nitrogen and phosphorus loads in future periods can be explained by the reduction or marginal increase in stream discharge (Table 5.5). Similar findings were found in other studies, suggesting that the change in nutrient export to streams would still be governed by the stream discharge under climate change (Jennings et al., 2009; Costa et al., 2023).

Several factors influenced the model performance in predicting water quality. Firstly, utilizing the regional estimates of water yield at the ecoprovince scale as the observations for assessment introduced high levels of uncertainty, which propagated when calculating the water quality observations with the established discharge-nutrient load relationships derived from Swan Creek.

Calibration with observations at a finer spatial resolution would yield a more representative model, which should enhance the performance in simulating water quality (Arheimer et al., 2012).

Secondly, the water quality station in Swan Creek did not measure hydrometric data, and the only gauging station nearby was located upstream. Thus, to estimate the flow rate data at the water quality station, approximation was used to proportionally scale up the flow rate data reported at the gauging station by the ratio of drainage areas. Although this method has been extensively applied in data-sparse watersheds (Emerson et al., 2005), caution should be exercised as the bias could become significant if the distance between two stations is large, making the underlying assumption of shared precipitation inputs and runoff generation across two stations untenable (Asquith et al., 2006). Furthermore, when determining the discharge-nutrient loads relationship in Swan Creek, only seasonal water chemistry data between 2013 and 2021 were available. Despite successfully obtaining a strong relationship, the extrapolation of this relationship for predicting nutrient fluxes in streams outside of the reported range would impose substantial uncertainties.

Lastly, it is important to acknowledge the uncertainties associated with the use of climate modelled data, stemming from sources including climate models, emission scenarios, and natural internal climate variability (Schwarzwald and Lenssen, 2022; Wu et al., 2022). The variations in meteorological input data not only affected the hydrological simulation, but also influenced the simulated nitrogen and phosphorus concentrations in both manure and plant residues using IFSM. Specifically, the nitrogen content in manure and grass residues ranged from 4.66 ± 0.015 and $26.6 \pm 1.59 \text{ kg ha}^{-1}$, respectively. In contrast, the range of phosphorus content in manure and residues were 0.36 ± 0.001 and $1.96 \pm 0.12 \text{ kg ha}^{-1}$. Considering that 72% of the study area

comprises pastureland (3355 ha), even trivial fluctuations could result in significant alternations in annual nutrient inputs.

5.6 Conclusion

To assess the impact of climate change on water quality within a 46.6 km² pasture-dominated watershed in Manitoba, the HYPE model was used. Initially, model forcing with the historical dataset produced the annual load of total nitrogen ranging from 158 to 9,045 kg with a NSE of 0.586 and a PBIAS of -11.5%, while the range of total phosphorus was between 15 and 315 kg with a NSE of 0.544 and a PBIAS of -3.8% for total phosphorus load. Afterward, model forecast was simulated with future climate datasets. The results indicated a projected reduction in the release of total nitrogen and phosphorus under both RCP 4.5 and RCP 8.5, respectively. These findings reflected a general trend in water quality that mostly mirrored the patterns observed in stream discharge primarily generated during spring snowmelt.

CHAPTER 6: GENERAL CONCLUSIONS

The following general conclusions can be drawn from the different modelling exercises conducted in this research:

1. Based on the Mann-Kendall test, statistically significant increasing trends ($p < 0.05$) were observed for daily average temperature and heat unit accumulation in future periods under RCP 4.5 and 8.5, as well as the entire simulation period between 2000 and 2079. However, no evidence was found to confirm a monotonically increasing trend in the projection of annual precipitation. Despite the overall slight increase in annual precipitation, a pronounced reduction in summer precipitation was observed. This decline poses a substantial threat to crop growth and agricultural activities;
2. With the climate modelled data, IFSM predicted pasture yield to decrease by 2 to 6.8% in general, which was likely attributed to the overall warming climate with less precipitation during growing seasons. This decrease was most substantial in the distant future under RCP 8.5. Furthermore, manure production was relatively stable, with the largest difference of -0.39%;
3. By comparing to regional estimates of water yield, both CRHM and HYPE models indicated a reduction in the near future period under RCP 4.5 by 20% and 40% on average, respectively. Under RCP 8.5, CRHM had a substantial increase by 26% and 39%, whereas HYPE had a marginal increase by 2% on average in the near future and distant future periods, respectively. Both models predicted that the timing of peak discharge, would occur on an earlier date, ranging from 6 to 21 days. The only exception was captured using CRHM during the near future period under RCP 8.5, which had a 2-

day delay. This implied that the snow-covered duration would be shorter, resulting in a potentially longer growing season;

4. The magnitude of stream discharge simulations by CRHM and HYPE did not agree, which was likely caused by several factors, such as model structure, parameterization, forcing data at different timesteps, and high levels of uncertainties associated with the observations. Nevertheless, the general trend of stream discharge was still captured, and it was in agreement between both models that earlier snowmelt event is expected;
5. A reduction in the projected total nitrogen load by 33% and 4.5% was observed under both RCP 4.5 and RCP 8.5, respectively. Similarly, the total phosphorus load also decreased by 50% and 35% under RCP 4.5 and RCP 8.5, respectively. It was evident that the fluctuation in nutrient load simulations closely followed the pattern of stream discharge, reinforcing that the water movement is the governing facilitator which redistributes and relocates nutrients in the vegetation, manure, and soil pools.

CHAPTER 7: RECOMMENDATIONS FOR FUTURE RESEARCH

The following are recommendations for future research:

1. Changes in pasture management were not assessed using IFSM, which could provide insights on the response of the model output when incorporating other management practices, such as a shift in stand composition to encompass other grass species, particularly those known for their high heat tolerance and drought resistance. New practices are likely to take place and constitute an important adaptation strategy to cope with the effects climate change. It is important to keep in mind, though, that changes in management will not have an isolated effect; rather, they will impact other aspects of the pasture system. For example, changes in forage type as an adaptation to climate change will likely impact pasture quality and, consequently, cattle nutrient utilization and grazing period. Pasture quality would impact manure composition and subsequent nutrient release as well. Also, structural changes in the grass canopy architecture due to species changes will likely affect snow trapping, leading to potential changes in the snow melt regime. All these aspects should be assessed concomitantly through dynamics modelling;
2. Instead of using the annual average forage yield from the Benchmark project, it would be better to seek a local forage yield as the reference value to be use for calibration. Therefore, monitoring pasture yield in the study area would enhance the predictability and generate a more representative pasture yield for the Beaver Creek watershed;
3. Similarly, the values that were used for model calibration (i.e., regional estimates of water yield, total nitrogen load, and total phosphorus load) associated with high level of uncertainty, hindering the model performance with substantial biases during model

hindcast. Collecting hydrometric and water quality data through on-site measurement should enhance the model representation with more reliable simulation results;

4. The implication of longer grazing season due to earlier snowmelt should be assessed. The longer grazing season implies a reduction in pasture residues, and more manure would be produced, affecting the nutrient contents in the vegetation and manure pools. To achieve a more comprehensive assessment, it is essential to incorporate these scenario evaluation into the analysis;
5. Lastly, there were only three climate models used for the ensemble approach in this study. Inclusion of more climate models would provide stronger confidence in our model predictions.

REFERENCES

- Agriculture and Agri-Food Canada. 2019. Manitoba Forage Benchmarking Project [Microsoft Excel spreadsheet].
- Agriculture and Agri-Food Canada. 2020. Climate change impacts on agriculture.
- Agriculture and Agri-Food Canada. 2023. Annual Crop Inventory 2016. [Online] Available: open.canada.ca/data/en/dataset/b8e4da73-fb5f-4e6e-93a4-8b1f40d95b51
- Ahmed, M., S. Ahmad, H.M. Waldrip, M. Ramin and M.A. Raza. 2020. Whole Farm Modeling: A Systems Approach to Understanding and Managing Livestock for Greenhouse Gas Mitigation, Economic Viability and Environmental Quality. *Animal Manure* 345–371. doi: 10.2134/asaspecpub67.c25.
- Ahmed, M.I., K. Shook, A. Pietroniro, T. Stadnyk, J.W. Pomeroy, C. Pers and D. Gustafsson. 2023. Implementing a parsimonious variable contributing area algorithm for the prairie pothole region in the HYPE modelling framework. *Environmental Modelling & Software* 167: 105769. doi: 10.1016/j.envsoft.2023.105769.
- Ajiboye, B., O.O. Akinremi and G.J. Racz. 2004. Laboratory characterization of phosphorus in fresh and oven-dried organic amendments. *J. Environ. Qual.* 33: 1062 – 1069.
- Aladenola, O.O., and C.A., Madramootoo. 2014. Evaluation of solar radiation estimation methods for reference evapotranspiration estimation in Canada. *Theoretical and Applied Climatology* 118(3): 377–385. doi: 10.1007/s00704-013-1070-2
- Allen, R.G., L.S. Pereira, D. Raes, and M. Smith. 1998. Crop evapotranspiration - Guidelines for computing crop water requirements. *FAO Irrigation and Drainage Paper No. 56*. ISBN 92-5-104219-5
- Andersson, J., I. Pechlivanidis, D. Gustafsson, C. Donnelly and B. Arheimer. 2015. Key factors for improving large-scale hydrological model performance. *European Water*.
- Annandale, J.G., N.Z. Jovanovic, N. Benad and R.G. Allen. 2002. Software for missing data analysis of Penman-Monteith reference evapotranspiration. *Irrigation Science* 21: 57-67.
- Appleyard, D.R. 2023. Strategic supplementation to improve beef cattle performance and expand utilization of pasture-based production systems. Master of Science Thesis. University of Manitoba, Winnipeg, MB. <https://mspace.lib.umanitoba.ca/items/c91912b0-58a1-4fb0-8a64-fd2c8efeff81> (2023/11/08)
- Archfield, S.A. and R.M. Vogel. 2010. Map correlation method: Selection of a reference streamgage to estimate daily streamflow at ungaged catchments. *Water Resources Research* 46(10). doi: 10.1029/2009wr008481.
- Arheimer, B., J. Dahné, C. Donnelly, G. Lindström and J. Strömqvist. 2012. Water and nutrient simulations using the HYPE model for Sweden vs. the Baltic Sea basin – influence of input-data quality and scale. *Hydrology Research* 43(4): 315–329. doi: 10.2166/nh.2012.010.
- Arheimer, B., J. Dahné, G. Lindström, L. Marklund, and J. Strömqvist. 2011. Multi-variable evaluation of an integrated model system covering Sweden (S-HYPE). IAHS-AISH Publication
- Arheimer, B., R. Pimentel, K. Isberg, L. Crochemore, J.C.M. Andersson, A. Hasan and L. Pineda. 2020. Global catchment modelling using World-Wide HYPE (WWH), open data, and stepwise parameter estimation. *Hydrology and Earth System Sciences* 24(2): 535–559. doi: 10.5194/hess-24-535-2020.
- Arnold, J.G., R. Srinivasan, R.S. Muttiah, and J.R. Williams. 1998. Large Area Hydrological

- Modelling and Assessment Part I: Model Development. *Journal of the American Water Resources Association* 34(1): 73-89. doi: 10.1111/j.1752-1688.1998.tb05961.x
- Ashmore, P. and M. Church. 2001. The impact of climate change on rivers and river processes in Canada. Geological Survey of Canada Bulletin 555.
- Asquith, W.H., M.C. Roussel, and J. Vrabel. 2006, Statewide analysis of the drainage-area ratio method for 34 streamflow percentile ranges in Texas: U.S. Geological Survey Scientific Investigations Report 2006–5286, 34 p., 1 appendix.
- Association of Manitoba Community Pasture. 2021. Ellice-Archi and Spy Hill Community Pastures [Microsoft Excel spreadsheet].
- Atwell, K., S.-J. Dunn, J.M. Osborne, H. Kugler, and E.J.A. Hubbard. 2016. How computational models contribute to our understanding of the germ line. *Mol Reprod Dev.* 2016 83(11):944-957. doi: 10.1002/mrd.22735
- Ayers, H.D. 1959. Influence of soil profile and vegetation characteristics on net rainfall supply to runoff, in: Proceedings of Hydrology Symposium No. 1: Spillway Design Floods, National Research Council Canada, Ottawa, 198-205.
- Baek, H.-J., J. Lee, H.-S. Lee, Y.-K. Hyun, C. Cho, W.-T. Kwon, C. Marzin, S.-Y. Gan, M.-J. Kim, D.-H. Choi, J. Lee, J. Lee, K.-O. Boo, H.-S. Kang and Y.-H. Byun. 2013. Climate change in the 21st century simulated by HadGEM2-AO under representative concentration pathways. *Asia-Pacific Journal of Atmospheric Sciences* 49(5): 603–618. doi: 10.1007/s13143-013-0053-7.
- Bajracharya, A.R. 2023. Process-based calibration of HYPE model for climate change impact assessment of Nelson Churchill River Basin. University of Manitoba, Winnipeg, MB. <https://mspace.lib.umanitoba.ca/items/c2fb2dc2-21ce-4aaf-b652-e3685c7e84ff> (2023/11/08)
- Bargo, F., L.D. Muller, E.S. Kolver and J.E. Delahoy. 2003. Invited Review: Production and Digestion of Supplemented Dairy Cows on Pasture. *Journal of Dairy Science* 86(1): 1–42. doi: 10.3168/jds.s0022-0302(03)73581-4.
- Barnhart, T.B., N.P. Molotch, B. Livneh, A.A. Harpold, J.F. Knowles and D. Schneider. 2016. Snowmelt rate dictates streamflow. *Geophysical Research Letters* 43(15): 8006–8016. doi: 10.1002/2016gl069690.
- Baronti, S., F. Ungaro, A. Maienza, F. Ugolini, A. Lagomarsino, A.E. Agnelli, C. Calzolari, F. Pisseri, G. Robbiati and F.P. Vaccari. 2022. Rotational pasture management to increase the sustainability of mountain livestock farms in the Alpine region. *Regional Environmental Change* 22, 50. doi: 10.1007/s10113-022-01896-1
- Barrow, E.M. and D.J. Sauchyn. 2019. Uncertainty in climate projections and time of emergence of climate signals in the western Canadian Prairies. *International Journal of Climatology* 39(11): 4358–4371. doi: 10.1002/joc.6079.
- Bechmann, M.E., P.J.A. Kleinman, A.N. Sharpley and L.S. Saporito. 2005. Freeze-Thaw Effects on Phosphorus Loss in Runoff from Manured and Catch-Cropped Soils. *J. Environ. Qual.* 34: 2301-2309. doi: 10.2134/jeq2004.0415
- Beetz, A.E. 2002. A brief overview of nutrient cycling in pastures. Appropriate Technology Transfer for Rural Areas. [Online] Available: www.canr.msu.edu/foodsystems/uploads/files/a-brief-overviewnutcycle.pdf
- Bellows, B. 2001. Nutrient cycling in pastures. Appropriate Technology Transfer for Rural Areas.
- Bengtsson, J., J.M. Bullock, B. Egoh, C. Everson, T. Everson, T. O'Connor, P.J. O'Farrell, H.G. Smith and R. Lindborg. 2019. Grasslands-more important for ecosystem services than you might think. *Ecosphere* 10(2): e02582. doi: 10.1002/ecs2.2582.

- Bernier, J.N., M. Undi, K.H. Ominski, G. Donohoe, M. Tenuta, D. Flaten, J.C. Plaizier, and K.M. Wittenberg. 2014. Nitrogen and phosphorus utilization and excretion by beef cows fed a low quality forage diet supplemented with dried distillers grains with solubles under thermal neutral and prolonged cold conditions. *Anim. Feed Sci. Technol.* 193:9–20. doi: 10.1016/j.anifeedsci.2014.03.010
- Bo, L., Z. Li, P. Li, G. Xu, L. Xiao and B. Ma. 2021. Soil Freeze-Thaw and Water Transport Characteristics Under Different Vegetation Types in Seasonal Freeze-Thaw Areas of the Loess Plateau. *Frontiers in Earth Science* 9. doi: 10.3389/feart.2021.704901
- Bogunovic, I., K. Kljak, I. Dugan, D. Grbeša, L.J. Telak, M. Duvnjak, I. Kisić, M. Kapović Solomun and P. Pereira. 2022. Grassland Management Impact on Soil Degradation and Herbage Nutritional Value in a Temperate Humid Environment. *Agriculture* 12(7): 921. doi: 10.3390/agriculture12070921.
- Bonsal, B.R., D.L. Peters, F. Seglenieks, A. Rivera, and A. Berg. 2019. Changes in freshwater availability across Canada; *Chapter 6 in Canada's Changing Climate Report*, (ed.) E. Bush and D.S. Lemmen: 261–342.
- Bonsal, B.R., E.E. Wheaton, A.C. Chipanshi, C. Lin, D.J. Sauchyn and L. Wen. 2011. Drought research in Canada: a review. *Atmosphere-Ocean* 49(4): 303-319. doi: 10.1080/07055900.2011.555103
- Bouffard, J.-S. 2014. A Comparison of Conceptual Rainfall-Runoff Modelling Structures and Approaches for Hydrologic Prediction in Ungauged Peatland Basins of the James Bay Lowlands. Carleton University.
- Bourke, D., D. Jeffrey, P. Dowding, I. Kurz and H. Tunney. 2008. Eutrophication from Agricultural Sources – The Impact of the Grazing Animal on Phosphorus, Nitrogen, Potassium and Suspended Solids Loss from Grazed Pastures - Phosphorus Dynamics in Grazed Grassland. Environmental Protection Agency. ISBN: 1-84095-266-0
- Bourne, A., N. Armstrong, and G. Jones. 2002. A preliminary estimate of total nitrogen and total phosphorus loading to streams in Manitoba, Canada. Manitoba Conservation Report No. 2002-04. [Online] Available: <https://citeseerx.ist.psu.edu/viewdoc/download?doi=10.1.1.528.6798>
- Byun, K., C.-M. Chiu and A.F. Hamlet. 2019. Effects of 21st century climate change on seasonal flow regimes and hydrologic extremes over the Midwest and Great Lakes region of the US. *Science of The Total Environment* 650: 1261–1277. doi: 10.1016/j.scitotenv.2018.09.063.
- Canadian Cattlemen's Association. 2023 Canadian Beef Economics. [Online] Available: www.cattle.ca/canadian-beef-economics
- Canadian Cattlemen's Association. n.d.b. Environment: Beef production and climate change. [Online] Available: <https://www.cattle.ca/ccca-resources/environment/>
- Ceballos, G., A. Davidson, R. List, J. Pacheco, P. Manzano-Fischer, G. Santos-Barrera and J. Cruzado. 2010. Rapid Decline of a Grassland System and Its Ecological and Conservation Implications. *PLoS ONE* 5(1): e8562. doi: 10.1371/journal.pone.0008562.
- Census of Agriculture. 2016. Agriculture Statistics: Manitoba Crop Highlights. [Online] Available: www.gov.mb.ca/agriculture/markets-and-statistics/crop-statistics/pubs/crop-highlights-census.pdf
- Chakraborty, D., R. Prasad and E. Brantley. 2020. Phosphorus Basics: Understanding Pathways of Soil Phosphorus Loss. Alabama Cooperative Extension System.
- Chambers, P.A., M. Guy, E.S. Roberts, M.N. Charlton, R. Kent, C. Gagnon, G. Grove and N.

- Foster. 2001. Nutrients and their impact on the Canadian environment. Agriculture and AgriFood Canada, Environment Canada, Fisheries and Oceans Canada, Health Canada and Natural Resources Canada. 241 p.
- Chastain, J.P. and J.J. Camberato. 2004. Dairy Manure Production and Nutrient Content. Confined animal manure managers certification program manual B dairy version. [Online] Available: www.clemson.edu/extension/camm/manuals/dairy/dch3a_04.pdf
- Chen, X., G. Tang, T. Chen and X. Niu. 2022. An Assessment of the Impacts of Snowmelt Rate and Continuity Shifts on Streamflow Dynamics in Three Alpine Watersheds in the Western U.S. *Water* 14(7): 1095. doi: 10.3390/w14071095.
- Cherkauer, K.A., L.C. Bowling, and D.P. Lettenmaier. 2003. Variable infiltration capacity cold land process model updates. *Global and Planetary Change* 38(1-2):151-159. doi: 10.1016/S0921-8181(03)00025-0
- Chiang, Y.-M., R.-N. Hao, H.-C. Ho, T.-J. Chang and Y.-P. Xu. 2017. Evaluating the contribution of multi-model combination to streamflow hindcasting by empirical and conceptual models. *Hydrological Sciences Journal* 62(9): 1456–1468. doi: 10.1080/02626667.2017.1330543.
- Chiwa, M. 2020. Ten-year determination of atmospheric phosphorus deposition at three forested sites in Japan. *Atmospheric Environment* 223: 117247. doi: 10.1016/j.atmosenv.2019.117247.
- Chow, V.T. 1964. Handbook of Applied Hydrology, McGraw-Hill, Inc., New York.
- Clarke, B., F. Otto, R. Stuart-Smith and L. Harrington. 2022. Extreme weather impacts of climate change: an attribution perspective. *Environmental Research: Climate* 1(1): 012001. doi: 10.1088/2752-5295/ac6e7d.
- Clarke, B., F. Otto, R. Stuart-Smith and L. Harrington. 2022. Extreme weather impacts of climate change: an attribution perspective. *Environmental Research: Climate* 1(1): 012001. doi: 10.1088/2752-5295/ac6e7d.
- Clean Water Team. 2004. pH Fact Sheet, FS-3.1.4.0(pH). in: The Clean Water Team Guidance Compendium for Watershed Monitoring and Assessment, Version 2.0. Division of Water Quality, California State Water Resources Control Board (SWRCB), Sacramento, CA.
- Climate Data Store. 2021. CMIP6 climate projections. Copernicus Climate Change Service (C3S). doi: 10.24381/cds.c866074
- Cober, J.R., M.L. Macrae and L.L. Van Eerd. 2018. Nutrient Release from Living and Terminated Cover Crops Under Variable Freeze–Thaw Cycles. *Agronomy Journal* 110(3): 1036–1045. doi: 10.2134/agronj2017.08.0449.
- Cole, N.A., and R.W. Todd. 2009. Nitrogen and phosphorus balance of beef cattle feedyards, p. 17-24 Proceedings of the Texas animal manure management issues conference. Round Rock, TX.
- Coles, A.E. and J.J. McDonnell. 2018. Fill and spill drives runoff connectivity over frozen ground. *Journal of Hydrology* 558: 115–128. doi: 10.1016/j.jhydrol.2018.01.016.
- Cordeiro, M.R., H.F. Wilson, J. Vanrobaeys, J.W. Pomeroy, X. Fang, and The Red-Assiniboine Project Biophysical Modelling Team. 2017. Simulating cold-region hydrology in an intensively drained agricultural watershed in Manitoba, Canada, using the Cold Regions Hydrological Model. *Hydrol. Earth Syst. Sci.*, 21, 3483–3506. doi: 10.5194/hess-21-3483-2017
- Cordeiro, M.R., K. Liang, H.F. Wilson, J. Vanrobaeys, D.A. Lobb, X. Fang, and J.W. Pomeroy. 2022. Simulating the hydrological impacts of land use conversion from annual crop to perennial forage in the Canadian Prairies using the Cold Regions Hydrological Modelling platform. *Hydrol. Earth Syst. Sci.*, 26: 5917–5931. <https://doi.org/10.5194/hess-26-5917-2022>

- Cordeiro, M.R.C., G. Lelyk, R. Kröbel, G. Legesse, M. Faramarzi, M.B. Masud, and T. McAllister. 2018. Deriving a dataset for agriculturally relevant soils from the Soil Landscapes of Canada (SLC) database for use in Soil and Water Assessment Tool (SWAT) simulations. *Earth Syst. Sci. Data* 10(3): 1673–1686. doi: 10.5194/essd-10-1673-2018
- Cordeiro, M.R.C., H.F. Wilson, J. Vanrobaeys, J.W. Pomeroy and X. Fang. 2017. Simulating cold-region hydrology in an intensively drained agricultural watershed in Manitoba, Canada, using the Cold Regions Hydrological Model. *Hydrology and Earth System Sciences* 21(7): 3483–3506. doi: 10.5194/hess-21-3483-2017.
- Cordeiro, M.R.C., J.A. Vanrobaeys and H.F. Wilson. 2019. Long-term weather, streamflow, and water chemistry datasets for hydrological modelling applications at the upper La Salle River watershed in Manitoba, Canada. *Geoscience Data Journal* 6(1): 41–57. doi: 10.1002/gdj3.67.
- Cordeiro, M.R.C., K. Liang, H.F. Wilson, J. Vanrobaeys, D.A. Lobb, X. Fang and J.W. Pomeroy. 2022. Simulating the hydrological impacts of land use conversion from annual crop to perennial forage in the Canadian Prairies using the Cold Regions Hydrological Modelling platform. *Hydrology and Earth System Sciences* 26(22): 5917–5931. doi: 10.5194/hess-26-5917-2022.
- Costa, D., C. Sutter, A. Shepherd, H. Jarvie, H. Wilson, J. Elliott, J. Liu and M. Macrae. 2023. Impact of climate change on catchment nutrient dynamics: insights from around the world. *Environmental Reviews* 31(1): 4–25. doi: 10.1139/er-2021-0109.
- Costa, D., J. Liu, J. Roste, and J. Elliott. 2019. Temporal Dynamics of Snowmelt Nutrient Release from Snow–Plant Residue Mixtures: An Experimental Analysis and Mathematical Model Development. *J. Environ. Qual.*, 48: 869-879. doi: 10.2134/jeq2018.12.0440
- Costa, D., J. Roste, J.W. Pomeroy, H. Baulch, J. Elliott, H. Wheeler and C. Westbrook. 2017. A modelling framework to simulate field-scale nitrate response and transport during snowmelt: The WINTRA model. *Hydrological Processes* 31(24): 4250-4268. doi: 10.1002/hyp.11346
- Costa, D., J.W. Pomeroy, T. Brown, H. Baulch, J. Elliott and M. Macrae. 2021. Advances in the simulation of nutrient dynamics in cold climate agricultural basins: Developing new nitrogen and phosphorus modules for the Cold Regions Hydrological Modelling Platform. *Journal of Hydrology* 603: 126901. doi: 10.1016/j.jhydrol.2021.126901
- De Baets, S., J. Poesen, J. Meersmans, L. Serlet. 2011. Cover crops and their erosion reducing effects during concentrated flow erosion. *Catena* 85:237–244
- Deb, P. and A.S. Kiem. 2020. Evaluation of rainfall–runoff model performance under non-stationary hydroclimatic conditions. *Hydrological Sciences Journal* 65(10): 1667–1684. doi: 10.1080/02626667.2020.1754420.
- Del Prado, A., P. Crosson, J.E. Olesen and C.A. Rotz. 2013. Whole-farm models to quantify greenhouse gas emissions and their potential use for linking climate change mitigation and adaptation in temperate grassland ruminant-based farming systems. *Animal* 7: 373–385. doi: 10.1017/s1751731113000748
- Dellar, M., C.F.E. Topp, G. Banos and E. Wall. 2018. A meta-analysis on the effects of climate change on the yield and quality of European pastures. *Agriculture, Ecosystems & Environment* 265: 413–420. doi: 10.1016/j.agee.2018.06.029.
- Delos Reyes, J. R. M., R. V. Parsons and R. Hoemsen. 2016. Winter Happens: The Effect of Ambient Temperature on the Travel Range of Electric Vehicles. in *IEEE Transactions on Vehicular Technology*, vol. 65, no. 6: 4016-4022. doi: 10.1109/TVT.2016.2544178.
- Devia, G.K., B.P. Ganasri, and G.S. Dwarakish. 2015. A Review on Hydrological Models. *Aquatic Procedia* 4 (2015): 1001 -1007. doi:10.1016/j.aqpro.2015.02.126

- Dile, Y., R. Srinivasan, and C. George. 2019. QGIS Interface for SWAT (QSWAT) Version 1.9. [Online] Available: swat.tamu.edu/software/qswat/
- Donnelly, C., B. Arheimer, R. Capell, J. Dahné, and J. Strömqvist. 2013. Regional overview of nutrient load in Europe – challenges when using a large-scale model approach, E-HYPE, IAHS Publ., 361, 49–58.
- Donnelly, C., J. Strömqvist, and B. Arheimer. 2011. Modelling climate change effects on nutrient discharges from the Baltic Sea catchment: processes and results. Water Quality: Current Trends and Expected Climate Change Impacts (Proceedings of symposium H04 held during IUGG2011 in Melbourne, Australia, July 2011) (IAHS Publ. 348, 2011)
- Donnelly, C., J. Strömqvist, and B. Arheimer. 2011. Modelling climate change effects on nutrient discharges from the Baltic Sea catchment: Processes and results. IAHS-AISH Publication.
- Drury, C.F., J.Y. Yang, R. De Jong, X.M. Yang, E.C. Huffman, V. Kirkwood and K. Reid. 2007. Residual soil nitrogen indicator for agricultural land in Canada. *Canadian Journal of Soil Science* 87(Special Issue): 167–177. doi: 10.4141/s06-064
- Du, T.L.T., H. Lee, D.D. Bui, B. Arheimer, H.-Y. Li, J. Olsson, S.E. Darby, J. Sheffield, D. Kim and E. Hwang. 2020. Streamflow prediction in “geopolitically ungauged” basins using satellite observations and regionalization at subcontinental scale. *Journal of Hydrology* 588: 125016. doi: 10.1016/j.jhydrol.2020.125016.
- Duethmann, D., G. Blöschl and J. Parajka. 2020. Why does a conceptual hydrological model fail to correctly predict discharge changes in response to climate change? *Hydrology and Earth System Sciences* 24(7): 3493–3511. doi: 10.5194/hess-24-3493-2020.
- Dumont, B., D. Andueza, V. Niderkorn, A. Lüscher, C. Porqueddu, and C. Picon-Cochard. 2015. A meta-analysis of climate change effects on forage quality in grasslands: specificities of mountain and Mediterranean areas. *Grass and Forage Science* 70: 239–254. doi: 10.1111/gfs.12169
- Duncan, E.W., P.J.A. Kleinman, D.B. Beegle and C.A. Rotz. 2017. Coupling Dairy Manure Storage with Injection to Improve Nitrogen Management: Whole-Farm Simulation Using the Integrated Farm System Model. *Agric. Environ. Lett.* 2:160048. doi:10.2134/aer2016.12.0048
- Dwarakish, G.S. and B.P. Ganasri. 2015. Impact of land use change on hydrological systems: A review of current modeling approaches. *Cogent Geoscience*, Article 1115691. doi: 10.1080/23312041.2015.1115691
- Environment and Climate Change Canada. 2020. Wet Deposition Maps. [Online] Available: <https://open.canada.ca/data/en/dataset/e8896575-1fb8-4e53-8acd-8579c3c055c2>
- Eldridge, S. 2004. Soil management for dairy and beef cattle grazing. NSW Agriculture.
- Elliott, J. 2013. Evaluating the potential contribution of vegetation as a nutrient source in snowmelt runoff. *Can. J. Soil Sci.* 93: 435–443. doi: 10.4141/cjss2012–050
- Emerson, D.G., A.V. Vecchia, and A.L. Dahl. 2005. Evaluation of Drainage-Area Ratio Method Used to Estimate Streamflow for the Red River of the North Basin, North Dakota and Minnesota. Scientific Investigations Report 2005-5017
- Environment and Climate Change Canada. 2020. Engineering Climate Datasets. [Online] Available: [Online] Available: climate.weather.gc.ca/prods_servs/engineering_e.html
- Environment and Climate Change Canada. 2023a. Historical climate data. [Online] Available: climate.weather.gc.ca/historical_data/search_historic_data_e.html
- Environment and Climate Change Canada. 2023b. National Water Data Archive: HYDAT. [Online] Available: <https://collaboration.cmc.ec.gc.ca/cmc/hydrometrics/www/>
- Escanilla-Minchel, R., H. Alcayaga, M. Soto-Alvarez, C. Kinnard and R. Urrutia. 2020.

- Evaluation of the Impact of Climate Change on Runoff Generation in an Andean Glacier Watershed. *Water* 12(12): 3547. doi: 10.3390/w12123547.
- Fang, X. and J.W. Pomeroy. 2007. Snowmelt runoff sensitivity analysis to drought on the Canadian prairies. *Hydrol. Process.* **21**: 2594-2609. [Online] Available: doi: 10.1002/hyp.6796
- Fang, X. and J.W. Pomeroy. 2009. Modelling blowing snow redistribution to prairie wetlands. *Hydrological Processes* 23(18): 2557–2569. doi: 10.1002/hyp.7348.
- Fang, X. and J.W. Pomeroy. 2020. Diagnosis of future changes in hydrology for a Canadian Rockies headwater basin. *Hydrology and Earth System Sciences* 24(5): 2731–2754. doi: 10.5194/hess-24-2731-2020.
- Fang, X. and J.W. Pomeroy. 2023. Simulation of the impact of future changes in climate on the hydrology of Bow River headwater basins in the Canadian Rockies. *Journal of Hydrology* 620: 129566. doi: 10.1016/j.jhydrol.2023.129566.
- Fang, X., J.W. Pomeroy, C.J. Westbrook, X. Guo, A.G. Minke and T. Brown. 2010. Prediction of snowmelt derived streamflow in a wetland dominated prairie basin. *Hydrology and Earth System Sciences* 14(6): 991-1006. doi: 10.5194/hess-14-991-2010
- FAO. 2001. Mixed crop-livestock farming: A review of traditional technologies based on literature and field experience. [Online] Available: www.fao.org/3/y0501e/y0501e03.htm
- FAO. 2023. Food Balances. [Online] Available: www.fao.org/faostat/en/#data/FBS
- Farjad, B., A. Gupta, H. Sartipizadeh and A.J. Cannon. 2019. A novel approach for selecting extreme climate change scenarios for climate change impact studies. *Science of The Total Environment* 678: 476–485. doi: 10.1016/j.scitotenv.2019.04.218.
- Ficchi, A., C. Perrin and V. Andréassian. 2019. Hydrological modelling at multiple sub-daily time steps: Model improvement via flux-matching. *Journal of Hydrology* 575: 1308–1327. doi: 10.1016/j.jhydrol.2019.05.084.
- Freedman, B. 1995. Acidification. In *Environmental Ecology (Second Edition)*. doi: 10.1016/B978-0-08-050577-0.50009-1
- Freyer, B., P. Ellssel, J.K. Friedel and K. Möller. 2023. The contribution of organic farming systems to soil fertility—A systems perspective. *Encyclopedia of Soils in the Environment* 135–145. doi: 10.1016/b978-0-12-822974-3.00240-8.
- Fry, J. and B. Huang. 2004. *Applied turfgrass science and physiology*. Wiley. ISBN: 978-0-471-47270-4
- Gage, A.M., S.K. Olinb and J. Nelson. 2016. Plowprint: Tracking Cumulative Cropland Expansion to Target Grassland Conservation. *Great Plains Research* 26(2): 107-116. [Online] Available: www.jstor.org/stable/44685737
- Gandra, J.R., J. Freitas Jr, R.V. Barletta, M. Maturana Filho, L. Gimenes, F. Vilela, P.S. Baruselli, and F.P. Rennó. 2011. Productive performance, nutrient digestion and metabolism of Holstein (*Bos taurus*) and Nellore (*Bos taurus indicus*) cattle and Mediterranean Buffaloes (*Bubalis bubalis*) fed with corn-silage based diets. *Livest. Sci.* 140:283–291. doi:10.1016/j.livsci.2011.04.005
- Gaudio, N., S. Belyazid, X. Gendre, A. Mansat, M. Nicolas, S. Rizzetto, H. Sverdrup and A. Probst. 2015. Combined effect of atmospheric nitrogen deposition and climate change on temperate forest soil biogeochemistry: A modeling approach. *Ecological Modelling* 306: 24–34. doi: 10.1016/j.ecolmodel.2014.10.002.
- Geisert, B.G., G.E. Erickson, T.J. Klopfenstein, C.N. Macken, M.K. Luebbe, and J.C.

- MacDonald. 2010. Phosphorus requirement and excretion of finishing beef cattle fed different concentrations of phosphorus. *J. Anim. Sci.* 88:2393–2402. doi:10.2527/jas.2008-1435
- Gelfan, A., D. Gustafsson, Y. Motovilov, B. Arheimer, A. Kalugin, I. Krylenko and A. Lavrenov. 2017. Climate change impact on the water regime of two great Arctic rivers: modeling and uncertainty issues. *Climatic Change* 141(3): 499–515. doi: 10.1007/s10584-016-1710-5.
- Geng, Y., F. Baumann, C. Song, M. Zhang, Y. Shi, P. Kühn, T. Scholten and J.-S. He. 2017. Increasing temperature reduces the coupling between available nitrogen and phosphorus in soils of Chinese grasslands. *Scientific Reports* 7(1). doi: 10.1038/srep43524.
- Ghaffar, S., S. Jomaa, G. Meon and M. Rode. 2021. Spatial validation of a semi-distributed hydrological nutrient transport model. *Journal of Hydrology* 593: 125818. doi: 10.1016/j.jhydrol.2020.125818.
- Glozier, N.E., J.A. Elliott, B. Holliday, J. Yarotski, and B. Harker. 2006. Water quality characteristics and trends in a small agricultural watershed: South Tobacco Creek, Manitoba, 1992–2001. Environment Canada, Ottawa, ON.
- Gong, X., A. Xu, S. Du and Y. Zhou. 2022. Spatiotemporal variations in the elasticity of runoff to climate change and catchment characteristics with multi-timescales across the contiguous United States. *Journal of Water and Climate Change* 13(3): 1408–1424. doi: 10.2166/wcc.2022.242
- Gordon, N.D., T.A. McMahon, and B.L. Finlayson. 1992. Stream hydrology: an introduction for ecologists. Wiley, New York.
- Government of Alberta. 2009. Nutrient Management on Intensively Managed Pastures. [Online] Available: <https://open.alberta.ca/publications/4416930>
- Government of Canada. 2019. Changes in snow.
- Government of Manitoba. 2009. Manure Nutrients and their Behaviour in Soil.
- Government of Manitoba. 2015. Properties of Manure. [Online] Available: www.gov.mb.ca/agriculture/environment/nutrient-management/pubs/properties-of-manure.pdf
- Government of Manitoba. n.d. Prevention of Pasture Bloat in Cattle Grazing Alfalfa. [Online] Available: <https://www.gov.mb.ca/agriculture/livestock/beef/prevention-of-pasture-bloat-in-cattle-grazing-alfalfa.html>
- Gray, D.M. and P.G. Landine. 1987. Albedo model for shallow prairie snow covers. *Canadian Journal of Earth Sciences* 24: 1760-1768.
- Gray, D.M. and P.G. Landine. 1988. An energy-budget snowmelt model for the Canadian Prairies. *Canadian Journal of Earth Sciences* 25: 1292-1303.
- Gray, D.M., P.G. Landine and R.J. Granger. 1985. Simulating infiltration into frozen Prairie soils in stream flow models. *Canadian Journal of Earth Science* 22: 464-474.
- Grillakis, M.G., A.G. Koutroulis and I.K. Tsanis. 2011. Climate change impact on the hydrology of Spencer Creek watershed in Southern Ontario, Canada. *Journal of Hydrology* 409(1–2): 1–19. doi: 10.1016/j.jhydrol.2011.06.018.
- Groot, J.C.J., G.J.M. Oomen and W.A.H. Rossing. 2012. Multi-objective optimization and design of farming systems. *Agricultural Systems* 110: 63–77. doi: 10.1016/j.agsy.2012.03.012.
- Guo, Z., C. Chang and R. Wang. 2016. A Novel Method to Downscale Daily Wind Statistics to Hourly Wind Data for Wind Erosion Modelling. *Geo-Informatics in Resource Management and Sustainable Ecosystem*, 2016, Volume 569: 611-619. doi: 10.1007/978-3-662-49155-3_64
- Hamel, C., E. Reimer. 2004. The St. Lazare area of Manitoba: a biodiversity hotspot. *Blue Jay* 62: 203-210.

- Hamza, M.A. and W.K. Anderson. 2005. Soil compaction in cropping systems. *Soil and Tillage Research* 82(2): 121–145. doi: 10.1016/j.still.2004.08.009.
- Haruna, A., P.-A. Garambois, H. Roux, P. Javelle and M. Jay-Allemand. 2022. Does Flash Flood Model Performance Increase with Complexity? Signature and Sensitivity-Based Comparison of Conceptual and Process-Oriented Models on French Mediterranean Cases. *Hydrology* 9(8): 141. doi: 10.3390/hydrology9080141.
- Harvriilla, C.A., J.B. Bradford, C.B. Yackulic, and S.M. Munson. 2022. Divergent climate impacts on C3 versus C4 grasses imply widespread 21st century shifts in grassland functional composition. *Diversity and Distributions* 29(3): 379-394. doi: 10.1111/ddi.13669
- He, S., K. Chen, Z. Liu and L. Deng. 2023. Exploring the impacts of climate change and human activities on future runoff variations at the seasonal scale. *Journal of Hydrology* 619: 129382. doi: 10.1016/j.jhydrol.2023.129382.
- Herrero, M., P.K. Thornton, P. Gerber, and R.S. Reid. 2009. Livestock, livelihoods and the environment: understanding the trade-offs. *Current Opinion in Environmental Sustainability* 1(2): 111-120. doi: 10.1016/j.cosust.2009.10.003
- Hoar, B., and J. Angelos. n.d. Beef Cattle Production. In *Food Animal Production Manual: 22-34*. Western Institute for Food Safety & Security at the University of California - Davis and the Food and Drug Administration.
- Hock, R. 2003. Temperature index melt modelling in mountain areas. *Journal of Hydrology* 282(1–4): 104–115. doi: 10.1016/s0022-1694(03)00257-9.
- Hofmann, N. 2008. A geographical profile of livestock manure production in Canada, 2006. *EnviroStats, Winter 2008* 2(4): 12-16. [Online] Available: www150.statcan.gc.ca/n1/en/pub/16-002-x/16-002-x2008004-eng.pdf?st=-YfO_ZGI
- Holzworth, D.P., N.I. Huth, P.G. deVoil, E.J. Zurcher, N.I. Herrmann, G. McLean, K. Chenu, E.J. van Oosterom, V. Snow, C. Murphy, A.D. Moore, H. Brown, J.P.M. Whish, S. Verrall, J. Fainges, L.W. Bell, A.S. Peake, P.L. Poulton, Z. Hochman, P.J. Thorburn, D.S. Gaydon, N.P. Dalgliesh, D. Rodriguez, H. Cox, S. Chapman, A. Doherty, E. Teixeira, J. Sharp, R. Cichota, I. Vogeler, F.Y. Li, E. Wang, G.L. Hammer, M.J. Robertson, J.P. Dimes, A.M. Whitbread, J. Hunt, H. van Rees, T. McClelland, P.S. Carberry, J.N.G. Hargreaves, N. MacLeod, C. McDonald, J. Harsdorf, S. Wedgwood and B.A. Keating. 2014. APSIM – Evolution towards a new generation of agricultural systems simulation. *Environmental Modelling & Software* 62: 327–350. doi: 10.1016/j.envsoft.2014.07.009
- Houlbrooke, D.J. and S. Laurenson. 2013. Effect of sheep and cattle treading damage on soil microporosity and soil water holding capacity. *Agricultural Water Management* 121: 81–84. doi: 10.1016/j.agwat.2013.01.010.
- Howe, E., W. Howland, and S. Strouse. 2011. Modeling Efforts and Identification of Critical Source Areas of Phosphorus Within the Vermont Sector of the Missisquoi Bay Basin. Lake Champlain Basin Program, Technical Report No. 63A. [Online] Available: www.lcbp.org/wp-content/uploads/2013/07/63A_Missisquoi_CSA-3.pdf
- Huang, J., C. Xu, B.G. Ridoutt, X. Wang and P. Ren. 2017. Nitrogen and phosphorus losses and eutrophication potential associated with fertilizer application to cropland in China. *Journal of Cleaner Production* 159: 171–179. doi: 10.1016/j.jclepro.2017.05.008.
- Huang, J.-C., and C. Shang. 2006. Air Stripping. In: Wang, L.K., Hung, Y.T., Shammas, N.K. (eds) *Advanced Physicochemical Treatment Processes. Handbook of Environmental Engineering*, vol 4. Humana Press. doi: 10.1007/978-1-59745-029-4_2

- Hubbard, R. K., G. L. Newton, and G. M. Hill. 2004. Water quality and the grazing animal. *J Anim Sci.* 2004;82 E-Suppl:E255-263. doi: 10.2527/2004.8213_supplE255x. PMID: 15471806
- Huber, R., S. Le’Clec’h, N. Buchmann and R. Finger. 2022. Economic value of three grassland ecosystem services when managed at the regional and farm scale. *Scientific Reports* 12(1). doi: 10.1038/s41598-022-08198-w.
- Hünerberg, M., S. McGinn, K. Beauchemin, E. Okine, O. Harstad, and T. McAllister. 2013. Effect of dried distillers grains plus solubles on enteric methane emissions and nitrogen excretion from growing beef cattle. *J. Anim. Sci.* 91:2846–2857. doi:10.2527/jas.2012-5564
- Ide, J., I. Takeda, H. Somura, Y. Mori, Y. Sakuno, Y. Yone, and E. Takahashi. 2019. Impacts of Hydrological Changes on Nutrient Transport From Diffuse Sources in a Rural River Basin, Western Japan. *Journal of Geophysical Research: Biogeosciences*, 124, 2565– 2581. doi: 10.1029/2018JG004513
- Idrissou, M., B. Diekkrüger, B. Tischbein, B. Ibrahim, Y. Yira, G. Steup and T. Poméon. 2020. Testing the Robustness of a Physically-Based Hydrological Model in Two Data Limited Inland Valley Catchments in Dano, Burkina Faso. *Hydrology* 7(3): 43. doi: 10.3390/hydrology7030043.
- Irshad, M., A.E. Eneji, Z. Hussain, and M. Ashraf. 2013. Chemical characterization of fresh and composted livestock manures. *Journal of Soil Science and Plant Nutrition* 2013, 13(1): 115-121. doi: 10.4067/S0718-95162013005000011
- Izaurrealde, R.C., A.M. Thomson, J.A. Morgan, P.A. Fay, H.W. Polley and J.L. Hatfield. 2011. Climate Impacts on Agriculture: Implications for Forage and Rangeland Production. *Agronomy Journal* 103(2): 371–381. doi: 10.2134/agronj2010.0304.
- Jégo, G., A. Rotz, G. Bélanger, G.F. Tremblay, E. Charbonneau and D. Pellerin. 2015. Simulating forage crop production in a northern climate with the Integrated Farm System Model. *Can. J. Plant Sci.* (2015) 95: 745-757. doi:10.4141/CJPS-2014-375
- Jenicek, M., J. Hnilica, O. Nedelcev and V. Sipek. 2021. Future changes in snowpack will impact seasonal runoff and low flows in Czechia. *Journal of Hydrology: Regional Studies* 37: 100899. doi: 10.1016/j.ejrh.2021.100899.
- Jennings, E., N. Allott, D.C. Pierson, E.M. Schneiderman, D. Lenihan, P. Samuelsson and D. Taylor. 2009. Impacts of climate change on phosphorus loading from a grassland catchment: Implications for future management. *Water Research* 43(17): 4316–4326. doi: 10.1016/j.watres.2009.06.032.
- Johnson, C., G. Albrecht, Q. Ketterings, J. Beckman, and K. Stockin. 2005. Nitrogen Basics – The Nitrogen Cycle. *Agronomy Fact Sheet Series: fact sheet 2.*
- Johnson, M.P. 2016. Photosynthesis. *Essays Biochem.* 60(3): 255–273. doi: 10.1042/EBC20160016
- Jones, C., B.D. Brown, R. Engel, D. Horneck and K. Olson-Rutz. 2013. Factors affecting nitrogen fertilizer volatilization. Montana State University Extension.
- Jones, J.W., G. Hoogenboom, C.H. Porter, K.J. Boote, W.D. Batchelor, L.A. Hunt, P.W. Wilkens, U. Singh, A.J. Gijsman, and J.T. Ritchie. 2003. The DSSAT cropping system model. *Europ. J. Agronomy* 18 (2003): 235-265.
- Josan, M., B. Taylor and K. Grace. 2019. Appendix 5C-3: Use of Soil Inversion to Control Phosphorus Flux. In 2019 South Florida Environmental Report – Volume I.
- Kalcic, M.M., I. Chaubey, and J. Frankenberger. 2015. Defining Soil and Water Assessment Tool

- (SWAT) hydrologic response units (HRUs) by field boundaries. *Int J Agric & Biol Eng* 8(3): 69 – 80. doi: 10.3965/j.ijabe.20150803.951
- Kendall, M.G., 1975. Rank correlation methods. London: Charles Griffin.
- Ketterings, Q.M., G. Albrecht, K. Czymmek, and S. Bossard. 2005. Nitrogen Credits from Manure. Agronomy Fact Sheet Series: fact sheet 4. [Online] Available: <http://cceonondaga.org/resources/nitrogen-credits-from-manure>
- Khan, M.N. and F. Mohammad. 2013. Eutrophication: Challenges and Solutions. *Eutrophication: Causes, Consequences and Control* 1–15. doi: 10.1007/978-94-007-7814-6_1.
- Kharel, G., H. Zheng and A. Kirilenko. 2016. Can land-use change mitigate long-term flood risks in the Prairie Pothole Region? The case of Devils Lake, North Dakota, USA. *Regional Environmental Change* 16(8): 2443–2456. doi: 10.1007/s10113-016-0970-y.
- Khorasani, G.R., P.E. Jedel, J.H. Helm and J.J. Kennelly. 1997. Influence of stage of maturity on yield components and chemical composition of cereal grain silages. *Canadian Journal of Animal Science* 77(2): 259–267. doi: 10.4141/a96-034.
- Kim, S.-B., H.-T., Huang, L. Tsang, T. Jackson, H. McNairn, and J.V. Zyl. 2014. Soil moisture retrieval using L-band time-series SAR data from the SMAPVEX12 experiment, Proceedings of EUSAR 2014; 10th European Conference on Synthetic Aperture Radar, 1–4.
- Kirtman, B., S.B. Power, J.A. Adedoyin, G.J. Boer, R. Bojariu, I. Camilloni, F.J. Doblas-Reyes, A.M. Fiore, M. Kimoto, G.A. Meehl, M. Prather, A. Sarr, C. Schär, R. Sutton, G.J. van Oldenborgh, G. Vecchi and H.J. Wang. 2013. Near-term Climate Change: Projections and Predictability. In: *Climate Change 2013: The Physical Science Basis. Contribution of Working Group I to the Fifth Assessment Report of the Intergovernmental Panel on Climate Change* [Stocker, T.F., D. Qin, G.-K. Plattner, M. Tignor, S.K. Allen, J. Boschung, A. Nauels, Y. Xia, V. Bex and P.M. Midgley (eds.)]. Cambridge University Press, Cambridge, United Kingdom and New York, NY, USA.
- Köchy, M. and S.D. Wilson. 2001. Nitrogen deposition and forest expansion in the northern Great Plains. *Journal of Ecology* 89(5): 807–817. doi: 10.1046/j.0022-0477.2001.00600.x.
- Koenig, K.M., and K.A. Beauchemin. 2018. Effect of feeding condensed tannins in high protein finishing diets containing corn distillers grains on ruminal fermentation, nutrient digestibility, and route of nitrogen excretion in beef cattle. *J. Anim. Sci.* 96:4398–4413. doi:10.1093/jas/sky273
- Koenig, K.M., and K.A. Beauchemin. 2013. Nitrogen metabolism and route of excretion in beef feedlot cattle fed barley-based backgrounding diets varying in protein concentration and rumen degradability. *J. Anim. Sci.* 91:2295–2309. doi:10.2527/jas.2012-5652
- Kossieris, P., H. Tyralis, D. Koutsoyiannis, C. Makropoulos, and A. Efstratiadis. 2016. HyetosMinute: A package for temporal stochastic simulation of rainfall at fine time scales. R package version 2.0. [Online] Available: www.itia.ntua.gr/en/softinfo/3/
- Kreyling, J., C. Beierkuhnlein and A. Jentsch. 2010. Effects of soil freeze–thaw cycles differ between experimental plant communities. *Basic and Applied Ecology* 11(1): 65–75. doi: 10.1016/j.baae.2009.07.008.s
- Kuo, C.C., T.Y. Gan and K. Higuchi. 2017. Evaluation of Future Streamflow Patterns in Lake Simcoe Subbasins Based on Ensembles of Statistical Downscaling. *Journal of Hydrologic Engineering* 22(9). doi: 10.1061/(asce)he.1943-5584.0001548.
- Laforge, J., V. Corkal, and A. Cosby. 2021. Farming the Future: Agriculture and climate change

- on the Canadian Prairies. International Institute for Sustainable Development. [Online] Available: www.iisd.org/publications/report/farming-future-agriculture-and-climate-change-canadian-prairies
- Lastoria, B. 2008. Hydrological processes on the land surface: A survey of modelling approaches.
- Legesse, G., M.R.C. Cordeiro, K.H. Ominski, K.A. Beauchemin, R. Kroebel, E.J. McGeough, S. Pogue and T.A. McAllister. 2018. Water use intensity of Canadian beef production in 1981 as compared to 2011. *Science of The Total Environment* 619–620: 1030–1039. doi: 10.1016/j.scitotenv.2017.11.194.
- Lessmann, M., A. Kanellopoulos, J. Kros, F. Orsi and M. Bakker. 2023. Maximizing agricultural reuse of recycled nutrients: A spatially explicit assessment of environmental consequences and costs. *Journal of Environmental Management* 332: 117378. doi: 10.1016/j.jenvman.2023.117378.
- Leuther, F. and S. Schlüter. 2021. Impact of freeze–thaw cycles on soil structure and soil hydraulic properties. *SOIL* 7: 179–191. doi: 10.5194/soil-7-179-2021
- Li, C. 2017. The role of beef in human nutrition and health. *Burleigh Dodds Science Publishing Limited*. doi: 10.19103/AS.2016.0009.16
- Lindström, G., C. Pers, J. Rosberg, J. Strömqvist and B. Arheimer. 2010. Development and testing of the HYPE (Hydrological Predictions for the Environment) water quality model for different spatial scales. *Hydrology Research* 41(3-4): 295-319. doi:10.2166/nh.2010.007
- Little, S.M., J. Lindeman, K. Maclean and H.H. Janzen. 2008. Holos - A tool to estimate and reduce GHGs from farms. Methodology and algorithms for Version 1.1.x. Agriculture & Agri-Food Canada. ISBN 978-1-100-11424-8
- Littlewood, I.G. and B.F.W. Croke. 2008. Data time-step dependency of conceptual rainfall—streamflow model parameters: an empirical study with implications for regionalisation. *Hydrological Sciences Journal* 53(4): 685–695. doi: 10.1623/hysj.53.4.685.
- Liu, J., B. Ulen, G. Bergkvist and H. Aronsson. 2014. Freezing-thawing effects on phosphorus leaching from catch crops. *Nutr. Cycling Agroecosyst.* 99: 17–30. doi: 10.1007/s10705–014–9615–z
- Liu, J., H.M. Baulch, M.L. Macrae, H.F. Wilson, J.A. Elliott, L. Bergström, A.J. Glenn and P.A. Vadas. 2019. Agricultural Water Quality in Cold Climates: Processes, Drivers, Management Options, and Research Needs. *Journal of Environmental Quality* 48(4): 792–802. doi: 10.2134/jeq2019.05.0220.
- Liu, J., R. Khalaf, and B. Ulen. 2013a. Potential phosphorus release from catch crop shoots and roots after freezing-thawing. *Plant Soil* 371: 543-557. doi: 10.1007/s11104-013-1716-y
- Liu, K., J.A. Elliott, D.A. Lobb, D.N. Flaten, and J. Yaroski. 2013b. Critical Factors Affecting Field-Scale Losses of Nitrogen and Phosphorus in Spring Snowmelt Runoff in the Canadian Prairies. *J. Environ. Qual.* 42: 484 - 496. doi: 10.2134/jeq2012.0385
- López-Moreno, J.I., J.W. Pomeroy, J. Revuelto, and S.M. Vicente-Serrano. 2013. Response of snow processes to climate change: spatial variability in a small basin in the Spanish Pyrenees. *Hydrological Processes* 27(18): 2637-2650. doi: 10.1002/hyp.9408
- Lorimor, J. and W. Powers. 2004. Manure Characteristics. [Online] Available: www.canr.msu.edu/uploads/files/ManureCharacteristicsMWPS-18_1.pdf
- Luebke, M.K., J.M. Patterson, K.H. Jenkins, E.K. Buttrey, T.C. Davis, B.E. Clark, F.T. McCollum, N.A. Cole, and J.C. MacDonald. 2012. Wet distillers grains plus solubles concentration in steam-flaked-corn-based diets: Effects on feedlot cattle performance, carcass

- characteristics, nutrient digestibility, and ruminal fermentation characteristics. *J. Anim. Sci.* 90:1589–1602. doi:10.2527/jas.2011-4567
- Luo, C., Z. Li, H. Liu, H. Li, R. Wan, J. Pan and X. Chen. 2020. Differences in the responses of flow and nutrient load to isolated and coupled future climate and land use changes. *Journal of Environmental Management* 256: 109918. doi: 10.1016/j.jenvman.2019.109918.
- Mackey, K.R.M. and A. Paytan. 2009. Phosphorus Cycle. *Encyclopedia of Microbiology* 322–334. doi: 10.1016/b978-012373944-5.00056-0.
- Mahat, V. and A. Anderson. 2013. Impacts of climate and catastrophic forest changes on streamflow and water balance in a mountainous headwater stream in Southern Alberta. *Hydrology and Earth System Sciences* 17(12): 4941–4956. doi: 10.5194/hess-17-4941-2013.
- Mahmood, T.H., J.W. Pomeroy, H.S. Wheatler, and H.M. Baulch. 2017. Hydrological responses to climatic variability in a cold agricultural region. *Hydrological Processes* 31(4): 854-870. doi: 10.1002/hyp.11064
- Mahoney, K., J.D. Scott, M. Alexander, R. McCrary, M. Hughes, D. Swales, and M. Bukovsky. 2021. Cool season precipitation projections for California and the Western United States in NA-CORDEX models. *Climate Dynamics* 56: 3081–3102. doi: 10.1007/s00382-021-05632-z
- Man, Z., C. Xie, R. Jiang and S. Che. 2022. Freeze–thaw cycle frequency affects root growth of alpine meadow through changing soil moisture and nutrients. *Sci Rep* 12, 4436. doi: 10.1038/s41598-022-08500-w
- Manitoba Agricultural Services Corporation. 2023. Manitoba Management Plus Program. [Online] Available: www.masc.mb.ca/masc.nsf/mmpp_index.html
- Manitoba Agriculture. 2019. The Manitoba Protein Advantage. [Online] Available: www.gov.mb.ca/agriculture/protein/pubs/manitoba-protein-strategy.pdf
- Manitoba Agriculture. 2022. Birtle. [Microsoft Excel spreadsheet]
- Manitoba Agriculture. n.d.a. Agricultural Climate of Manitoba. [Online] Available: www.gov.mb.ca/agriculture/weather/agricultural-climate-of-mb.html
- Manitoba Agriculture. n.d.b. Crop report. [Online] Available: www.gov.mb.ca/agriculture/crops/seasonal-reports/crop-report-archive/index.html
- Mann, H.B., 1945. Nonparametric tests against trend. *Econometrica*, 13(3): 245–259. doi: 10.2307/1907187
- March-Salas, M. and P.S. Fitze. 2019. A multi-year experiment shows that lower precipitation predictability encourages plants’ early life stages and enhances population viability. *PeerJ* 7: e6443. doi: 10.7717/peerj.6443.
- Martina, M.L.V., and E. Todini. 2009. Watershed Hydrological Modeling: Toward Physically Meaningful Processes Representation. In: Sorooshian S., Hsu KL., Coppola E., Tomassetti B., Verdecchia M., Visconti G. (eds) *Hydrological Modelling and the Water Cycle*. Water Science and Technology Library, vol 63: 229-241. doi: 10.1007/978-3-540-77843-1_10
- Martina, M.L.V., and E. Todini. 2009. Watershed Hydrological Modeling: Toward Physically Meaningful Processes Representation. In: Sorooshian S., Hsu KL., Coppola E., Tomassetti B., Verdecchia M., Visconti G. (eds) *Hydrological Modelling and the Water Cycle*. Water Science and Technology Library, vol 63: 229-241. doi: 10.1007/978-3-540-77843-1_10
- McMaster, G.S., and W.W. Wilhelm. 1997. Growing degree-days: one equation, two interpretations. *Agricultural and Forest Meteorology* 87(4): 291–300. doi: 10.1016/s0168-1923(97)00027-0
- Mearns, L.O., S. McGinnis, D. Korytina, R. Arritt, S. Biner, M. Bukovsky, H.-I. Chang, O.

- Christensen, D. Herzmann, Y. Jiao, S. Kharin, M. Lazare, G. Nikulin, M. Qian, J. Scinocca, K. Winger, C. Castro, A. Frigon, and W. Gutowski. 2017. The NA-CORDEX dataset, version 1.0. NCAR Climate Data Gateway. doi: 10.5065/D6SJ1JCH
- Melsen, L., A. Teuling, P. Torfs, M. Zappa, N. Mizukami, M. Clark, and R. Uijlenhoet. 2016. Representation of spatial and temporal variability in large-domain hydrological models: case study for a mesoscale pre-Alpine basin. *Hydrol. Earth Syst. Sci.*, **20**: 2207–2226. doi: 10.5194/hess-20-2207-2016
- Meyer, J.H., G.P. Lofgreen, and J.L. Hull. 1957. Selective Grazing by Sheep and Cattle. *Journal of Animal Science* 16(4): 766–772. doi: 10.2527/jas1957.164766x
- Michiels, K. Gottfried, and Z. Yu. 2017. Simulating cold-region hydrology in an intensively drained agricultural watershed in Manitoba, Canada, using the Cold Regions Hydrological Model. *Hydrology and Earth System Sciences*, 21: 3483-3506. doi: 10.5194/hess-21-3483-2017
- Monteith, J.L. 1965. Evaporation and environment. In *State and movement of water in living organisms*. 19th Symposium of the Society for Experimental Biology. Cambridge University Press: Cambridge, 205-234.
- Moore, A., G. Pirelli, S. Filley, S. Fransen, D. Sullivan, M. Fery, and T. Thomson. 2019. Nutrient management for pastures: Western Oregon and Western Washington. Oregon State University Extension Service. [Online] Available: <https://catalog.extension.oregonstate.edu/sites/catalog/files/project/pdf/em9224.pdf>
- Moriasi, D.N., J.G. Arnold, M.W. Van Liew, R.L. Bingner, R.D. Harmel and T.L. Veith. 2007. Model Evaluation Guidelines for Systematic Quantification of Accuracy in Watershed Simulations. *Transactions of the ASABE* 50(3): 885–900. doi: 10.13031/2013.23153.
- Moriasi, D.N., M.W. Gitau, N. Pai, and P. Daggupati. 2015. Hydrologic and Water Quality Models: Performance Measures and Evaluation Criteria. *American Society of Agricultural and Biological Engineers* 58(6): 1763-1785. doi: 10.13031/trans.58.10715
- Mouelhi, S., C. Michel, C. Perrin and V. Andréassian. 2006. Stepwise development of a two-parameter monthly water balance model. *Journal of Hydrology* 318(1–4): 200–214. doi: 10.1016/j.jhydrol.2005.06.014.
- Müller, L., J. Lipiec, T.S. Kornecki, S. Gebhardt. 2011. Trafficability and Workability of Soils. *Encyclopedia of Agrophysics*. doi: 10.1007/978-90-481-3585-1_176
- Mus, F., M.B. Crook, K. Garcia, A. Garcia Costas, B.A. Geddes, E.D. Kouri, P. Paramasivan, M.-H. Ryu, G.E.D. Oldroyd, P.S. Poole, M.K. Udvardi, C.A. Voigt, J.-M. Ané and J.W. Peters. 2016. Symbiotic Nitrogen Fixation and the Challenges to Its Extension to Nonlegumes. *Applied and Environmental Microbiology* 82(13): 3698–3710. doi: 10.1128/aem.01055-16.
- Nair, J., G.B. Penner, P. Yu, H.A. Lardner, T.A. McAllister, D. Damiran, and J.J. McKinnon. 2016. Evaluation of canola meal derived from Brassica juncea and Brassica napus on rumen fermentation and nutrient digestibility by feedlot heifers fed finishing diets. *Can. J. Anim. Sci.* 96:342–353. doi:10.1139/cjas-2015-0184
- National Aeronautics and Space Administration. 2023. NASA POWER | Data Access Viewer. [Online] Available: <https://power.larc.nasa.gov/data-access-viewer/>
- Nemec, J. 1993. Comparison and selection of existing hydrological models for the simulation of the dynamic water balance processes in basins of different sizes and on different scales. ISBN 90-70980-16-9
- Noll, P. and M. Henkel. 2020. History and Evolution of Modeling in Biotechnology: Modeling &

- Simulation, Application and Hardware Performance. *Computational and Structural Biotechnology Journal* 18 (2020): 3309-3323. doi: 10.1016/j.csbj.2020.10.018
- Ochoa-Rodriguez, S., L. Wang, A. Gires, R.D. Pina, R. Reinoso-Rondinel, G. Bruni, A. Ichiba, S. Gaitan, E. Cristiano, J.V. Assel, S. Kroll, D. Murlà-Tuyls, B. Tisserand, D. Schertzer, I. Tchiguirinskaia, C. Onof, P. Willems, M.T. Veldhuis. 2015. Impact of spatial and temporal resolution of rainfall inputs on urban hydrodynamic modelling outputs: A multi-catchment investigation. *Journal of Hydrology* 531: 389-407. doi: 10.1016/j.jhydrol.2015.05.035
- Øgaard, A.F. 2015. Freezing and thawing effects on phosphorus release from grass and cover crop species cover crop species. *Acta Agric. Scand., Sect. B* 65:529–536. doi:10.1080/09064710.2015.1030444
- Organisation for Economic Co-operation and Development. 2022. Meat consumption: Beef and veal, Kilograms/capita, 2010-2022. [Online] Available: <https://data.oecd.org/>
- Osada, K., S. Ura, M. Kagawa, M. Mikami, T.Y. Tanaka, S. Matoba, K. Aoki, M. Shinoda, Y. Kurosaki, M. Hayashi, A. Shimizu and M. Uematsu. 2014. Wet and dry deposition of mineral dust particles in Japan: factors related to temporal variation and spatial distribution. *Atmospheric Chemistry and Physics* 14(2): 1107–1121. doi: 10.5194/acp-14-1107-2014
- Oschner, T. 2019. Rain or Shine: an introduction to soil physical properties and processes. Oklahoma State University. [Online] Available: <https://open.library.okstate.edu/rainorshine/>
- Pagliari, P.H., M. Wilson, H.M. Waldrip and Z. He. 2020. Nitrogen and Phosphorus Characteristics of Beef and Dairy Manure. In *Animal Manure* (eds H.M. Waldrip, P.H. Pagliari and Z. He). doi: 10.2134/aspectpub67.c4
- Palminteri, S., V. Wyart and E. Koechlin. 2017. The Importance of Falsification in Computational Cognitive Modeling. *Trends in Cognitive Sciences* 21(6): 425–433. doi: 10.1016/j.tics.2017.03.011.
- Parra, V., P. Fuentes-Aguilera and E. Muñoz. 2018. Identifying advantages and drawbacks of two hydrological models based on a sensitivity analysis: a study in two Chilean watersheds. *Hydrological Sciences Journal* 63(12): 1831–1843. doi: 10.1080/02626667.2018.1538593.
- Pavlovskii, I., M. Hayashi and D. Itenfisu. 2019. Midwinter melts in the Canadian prairies: energy balance and hydrological effects. *Hydrology and Earth System Sciences* 23(4): 1867–1883. doi: 10.5194/hess-23-1867-2019.
- Payant, C., G. Jégo, V. Ouellet, P. Grenier, G.F. Tremblay, G. Bélanger and É. Charbonneau. 2021. Modeled performance of forage mixtures and annual crops grown in eastern Canada under climate change. *Agronomy Journal* 113(6): 4945–4964. doi: 10.1002/agj2.20894
- Pechlivanidis, I. G., and B. Arheimer. 2015. Large-scale hydrological modelling by using modified PUB recommendations: The India-HYPE case. *Hydrology and Earth System Sciences*, 19(11): 4559–4579. doi: 10.5194/hess-19-4559-2015
- Picon-Cochard, C., F. Teyssonneyre, J.M. Besle and J.-F. Soussana. 2004. Effects of elevated CO₂ and cutting frequency on the productivity and herbage quality of a semi-natural grassland. *European Journal of Agronomy* 20(4): 363–377. doi: 10.1016/s1161-0301(03)00040-6
- Pierong, R. and M. Takman. 2014. Evaluation of the hydrological model India-HYPE With focus on precipitation driving data and regionalization quality. Uppsala University, Sweden.
- Pogue, S.J., R. Kröbel, H.H. Janzen, K.A. Beauchemin, G. Legesse, D. M. d. Souza, M. Iravani,

- C. Slin, J. Byrne, T.A. McAllister. 2018. Beef production and ecosystem services in Canada's prairie provinces: A review. *Agricultural Systems* 166: 152-172. doi: 10.1016/j.agsy.2018.06.011.
- Pomeroy, J.W. and Li, L. 2000. Prairie and Arctic areal snow cover mass balance using a blowing snow model. *Journal of Geophysical Research* 105: 26619-26634.
- Pomeroy, J.W., D.M. Gray and P.G. Landine. 1993. The Prairie Blowing Snow Model: characteristics, validation, operation. *Journal of Hydrology* 144(1-4): 165-192. doi: 10.1016/0022-1694(93)90171-5.
- Pomeroy, J.W., D.M. Gray, N.R. Hedstrom and J.R. Janowicz. 2002. Prediction of seasonal snow accumulation in cold climate forests. *Hydrological Processes* 16(18): 3543-3558. doi: 10.1002/hyp.1228.
- Pomeroy, J.W., D.M. Gray, T. Brown, N.R. Hedstrom, W.L. Quinton, R.J. Granger, and S.K. Carey. 2007. The cold regions hydrological model: a platform for basing process representation and model structure on physical evidence. *Hydrological Processes* 21(19): 2650-2667. doi: 10.1002/hyp.6787
- Pomeroy, J.W., T. Brown, X. Fang, K.R. Shook, D. Pradhananga, R. Armstrong, P. Harder, C. Marsh, D. Costa, S.A. Krogh, C. Aubry-Wake, H. Annand, P. Lawford, Z. He, M. Kompanizare and J.I. Lopez Moreno. 2022. The cold regions hydrological modelling platform for hydrological diagnosis and prediction based on process understanding. *Journal of Hydrology* 615: 128711. doi: 10.1016/j.jhydrol.2022.128711
- Pomeroy, J.W., X. Fang, K. Shook, and P.H. Whitfield. 2013. Predicting In Ungauged Basins using Physical Principles Obtained Using Deductive, Inductive and Abductive Reasoning Approach. In *Putting Prediction in Ungauged Basins into Practice*, J.W. Pomeroy, P.H. Whitfield, C. Spence(Ed.): 41-62.
- Pomeroy, J.W., X. Fang, K. Shook, and P.H. Whitfield. 2014. Predicting in ungauged basins using physical principles obtained using the deductive, inductive, and abductive reasoning approach.
- Prairie Province's Committee. 2004. Tri-Provincial Manure Application and Use Guidelines. [Online] Available: www.gov.mb.ca/agriculture/environment/nutrient-management/manure-management.html
- Prairies Regional Adaptation Collaborative. 2011. Vulnerability of Grasslands to Climate Change. SRC Publication No. 12855-2E11.
- Prasad, R. and D. Chakraborty. 2019. Phosphorus Basics: Understanding Phosphorus Forms and Their Cycling in the Soil. Alabama Cooperative Extension System.
- Pratap, S., and Y. Markonis. The response of the hydrological cycle to temperature changes in recent and distant climatic history. *Prog Earth Planet Sci* 9: 30. doi: 10.1186/s40645-022-00489-0
- Pulido, M., J. Barrena-Gonzalez, W. Badgery, J. Rodrigo-Comino, and A. Cerda. 2018. Sustainable grazing. *Current Opinion in Environmental Science & Health* 5: 42-46. doi: 10.1016/j.coesh.2018.04.004
- Putnam, D.H. and S.B. Orloff. 2014. Forage Crops. *Encyclopedia of Agriculture and Food Systems*: 381-405. doi: 10.1016/b978-0-444-52512-3.00142-x.
- Qi, J., X. Zhang, Q. Yang, R. Srinivasan, J.G. Arnold, J. Li, S.T. Waldhoff and J. Cole. 2020. SWAT ungauged: Water quality modeling in the Upper Mississippi River Basin. *Journal of Hydrology* 584: 124601. doi: 10.1016/j.jhydrol.2020.124601.

- Rasouli, K., J.W. Pomeroy, and P.H. Whitfield. 2019. Hydrological Responses of Headwater Basins to Monthly Perturbed Climate in the North American Cordillera. *Journal of Hydrometeorology* 20(5): 863-882. doi: 10.1175/JHM-D-18-0166.1
- Rawal, N., K.R. Pande, R. Shrestha and S.P. Vista. 2022. Phosphorus and potassium mineralization as affected by phosphorus levels and soil types under laboratory condition. *Agrosystems, Geosciences & Environment* 5(1). doi: 10.1002/agg2.20229.
- Rawls, W.J., D.L. Brakensiek and N. Miller. 1983. Green-ampt Infiltration Parameters from Soils Data. *Journal of Hydraulic Engineering* 109(1): 62–70. doi: 10.1061/(asce)0733-9429(1983)109:1(62).
- Revilla, I., J. Plaza, and C. Palacios. 2021. The Effect of Grazing Level and Ageing Time on the Physicochemical and Sensory Characteristics of Beef Meat in Organic and Conventional Production. *Animals (Basel)* 11(3): 635. doi: 10.3390/ani11030635
- Roberson, T., L.G. Bundy and T.W. Andraski. 2007. Freezing and Drying Effects on Potential Plant Contributions to Phosphorus in Runoff. *Journal of Environmental Quality* 36(2): 532–539. doi: 10.2134/jeq2006.0169.
- Roberson, T., L.G. Bundy and T.W. Andraski. 2007. Freezing and Drying Effects on Potential Plant Contributions to Phosphorus in Runoff. *Journal of Environmental Quality* 36(2): 532–539. doi: 10.2134/jeq2006.0169.
- Roesch, A., P. Weisskopf, H. Oberholzer, A. Valsangiacomo, and T. Nemecek. 2019. An Approach for Describing the Effects of Grazing on Soil Quality in Life-Cycle Assessment. *Sustainability* 11(18): 4870. doi: 10.3390/su11184870
- Romano, N., M. Palladino and G.B. Chirico. 2011. Parameterization of a bucket model for soil-vegetation-atmosphere modeling under seasonal climatic regimes. *Hydrology and Earth System Sciences* 15(12): 3877–3893. doi: 10.5194/hess-15-3877-2011.
- Roste, J. 2015. Development and evaluation of a Canadian prairie nutrient transport model. University of Saskatchewan. [Online] Available: <https://harvest.usask.ca/handle/10388/ETD-2015-07-2172?show=full>
- Rotz, C.A. 2004. The Integrated Farm System Model: A Tool for Developing more Economically and Environmentally Sustainable Farming Systems for the Northeast. doi: 10.13031/2013.16116
- Rotz, C.A., M.S. Corson, D.S. Chianese, F. Montes, S.D. Hafner, H.F. Bonifacio and C.U. Coiner. 2022. The Integrated Farm System Model reference manual version 4.7. USDA.
- Rotz, C.A., S. Asem-Hiablíe, S. Place, and G. Thoma. 2019. Environmental footprints of beef cattle production in the United States. *Agriculture Systems* 169 (2019): 1-13. doi: 10.1016/j.agsy.2018.11.005
- Safeeq, M. and A. Fares. 2011. Accuracy evaluation of ClimGen weather generator and daily to hourly disaggregation methods in tropical conditions. *Theoretical and Applied Climatology* 106(3–4): 321–341. doi: 10.1007/s00704-011-0438-4.
- Sajikumar, N. and R.S. Remya. 2015. Impact of land cover and land use change on runoff characteristics. *Journal of Environmental Management* 161: 460–468. doi: 10.1016/j.jenvman.2014.12.041.
- Sazib, N., J. Bolten and I. Mladenova. 2020. Exploring Spatiotemporal Relations between Soil Moisture, Precipitation, and Streamflow for a Large Set of Watersheds Using Google Earth Engine. *Water* 12(5): 1371. doi: 10.3390/w12051371.
- Schils, R.L.M., J.E. Olesen, A. del Prado, and J.F. Soussana. 2007. A review of farm level

- modelling approaches for mitigating greenhouse gas emissions from ruminant livestock systems. *Livestock Science* 112(3): 240-251. doi: 10.1016/j.livsci.2007.09.005
- Schlesinger, W.H. 1997. *Biogeochemistry: An Analysis of Global Change*. 2nd Edition. Academic Press, New York.
- Schwarzwalder, K. and N. Lenssen. 2022. The importance of internal climate variability in climate impact projections. *Proceedings of the National Academy of Sciences* 119(42). doi: 10.1073/pnas.2208095119.
- Sharpe, P. and E.B. Rayburn. 2019. Climate, Weather, and Plant Hardiness. *Horse Pasture Management*: 209–231. doi: 10.1016/b978-0-12-812919-7.00012-3
- Shrestha, R.R., Y.B. Dibike and T.D. Prowse. 2012. Modelling of climate-induced hydrologic changes in the Lake Winnipeg watershed. *Journal of Great Lakes Research* 38: 83–94. doi: 10.1016/j.jglr.2011.02.004.
- Silveira, M.L., J.M.B. Vendramini, H.M.D. Silva, and M. Azenha. 2019. Nutrient Cycling in Grazed Pastures. University of Florida Institute of Food and Agricultural Sciences. doi: 10.32473/edis-ss578-2013
- Šimůnek, J., M.Th. van Genuchten, and M. Šejna. 2012. HYDRUS: Model use, calibration, and validation. *Transactions of the ASABE*. 55(4): 1261-1274. doi: 10.13031/2013.42239
- Sitterson, J., C. Knightes, R. Parmar, K. Wolfe, M. Muche, and B. Avant. 2017. An overview of rainfall-runoff model types. U.S. Environmental Protection Agency.
- Slewisinski, T.L. 2012. Non-structural carbohydrate partitioning in grass stems: a target to increase yield stability, stress tolerance, and biofuel production. *Journal of Experimental Botany* 63(13): 4647–4670. doi: 10.1093/jxb/ers124
- Soana, E., M.P. Gervasio, T. Granata, D. Colombo and G. Castaldelli. 2023. Climate change impacts on eutrophication in the Po River (Italy): Temperature-mediated reduction in nitrogen export but no effect on phosphorus. *Journal of Environmental Sciences*. doi: 10.1016/j.jes.2023.07.008.
- Soil Landscapes of Canada Working Group, 2010. Soil Landscapes of Canada version 3.2. Agriculture and Agri-Food Canada. (digital map and database at 1:1 million scale).
- Soriano, E., L. Mediero and C. Garijo. 2019. Selection of Bias Correction Methods to Assess the Impact of Climate Change on Flood Frequency Curves. *Water* 11(11): 2266. doi: 10.3390/w11112266.
- Souza, V.C., P. Malafaia, B.R. Vieira, Y.T. Granja-Salcedo, and T.T. Berchielli. 2016. Phosphorus supplementation with or without other minerals, ionophore and antibiotic did not affect performance of Nellore bulls receiving high-grain diets, but increased phosphorus excretion and dietary costs. *Anim. Prod. Sci.* 58:871–877. doi:10.1071/AN16420
- Spence, C., Z. He, K.R. Shook, B.A. Mekonnen, J.W. Pomeroy, C.J. Whitfield and J.D. Wolfe. 2022. Assessing hydrological sensitivity of grassland basins in the Canadian Prairies to climate using a basin classification-based virtual modelling approach. *Hydrology and Earth System Sciences* 26(7): 1801–1819. doi: 10.5194/hess-26-1801-2022.
- Spiehs, M.J., and V.H. Varel. 2009. Nutrient excretion and odorant production in manure from cattle fed corn wet distillers grains with solubles. *J. Anim. Sci.* 87:2977–2984. doi:10.2527/jas.2008-1584
- Srivastava, A., P. Deb and N. Kumari. 2019. Multi-Model Approach to Assess the Dynamics of Hydrologic Components in a Tropical Ecosystem. *Water Resources Management* 34(1): 327–341. doi: 10.1007/s11269-019-02452-z.
- Stadnyk, T., S. Déry, M. MacDonald, and K. Koenig. 2019. The Freshwater System. In

- Integrated Regional Impact Study: Hudson Bay*; Kuzyk, Z.Z., Candlish, L.M., Eds.; Arctic Net: Québec City, QC, Canada; pp. 113–154.
- Statistics Canada. 2006. A Geographical Profile of Manure Production in Canada, 2001, Catalogue no. 21-601-M. [Online] Available: www.statcan.gc.ca/bsolc/olc-ccel/olccel?lang=eng&catno=21-601-M2006077
- Statistics Canada. 2006. Snapshot of Canadian agriculture. [Online] Available: www150.statcan.gc.ca/n1/ca-ra2006/articles/snapshot-portrait-eng.htm
- Statistics Canada. 2017. Table 32-10-0406-01. Land use, Census of Agriculture, 2011 and 2016, inactive. doi: 10.25318/3210040601-eng
- Statistics Canada. 2022a. Canadian Beef and Cattle Export Percentages 2010-2021.
- Statistics Canada. 2022b. Table 32-10-0130-01: Number of cattle, by class and farm type (x 1,000). doi: 10.25318/3210013001-eng
- Statistics Canada. 2022c. Table 32-10-0249-01. Land use, Census of Agriculture, 2021. doi: 10.25318/3210024901-eng
- Statistics Canada. 2023a. Table 38-10-0091-01. Annual water yield for selected ecoprovinces. doi: 10.25318/3810009101-eng
- Statistics Canada. 2023b. Table 32-10-0045-01. Farm cash receipts, annual (x 1,000). doi: 10.25318/3210004501-eng
- Stern, D.I., and R.K., Kaufmann. 2014. Anthropogenic and natural causes of climate change. *Climatic Change* 122: 257–269. doi: 10.1007/s10584-013-1007-x
- Strömqvist, J., B. Arheimer, J. Dahné, C. Donnelly and G. Lindström. 2012. Water and nutrient predictions in ungauged basins: set-up and evaluation of a model at the national scale. *Hydrological Sciences Journal* 57(2): 229–247. doi: 10.1080/02626667.2011.637497.
- Swedish Meteorological and Hydrological Institute. n.d. HYPE Model Documentation: Land routines. [Online] Available: www.smhi.net/hype/wiki/doku.php?id=start:hype_model_description:hype_land
- Tam, B.Y., K. Szeto, B. Bonsal, G. Flato, A.J. Cannon and R. Rong. 2018. CMIP5 drought projections in Canada based on the Standardized Precipitation Evapotranspiration Index. *Canadian Water Resources Journal / Revue Canadienne Des Ressources Hydriques* 44(1): 90–107. doi: 10.1080/07011784.2018.1537812.
- Tan, Z.X., R. Lal, and K.D. Wiebe. 2005. Global Soil Nutrient Depletion and Yield Reduction. *Journal of Sustainable Agriculture* 26(1): 123-146. doi: 10.1300/J064v26n01_10
- Taylor, K.E., R.J. Stouffer and G.A. Meehl. 2012. An Overview of CMIP5 and the Experiment Design. *Bulletin of the American Meteorological Society* 93(4): 485–498. doi: 10.1175/bams-d-11-00094.1
- Taylor, P. 1998. The Thermodynamic Effects of Sublimating, Blowing Snow in the Atmospheric Boundary Layer. *Boundary-Layer Meteorology* 89, 251–283. doi: 10.1023/A:1001712111718
- Thivierge, M.-N., G. Jégo, G. Bélanger, A. Bertrand, G.F. Tremblay, C.A. Rotz and B. Qian. 2016. Predicted Yield and Nutritive Value of an Alfalfa–Timothy Mixture under Climate Change and Elevated Atmospheric Carbon Dioxide. *Agronomy Journal* 108(2): 585–603. doi: 10.2134/agronj2015.0484.
- Thivierge, M.-N., G. Jégo, G. Bélanger, M.H. Chantigny, C.A. Rotz, É. Charbonneau, V.S. Baron and B. Qian. 2017. Projected impact of future climate conditions on the agronomic and environmental performance of Canadian dairy farms. *Agricultural Systems* 157: 241–257. doi: 10.1016/j.agsy.2017.07.003.
- Thorpe, J., S.A. Wolfe and B. Houston. 2008. Potential impacts of climate change on grazing

- capacity of native grasslands in the Canadian prairies. *Can. J. Soil Sci.* 88: 595-609. doi: 10.4141/CJSS07094
- Tsegaw, A.T., M. Pontoppidan, E. Kristvik, K. Alfredsen and T.M. Muthanna. 2020. Hydrological impacts of climate change on small ungauged catchments – results from a global climate model–regional climate model–hydrologic model chain. *Natural Hazards and Earth System Sciences* 20(8): 2133–2155. doi: 10.5194/nhess-20-2133-2020.
- Tunney, H., I. Kurz, D. Bourke, and C. O’Reilly. 2007. Eutrophication from Agricultural Sources: The Impact of the Grazing Animal on Phosphorous Loss from Grazed Pasture. ERTDI funded-project 2000-LS-2.1.2-M2. [Online] Accessible: www.epa.ie/publications/research/water/LS-212ppcalice_Web1.pdf
- Turner, D.W. and E. Lahav. 1985. Temperature influences nutrient absorption and uptake rates of bananas grown in controlled environments. *Scientia Horticulturae* 26(4): 311–322. doi: 10.1016/0304-4238(85)90015-9.
- U.S. Geological Survey. 2014. EarthExplorer. [Online] Available: <https://earthexplorer.usgs.gov/>
- Uddin, M.E. and E. Kebeab. 2020. Review: Impact of Food and Climate Change on Pastoral Industries. *Front. Sustain. Food Syst.*, Volume 4. doi: 10.3389/fsufs.2020.543403
- USAF. 1991. A Method for Estimating Missing Hourly Temperatures using Daily Maximum and Minimum Temperatures. USAFETAC/PR-91/017. USAF Environmental Technical Applications Center. Scott Air Force Base, IL
- USGS. 2018. Runoff: Surface and Overland Water Runoff.
- Vadas, P.A., and C.H. Bolster. 2022. Annual Phosphorus Loss Estimator theoretical documentation Version 3.0. [Online] Available: www.ars.usda.gov/midwest-area/bowling-green-kyenvironmental-systems-research/people/carl-bolster/aple/
- van der Kamp, G., d. Keir and M.S. Evans. 2013. Long-Term Water Level Changes in Closed-Basin Lakes of the Canadian Prairies. *Canadian Water Resources Journal* 33(1): 23–38. doi: 10.4296/cwrj3301023
- van der Kamp, G., M. Hayashi and D. Gallén. 2003. Comparing the hydrology of grassed and cultivated catchments in the semi-arid Canadian prairies. *Hydrological Processes* 17(3): 559–575. doi: 10.1002/hyp.1157.
- Van Horn, H.H. 1997. Factors affecting manure quantity, quality, and use. [Online] Available: www.txanc.org/Proceedings/1998/vanhorn3.pdf
- van Vuuren, D.P., J. Edmonds, M. Kainuma, K. Riahi, A. Thomson, K. Hibbard, G.C. Hurtt, T. Kram, V. Krey, J.-F. Lamarque, T. Masui, M. Meinshausen, N. Nakicenovic, S.J. Smith and S.K. Rose. 2011. The representative concentration pathways: an overview. *Climatic Change* 109: 5–31. doi: 10.1007/s10584-011-0148-z
- Vickers, G., S. Buzza, D. Schmidt and J. Mullock. 2001. The Weather of The Canadian Prairies Graphic Area Forecast 32. NAV Canada.
- Vogt, R.J., S. Sharma and P.R. Leavitt. 2018. Direct and interactive effects of climate, meteorology, river hydrology, and lake characteristics on water quality in productive lakes of the Canadian Prairies. *Can. J. Fish. Aquat. Sci.* 75: 47–59. doi: 10.1139/cjfas-2016-0520
- Ward, B.B. 2008. Nitrification. *Encyclopedia of Ecology* 2511–2518. doi: 10.1016/b978-008045405-4.00280-9.
- Wang, C., X. Zhou, D. Guo, J.-H. Zhao, Y. Li, G. Feng, Q. Gao, H. Yu and L. Zhao. 2019. Soil pH is the primary factor driving the distribution and function of microorganisms in farmland soils in northeastern China. *Annals of Microbiology*. doi: 10.1007/s13213-019-01529-9.
- Wang, S., Y. Yang, Y. Luo and A. Rivera. 2013. Spatial and seasonal variations in

- evapotranspiration over Canada's landmass. *Hydrology and Earth System Sciences* 17(9): 3561–3575. doi: 10.5194/hess-17-3561-2013.
- Water Quality Management Section Manitoba Environment and Climate. Box 14, 14 Fultz Blvd. Winnipeg MB R3Y 0L6
- Watson, A., G. Midgley, P. Ray, S. Kralisch, and J. Helmschrot. 2022. How Climate Extremes Influence Conceptual Rainfall-Runoff Model Performance and Uncertainty. doi: 10.3389/fclim.2022.859303
- Whetton, R.L., M.A. Harty and N.M. Holden. 2022. Communicating Nitrogen Loss Mechanisms for Improving Nitrogen Use Efficiency Management, Focused on Global Wheat. *Nitrogen* 3(2): 213–246. doi: 10.3390/nitrogen3020016.
- Williams, M. R., G. W. Feyereisen, D. B. Beegle, R. D. Shannon, G. J. Folmar and R. B. Bryant. 2011. Manure Application under Winter Conditions: Nutrient Runoff and Leaching Losses. *Transactions of the ASABE* 54(3): 891–899. doi: 10.13031/2013.37114
- Williams, M.R., G.W. Feyereisen, D.B. Beegle, and R.D. Shannon. 2012. Soil temperature regulates phosphorus loss from lysimeters following fall and winter manure application. *Transactions of the ASABE*. 55(2): 871-880. doi: 10.13031/2013.41529
- Williams, P.H., and R.J. Haynes. 1990. Influence of improved pastures and grazing animals on nutrient cycling within New Zealand soils. *New Zealand Journal of Ecology* 14: 49-57
- Wilson, H.F., N.J. Casson, A.J. Glenn, P. Badiou and L. Boychuk. 2019. Landscape Controls on Nutrient Export during Snowmelt and an Extreme Rainfall Runoff Event in Northern Agricultural Watersheds. *Journal of Environmental Quality* 48(4): 841–849. doi: 10.2134/jeq2018.07.0278.
- World Meteorological Organization. 2019. Atmospheric Deposition. [Online] Available: <https://public.wmo.int/en/our-mandate/focus-areas/environment/atmospheric-deposition>
- World Wildlife Fund. 2016. Plowprint report. [Online] Available: files.worldwildlife.org/wwfcmsprod/files/Publication/file/7xaffijdtj_plowprint_AnnualReport_2016_Final_REV09192016.pdf
- Wu, G., M. Baraldo, and M. Furlanut. 1995. Calculating percentage prediction error: a user's note. *Pharmacological Research* 32(4): 241-248. doi: 10.1016/S1043-6618(05)80029-5
- Wu, G., Z. Cheng, J.M. Alatalo, J. Zhao and Y. Liu. 2021. Climate Warming Consistently Reduces Grassland Ecosystem Productivity. *Earth's Future* 9(6). doi: 10.1029/2020ef001837.
- Wu, Y., C. Miao, X. Fan, J. Gou, Q. Zhang and H. Zheng. 2022. Quantifying the Uncertainty Sources of Future Climate Projections and Narrowing Uncertainties With Bias Correction Techniques. *Earth's Future* 10(11). doi: 10.1029/2022ef002963.
- Wu, Y., J. Liu, J. Zhai, L. Cong, Y. Wang, W. Ma, Z. Zhang and C. Li. 2018. Comparison of dry and wet deposition of particulate matter in near-surface waters during summer. *PLOS ONE* 13(6): e0199241. doi: 10.1371/journal.pone.0199241.
- Xu, Y., C. Zhan, and B. Huang. 2011. Heat Shock Proteins in Association with Heat Tolerance in Grasses. *International Journal of Proteomics 2011*: 1–11. doi: 10.1155/2011/529648
- Yang, J., L. Zhao and K. Oleson. 2023. Large humidity effects on urban heat exposure and cooling challenges under climate change. *Environmental Research Letters* 18(4): 044024. doi: 10.1088/1748-9326/acc475.
- Yang, J.Y., C.F. Drury, X.M. Yang, R. De Jong, E.C. Huffman, C.A. Campbell and V. Kirkwood. 2010. Estimating biological N₂ fixation in Canadian agricultural land using legume yields. *Agriculture, Ecosystems & Environment* 137(1–2): 192–201. doi: 10.1016/j.agee.2010.02.004.
- Yue, S. and C. Wang. 2004. The Mann-Kendall Test Modified by Effective Sample Size to Detect

- Trend in Serially Correlated Hydrological Series. *Water Resources Management* 18: 201-218. doi: 10.1023/B:WARM.0000043140.61082.60
- Yue, S. and C. Wang. 2004. The Mann-Kendall Test Modified by Effective Sample Size to Detect Trend in Serially Correlated Hydrological Series. *Water Resources Management* 18: 201-218. doi: 10.1023/B:WARM.0000043140.61082.60
- Zanetti, D., S.C. Valadares Filho, L.F. Prados, E. Detmann, M.V.C. Pacheco, L.A. Godoi, L.N. Rennó, and T.E. Engle. 2017. Impacts of reduction of phosphorus in finishing diets for Holstein× Zebu steers. *Livest. Sci.* 198:45–51. doi: 10.1016/j.livsci.2017.02.001
- Zeinali, A., T. Edeskär and J. Laue. 2020. Mechanism of thawing. *Cogent Engineering* 7(1): 1716438. doi: 10.1080/23311916.2020.1716438
- Zenobi, M.G., H.A. Lardner, P.G. Jefferson, and J.J. McKinnon. 2015. Effect of feeding strategically blended feed pellets on rumen fermentation and nutrient digestion. *Can. J. Anim. Sci.* 95:243–254. doi:10.4141/cjas-2014 -131
- Zhang, R., H. Wang, Q. Fu, P.J. Rasch and X. Wang. 2019. Unraveling driving forces explaining significant reduction in satellite-inferred Arctic surface albedo since the 1980s. *Proceedings of the National Academy of Sciences* 116(48): 23947–23953. doi: 10.1073/pnas.1915258116.
- Zhang, X., G. Flato, M. Kirchmeier-Young, L. Vincent, H. Wan, X. Wang, R. Rong, J. Fyfe, G. Li, and V.V. Kharin. 2019. Changes in Temperature and Precipitation Across Canada; Chapter 4 in Bush, E. and Lemmen, D.S. (Eds.) *Canada’s Changing Climate Report*: 112-193.
- Zhang, Z., D. L. Kane, and L. D. Hinzman. 2000. Development and application of a spatially-distributed Arctic hydrological and thermal process model. *Hydrological Processes* 14: 1017-1044. doi: 10.1002/(SICI)1099-1085(20000430)14:6<1017::AID-HYP982>3.0.CO;2-G
- Ziska, L.H. 2003. Evaluation of the growth response of six invasive species to past, present and future atmospheric carbon dioxide. *Journal of Experimental Botany* 54(381): 395–404. doi: 10.1093/jxb/erg027